Title
Basolateral amygdala circuits in detailed associative reward memory

Author
Sias, Ana

Publication Date
2022

Peer reviewed|Thesis/dissertation

UNIVERSITY OF CALIFORNIA

Los Angeles

Basolateral amygdala circuits in detailed associative reward memory

A dissertation submitted in partial satisfaction of the

requirements for the degree Doctor of Philosophy in

Neuroscience

by

Ana Sias

2022

ABSTRACT OF THE DISSERTATION

Basolateral amygdala circuits in detailed associative reward memory

by

Ana Sias

Doctor of Philosophy in Neuroscience

University of California, Los Angeles, 2022

Professor Kate Wassum, Chair

To make good decisions we often rely on detailed associative memories to infer the availability of prospective rewards from predictive cues within the environment. These stimulus-outcome relationships are essential elements of our cognitive map that links specific outcomes to antecedent cues and the specific actions needed to obtain them. This internal model enables us to project into the future, anticipate the consequences of our actions and adapt our behaviors accordingly (i.e., model-based decision making). The research presented here investigated neural circuitry mediating the encoding and subsequent retrieval of outcome-specific reward memories.

Targeted optical manipulation and recording methods revealed the basolateral amygdala (BLA) as a central hub for detailed stimulus-outcome associations. The BLA was robustly activated by the delivery of distinct food outcomes preceded by auditory stimuli and this activity was necessary for *encoding* sensory-specific cue-reward memories. This function was supported by modulatory inputs from ventral tegmental dopamine neurons (VTA_{DA}). Optically manipulating VTA_{DA}→BLA axonal terminals during Pavlovian conditioning and in a novel Pavlovian blocking paradigm revealed these inputs are both necessary and sufficient to drive outcome-specific learning. Excitatory projections from the lateral orbitofrontal cortex (lOFC) were also essential

for facilitating the BLA in encoding these associations. Moreover, reciprocal lOFC→BLA→lOFC connections formed an encoding and retrieval circuit. Associative memories are complex, containing information about stimuli, motivational state, outcome identity, value, etc. A pathway-specific serial disconnection revealed that the component of the associative memory that was encoded through activation of lOFC→BLA projections was the same as that which was later accessed through BLA→lOFC projections to enable cue motivated adaptive reward seeking. Collectively, these data uncover neural substrates for detailed associative reward memories that enable model-based decision making.

The dissertation of Ana Sias is approved.

Laura Anne Wilke

Melissa J. Sharpe

Avishek Adhikari

Edythe Danick London

Kate Wassum, Committee Chair

University of California Los Angeles

2022

Dedicated to my grandma, Aida Sias.

You're just too wonderful, too wonderful for words.

Table of Contents

Table of Figures

Acknowledgements

Graduate school has been the most trying and rewarding experience of my life. I would not be where I am today without the support of my mentor, friends, and family. First, I would like to acknowledge my advisor, Dr. Kate Wassum. Everyone who knows Kate will tell you that she is a driven and brilliant scientist. But only those lucky enough to have worked with her can say that she is also a thoughtful and generous mentor. Over the last five years Kate has spent countless hours pushing me to my full potential, guiding me in experimental design, data analysis and workshopping new ideas. She welcomes questions without judgement, even when they may seem trivial or small. For her patience and encouragement, I thank her. I would also like to recognize my dissertation committee members: Dr. Melissa Sharpe, Dr. Avishek Adhikari, Dr. Laura DeNardo and Dr. Edythe London. Each one challenged me to think critically about my project and provided invaluable advice that focused my research trajectory.

With the challenges I have faced in this journey has also come great friendships. Thank you, Mimi La-Vu, Ethan Rohrbach, Joselyn Soto and Scott Vincent, for your commiseration and for getting me through my first year. A special thanks to my lab mates, Alex Lamparelli, Baila Hall, Melissa Malvaez, Christine Shieh and Jackie Giovanniello for all their support along the way and for filling the bleak Franz Hall basement with laughter and good times. I would also like to thank Caitlin Goodpaster for being a truly thoughtful, fun, and kind friend.

Who I am as a person and as a student is intimately tied to the relationship I have with my family. My grandma, Aida, has always loved me with all her heart and has made me feel like I can accomplish anything. My sister Sara has gotten me through difficult times and brings light everywhere she goes. I also share a bond with my younger sisters, Gabriela and Rebecca, that can't be replaced. Christopher is the brother that I never had and will always be way cooler than me. My parents are especially proud of my accomplishments and provide me with optimism about the future. John and Marth Miller are two of the kindest and most welcoming people I have ever had the pleasure to meet. Thanks to all of them for being a part of my life. Last, I would like to

acknowledge my fiancée, Matthew Miller for inspiring me to pursue my PhD. We have been on this journey together and I cherish sharing in each other's successes. Matt motivates me to strive for more and be the best version of myself. Thank you for your boundless love and encouragement.

Permissions

Chapter 2 is a version of Sias, A.C., Morse, A.K., Wang, S., Greenfield, V.Y., Goodpaster, C.M., Wrenn, T.M., Wikenheiser, A.M., Holley, S.M., Cepeda, C., Levine, M.S. & Wassum, K.M. (2021). A bidirectional corticoamygdala circuit for the encoding and retrieval of detailed reward memories. eLife, 10, e68617. doi: 10.7554/eLife.68617

Author contributions: K.M.W. and A.K.M. designed the research, A.C.S., A.K.M., S.W., C.M.G., and T.M.W. performed the research, A.M.W. created a customized data processing pipeline, A.C.S. and A.K.M. analyzed the data, S.M.H., conducted *ex vivo* electrophysiology experiments. S.M.H., C.C., and M.S.L. contributed to manuscript preparation, and A.C.S. and K.M.W. wrote the paper. K.M.W. was the principal investigator for this project.

Chapter 3 is in preparation for publication.

Author contributions: A.C.S., M.J.S., and K.M.W. designed the research, A.C.S, Y.X.K, C.M.G, and T.M.W performed the research, N.G. assisted with figures, and A.C.S and K.M.W wrote the paper. K.M.W. was the principal investigator for this project.

Funding

This work was supported by NIH Research Project grant (R01DA035443, Wassum) and NIH Research Project grant (R01MH126285, Wassum and Ostlund). Additional funding was provided by the National Science Foundation Graduate Research Fellowship Program (DGE1650604) and the UCLA Training Program in the Translational Neuroscience of Drug Abuse (T32DA024635, London).

Vita

Education

University of California Los Angeles — 2017-present
PhD Candidate, Neuroscience Interdepartmental Ph.D. Program

University of California Berkeley — 2010-2014
Bachelor of Arts, Psychology, High Distinction

Awards and Honors

Samuel Eiduson Student Lecture Award	2022
National Science Foundation Graduate Research Fellowship	2019-2022
Society for Neuroscience Trainee Professional Development Award	2021
Brain Research Institute Society for Neuroscience Travel Award, UC Los Angeles	2021
Brain Research Institute Society for Neuroscience Travel Award, UC Los Angeles	2019
NIDA T32 Predoctoral Fellowship, UC Los Angeles	2018-2019

Selected Publications

Sias A. C., Morse, A. K., Wang, S., Greenfield V. Y., Goodpaster C. M., Wrenn T. M., Wikenheiser, A. M., Holley, S. M., Cepeda, C., Levine M. S., Wassum K. M. (2021). A bidirectional corticoamygdala circuit for the encoding and retrieval of detailed reward memories. *elife, 10*.

Lee S. E., **Sias A. C.**, Kosik E. L., Flagan T.M. , Deng J., Chu S. A., Brown J. A., Vidovszky A. A., Ramos E. M., Gorno-Tempini M. L., Karydas A. M., Coppola G., Geschwind D. H., Rademakers R., Boeve B. F., Boxer A. L., Rosen H. J., Miller B. L., Seeley W.W. (2019). Thalamo-cortical network hyperconnectivity in preclinical progranulin mutation carriers. *Neuroimage: Clinical, 22*.

Lee, S. E., **Sias, A. C.**, Mandelli, M. L., Brown, J. A., Brown, A. B., Khazenzon, A. M., Vidovszky, A. A., Zanto, T. P., Karydas, A. K., Pribadi, M., Dokuru, D., Coppola, G., Geschwind, D. H., Rademakers, R., Gorno-Tempini, M. L., Rosen, H. J., Miller, B. L., Seeley, W. W. (2017). Network degeneration and dysfunction in presymptomatic *C9ORF72* expansion carriers. *Neuroimage: Clinical, 14*, 286-297.

Greenhouse, I., **Sias, A.**, Labruna, L., Ivry, R. B. (2015). Nonspecific Inhibition of the Motor System during Response Preparation. *The Journal of Neuroscience, 35*(30), 10675-10684.

Selected Talks

Sias, A. C. Basolateral amygdala circuits are neural substrates for outcome-specific reward memories. (2022). *Samuel Eiduson Student Lecture*, Los Angeles, California.

Sias, A. C. Dopamine projections to the basolateral amygdala mediate the encoding of outcome-specific reward memories (2022). *Integrative Center for Learning and Memory – Young Investigator Lecture Series*, Los Angeles, California.

Sias, A. C. A reciprocal cortical-amygdala circuit for the encoding and retrieval of detailed associative reward memories. (2020). *Integrative Center for Learning and Memory – Young Investigator Lecture Series*, Los Angeles, California

Chapter 1: General Introduction

Being able to accurately anticipate available rewards in the environment is crucial to making adaptive decisions. To do this, we often rely on observable stimuli to make predictions about future outcomes. Previously learnt stimulus-outcome associations are fundamental elements of our internal model of the environment which enables us to infer the consequences of our actions and make advantageous choices (Dayan and Berridge, 2014). For example, as a child you might have learnt that on Sunday mornings your father comes home with a pink box filled with donuts. Years later, when seeing that same pink box on the snack table at a conference, you can anticipate delicious fried treats inside and decide to grab yourself a maple bar. When multiple cues are present, a mental map of each of their specific associated outcomes facilitates assessment of their current value based on our goals and needs. Comparing the Sweetgreen™ bag next to the pink donut box, you can infer salad is also an option and might be better given your high cholesterol. An inability to encode or successfully retrieve these detailed associations can distort outcome expectations leading to disrupted motivation and choice – cognitive symptoms that are characteristic of several psychiatric disorders (Grillon, 2002; Hogarth et al., 2013; Chen et al., 2015; Everitt and Robbins, 2016; Bishop and Gagne, 2018). Investigating how the brain forms these detailed associative memories is therefore essential to understanding the basis of both adaptive and maladaptive decision making.

Associative learning: Instrumental and Pavlovian processes

In navigating our world, we often toggle between decision processes that alternatively favor efficiency or flexibility. Efficient decisions can be mediated by a habitual behavioral control system in which actions are executed based on past success rather than consideration of potential future outcomes or consequences. Habitual behaviors can reduce cognitive effort through automaticity but are inflexible to changes in outcome value or the contingency between actions and associated outcomes (Dickinson, 1985; Robbins and Costa, 2017). Alternatively, encoding the associative relationship between our actions, or responses, and the resulting outcomes (R-O)

enables goal-directed behaviors. It has been proposed that for an action to be goal-directed, it must be 1) sensitive to the instrumental contingency between that action and the proceeding outcome and 2) the outcome's incentive value (Dickinson and Balleine, 1994; Balleine and Dickinson, 1998b). Indeed, early studies have demonstrated that instrumental behaviors driven by R-O associations are modulated by degradation in the causal relationship between actions and outcomes (Hammond, 1980) and by devaluation of the outcome (Adams and Dickinson, 1981). Furthermore, these changes in instrumental performance are specific to the actions for which the instrumental contingency is degraded, or for which the associated outcome's value is altered (Bolles et al., 1980; Colwill and Rescorla, 1985, 1986; Dickinson and Mulatero, 1989; Dickinson et al., 1996).

In addition to expectancies derived from instrumental associations, we can infer the availability of outcomes (unconditioned stimulus; US) within our environment from stimuli that we have learnt reliably predict those outcomes (i.e., conditioned stimuli; CS). In classical Pavlovian conditioning paradigms, a cue (CS) is paired with an ecologically salient outcome (US), facilitating the formation of a CS-US association in which the US is conditional upon the presence of the CS. Once this association is formed, the conditioned stimulus can itself elicit a response originally generated by the US itself (conditioned response; CR) or one that facilitates adaptive behavior in the face of the US (Pavlov, 1927; Fanselow and Wassum, 2015). Early theories suggest that these conditioned responses emerge through stimulus-response (S-R) learning (Hull, 1943; Spence, 1956; Fanselow and Wassum, 2015). Here, if a stimulus and response are followed by a reinforcing outcome the presence of the stimulus will increase the likelihood that the response is evoked, thus forming the S-R link. Similar accounts emerge from computational frameworks of Pavlovian learning which suggest that through repeated experience, the CS is imbued with motivational value of the predicted US (Dayan and Berridge, 2014). Temporal difference models of reinforcement learning suggest this is facilitated through a discrepancy between outcomes

predicted and outcomes experienced (prediction error) which acts as a teaching signal to retrospectively cache value and update associative strengths (Rescorla and Wagner, 1972; Sutton, 1988). This cached value enables the cue to elicit a CR, without the need for a representation of the US itself (Ludvig et al., 2012; Dayan and Berridge, 2014). Without the need to represent the features of outcomes or predictive stimuli, this value-driven form of learning can occur without a model of the external environment and is therefore often referred to as being "model-free".

Like habits, stimulus-response, or model-free, mechanisms of Pavlovian learning are efficient, but inflexible. To support behavioral flexibility, early theorists argued for a more cognitive association that involves a causal link between stimuli and the outcomes they predict (i.e., stimulus-outcome; S-O). Through these S-O relationships, stimuli can generate outcome expectations which can in turn elicit ecologically relevant behaviors related to the outcome (i.e., the conditioned response) (Bolles et al., 1980; Fanselow and Wassum, 2015). Within the computational reinforcement learning literature, the acquisition of a mental map containing causal associative links between stimuli and events within the environment is referred to as "model-based" learning. Support for model-based S-O associations come from several sources such as studies of sensory preconditioning and outcome revaluation. In sensory preconditioning, two neutral stimuli are paired together (S1→S2). S2 is subsequently paired with a US and in a final stage S1 is presented alone and is sufficient to elicit a CR (Brogden, 1939). Because S1 was never directly experienced with the US, the CR cannot be easily explained by an S-R strategy. More likely, the CR is driven through a series of S-O activations. S1 generates a representation of S2 which elicits a CR through its association with the US (Fanselow and Wassum, 2015). Studies implementing outcome revaluation have demonstrated that altering the value of either an aversive (Rescorla, 1973, 1974) or appetitive (Holland and Rescorla, 1976; Holland and Straub, 1980; Holland, 1981; Colwill and Motzkin, 1994) US can modify the CR. For example, post-conditioning devaluation of a food US through satiation can reduce food cup approach in a non-

reinforced probe test (Holland and Rescorla, 1976). Because this test is done in extinction, this behavioral modification reflects the subjects' ability to use the CS to generate an expectation of the US and its current value.

Through stimulus-outcome learning, the CS can associate with multiple attributes of the US including its general or incentive motivational properties (Konorski, 1967; Rescorla and Solomon, 1967; Bindra, 1968; Bolles, 1972; Bindra, 1974; Fanselow and Wassum, 2015) as well as it's specific identifying features (Konorski, 1967; Trapold, 1970; Overmier et al., 1972; Baxter and Zamble, 1982; Delamater, 1995). Evidence for a detailed representation of the US within S-O associations has been demonstrated through outcome-devaluation. A reduction in conditioned food-port approach following the devaluation of a US is selective to the CS predicting that US, but remains intact for a CS predictive of a similar, but non-devalued outcome (Colwill and Motzkin, 1994). Since the relationship between the CS and the newly devalued outcome is not learnt directly, this reflects an inferential process in which a cue-evoked representation of the associated outcome can be used to assess how advantageous it would be to pursue it given the current state.

Pavlovian-to-instrumental transfer

Cues previously paired with reward can excite ongoing actions (Estes, 1948). This is the Pavlovian-to-instrumental transfer phenomenon and can be governed by two processes. Pavlovian stimuli can enhance appetitive arousal and provide a source of motivation for instrumental performance generally (i.e., general PIT) (Rescorla and Solomon, 1967; Hall et al., 2001; Corbit and Balleine, 2005). Alternatively, predictive cues can selectively bias performance for actions associated with the same outcome (i.e., outcome-specific PIT) (Kruse et al., 1983; Colwill and Motzkin, 1994). Outcome-specific PIT assesses the ability to use previously learnt stimulus-outcome associations to, upon cue presentation, make inferences about the availability of specific rewards and choose accordingly. As such, this task is an invaluable tool to assess the circuit mechanisms underlying sensory-specific Pavlovian learning and memory (Corbit and Balleine, 2016).

BLA function in reward learning

The amygdala is a highly conserved limbic structure that can be divided into medial, central, lateral and basal subnuclei. These latter nuclei together form the basolateral amygdala (Janak and Tye, 2015). The BLA cell population is comprised primarily of glutamatergic principal neurons, but also contains local inhibitory interneurons and is laterally and medially flanked by GABAergic intercalated cell clusters (Millhouse and DeOlmos, 1983; McDonald, 1992; McDonald and Augustine, 1993). Sensory information is relayed through glutamatergic projections from thalamus and cortex primarily to the lateral amygdala, which sends excitatory projections to the central and basal compartments. But the basal amygdala also receives sensory inputs directly (McDonald, 1998; Duvarci and Pare, 2014). Reciprocal excitatory connections with cortical regions, including orbitofrontal cortex and sensory association areas (McDonald, 1998), in addition to the modulatory inputs it receives from midbrain dopamine neurons (Fallon and Ciofi, 1992), makes the BLA well positioned to integrate and utilize sensory information to inform adaptive decision making.

The BLA is a hub for emotional memory (Wassum and Izquierdo, 2015). This has been well exemplified by studies investigating the contribution of this region to aversive memories. Lesioning or inactivating the BLA disrupts acquisition and expression of conditioned fear responses (Davis, 1992; Fanselow and LeDoux, 1999) and active avoidance of an aversive stimulus (Killcross et al., 1997; Lázaro-Muñoz et al., 2010). That BLA involvement in associative learning also extends to appetitive events has led to the proposal that the BLA functions to assign negative or positive valence to emotionally salient stimuli (Janak and Tye, 2015; Pignatelli and Beyeler, 2019). But the BLA does more than process whether an event is “good” or “bad”. Rather, there is substantial evidence to suggest that the BLA is particularly important for memories that encode the sensory-specific details of outcomes.

Lesioning or inactivating the BLA has no impact on the acquisition of appetitive Pavlovian conditional responses or instrumental actions (Hatfield et al., 1996; Parkinson et al., 2000;

Balleine et al., 2003). However, these response strategies do not necessitate encoding the identifying features of associated outcomes. As such, they can be controlled by a model-free stimulus-response strategy that has been reinforced through past experience. In contrast, the BLA is a necessary component in the neural circuitry mediating outcome-specific reward memories. This is made clear in tasks that require these memories to promote adaptive behavioral responses and decision making. One example is sensory-specific outcome devaluation. Pre- and post-training BLA lesions or inactivation render Pavlovian conditional responses and instrumental actions insensitive to the devaluation of the associated outcome (Hatfield et al., 1996; Málková et al., 1997; Balleine et al., 2003; Pickens et al., 2003; Corbit and Balleine, 2005). This effect is pronounced in circumstances that require learning about multiple reinforcers. Johnson et al. (2009) found that post-training lesions of the BLA did not affect sensitivity to outcome devaluation when a single reinforcer was trained, but adaptation of Pavlovian and instrumental responses following outcome devaluation was impaired when multiple cue-outcome and action-outcome associations were learnt (Johnson et al., 2009). This further highlights a specific function for the BLA in outcome-specific associative learning as discriminating between distinct predictive events requires rich representation of the sensory-specific details of associated rewards (Blundell et al., 2001).

Converging evidence is provided by studies examining BLA involvement in outcome-specific Pavlovian-to-instrumental transfer. In this task, encoding and utilization of sensory-specific stimulus-outcome memories enable selective and adaptive pursuit of rewards. Glutamatergic activity in the BLA tracks this adaptive cue-directed decision making (Malvaez et al., 2015). Transient frequency is correlated with performance of an action that is known to earn the same outcome predicted by the CS, but not with actions that had previously earnt an alternative outcome. Post-training inactivation of either AMPA or NMDA glutamate receptors in the BLA demonstrates this activity is needed for the selective motivational influence of the cue over selective reward seeking (Malvaez et al., 2015). This is consistent with disrupted PIT

performance following lesions of the BLA (Blundell et al., 2001; Corbit and Balleine, 2005; Ostlund and Balleine, 2008; Morse et al., 2020). Critically, the BLA only mediates transfer effects that require sensory-specific stimulus-outcome representations to selectively motivate actions. Lesioning the BLA has no impact on the expression of general PIT (Corbit and Balleine, 2005), which assesses the general excitatory influence of a cue conditioned to a single reward on instrumental behavior (Corbit and Balleine, 2016).

The BLA is also essential for incentive learning. The degree to which a reward can incentivize reward seeking is dependent on the current internal need state. This state-dependent value must be learned through past experience with the reward in that need state (Dickinson and Balleine, 1994). For example, by eating a donut when you are hungry, you'll learn that the donut is really satisfying in that food deprived state. You can later use this knowledge to seek out donuts when you are hungry again in the future. BLA glutamate tracks an upshift in value during incentive learning (Malvaez et al., 2015). Transiently inactivating the BLA, or more selective blockade with mu opioid or NMDA receptor antagonists also disrupts state-dependent incentive value encoding (West et al., 2012; Parkes and Balleine, 2013; Malvaez et al., 2015). A shift in value driven by a change in physiological state is specific to the particular reward experienced in that state and does not typically influence behavioral pursuit of rewarding events more broadly (Balleine and Dickinson, 1998a). Thus, BLA mediated encoding and retrieval (Malvaez et al., 2015) of a reward's incentive value provides converging evidence for a larger role of this region in sensory-specific reward memory.

lOFC Function in reward learning

A large body of evidence implicates the lateral division of the orbitofrontal cortex (lOFC) in model-based decision making. lOFC activity encodes the sensory features of rewarding events (Schoenbaum et al., 2003; McDannald et al., 2014; Stalnaker et al., 2014; Lopatina et al.; Howard and Kahnt, 2017; Howard and Kahnt, 2018, 2021) and is needed in tasks where accurate representation of future rewards enables adaptive reward-seeking. Like the BLA, the lOFC is not

typically needed for the acquisition of a Pavlovian conditional approach response, but lOFC lesions render this behavior insensitive to devaluation of the associated outcome (Gallagher et al., 1999; Pickens et al., 2003; Izquierdo et al., 2004; Pickens et al., 2005; Ostlund and Balleine, 2007b). The lOFC is also needed to use cue-reward associations to guide selective choice in outcome-specific PIT (Ostlund and Balleine, 2007b; Scarlet et al., 2012). These deficits in cue-guided behaviors following lOFC lesions are selectively driven by an inability to encode or use detailed stimulus-outcome associations. Ostlund and Balleine (2007) found that neither pre- nor post-training lOFC lesions affected instrumental choice following outcome devaluation (Ostlund and Balleine, 2007b). Collectively these data indicate the lOFC is critical for using cues to make predictions about specific future rewarding events and generating inferences based on this information to guide the appropriate course of action.

Several proposals have been made regarding the precise function of the lOFC in model-based decision making. A popular perspective is that the lOFC enables adaptive behavior through the generation of outcome expectancies – signals that convey expectations about the features and value of rewards given the circumstance or cues in the environment (Schoenbaum and Roesch, 2005; Schoenbaum et al., 2016; Howard and Kahnt, 2021). Supporting evidence is provided by experiments demonstrating that lOFC activity not only encodes the delivery of rewarding events but also encodes anticipation of their receipt (Schoenbaum et al., 1998; Tremblay and Schultz, 2000; Schoenbaum et al., 2003; Feierstein et al., 2006; Stalnaker et al., 2006). As mentioned earlier, lOFC activity encodes the identity of anticipated outcomes, not just their value (Howard and Kahnt, 2021). The ability to generate these reward identity predictions is particularly crucial for flexible decision making in novel scenarios or in situations where rewards are not readily observable. In such cases, these outcome expectancies allow inferences to be made regarding the behaviors that would be most optimal given the circumstance. A role for the lOFC in generating outcome expectancies that enable inferential decision making has been demonstrated empirically

(Jones et al., 2012; Takahashi et al., 2013; Wang et al., 2020) and is consistent with its involvement in outcome-specific devaluation and PIT.

Building upon this is the proposal that the lOFC keeps track of a subject's position in a cognitive map of the task (Wilson et al., 2014b; Wikenheiser and Schoenbaum, 2016; Niv, 2019; Sharpe et al., 2019). This map connects task states, which represent a given situation or position within the task. A state can be either be fully or partially observable depending on the perceptual information available to the animal. It is hypothesized that the lOFC is critical for representing and separating partially observable states that signal internal information or are perceptually ambiguous (Wilson et al., 2014b). This does well to explain the effects of lOFC lesions on devaluation and PIT, as each of these tests pose novel scenarios in which subjects must mentally simulate the consequences of their actions within a cognitive model of the task. Proponents of this cognitive map hypothesis suggest that the lOFC is needed to represent these imagined states. Evidence for task state representation is also found at the neural level (Schuck et al., 2016; Riceberg and Shapiro, 2017; Zhou et al., 2019b; Zhou et al., 2019a). For example, Schoenbaum et al. observed that in an odor discrimination task, separate populations of neurons in the lOFC respond to rewarded vs non-rewarded cues. After a reversal, neurons that were originally non-selective to the cues now encoded the new cue-outcome associations (Schoenbaum et al., 1999, 2000), suggesting that the contingencies relevant to different task states are represented by distinct neuronal ensembles (Sharpe et al., 2019). In humans, OFC activity is a reliable predictor of hidden task states that are determined from memory of past events (Schuck et al., 2016).

In a recent configuration of the state space framework, the lOFC is proposed to be a "cartographer" of the cognitive map (Gardner and Schoenbaum, 2021). From this standpoint, the lOFC is not required to support the use of cognitive maps through signaling the current state but is needed for their formulation. This is an intriguing perspective that is concordant with findings that lOFC is needed for encoding stimulus-stimulus associations (Sadacca et al., 2018; Hart et al., 2020), incentive value (Malvaez et al., 2019) and stimulus-outcome contingency (Ostlund and

Balleine, 2007b), and for learning novel outcome estimates (Takahashi et al., 2013). A tenet of this hypothesis is that the cognitive map is not necessarily contained in the lOFC but could be created through lOFC mediated orchestration of map components represented in downstream regions (Gardner and Schoenbaum, 2021).

lOFC-BLA circuitry in stimulus-outcome learning

As discussed in previous sections, both the BLA and lOFC are critical components of the neural circuitry mediating sensory-specific stimulus-outcome memories. Lesions to either region produce similar disruptions in tasks that require use of these memories to inform adaptive decision making. Moreover, many reward-related behaviors depend on crosstalk between the lOFC and BLA. Disconnecting these regions impairs sensitivity to reinforcer devaluation (Baxter et al., 2000), cost-benefit decision making (Zeeb and Winstanley, 2013), and context-induced reinstatement of drug seeking (Lasseter et al., 2011). Furthermore, *in vivo* electrophysiology has revealed that associative encoding in one region is dependent on inputs from the other. Lesioning the BLA diminishes the acquisition of cue-selectivity in lOFC neurons across learning and abolishes contingency remapping in the lOFC during reversals (Schoenbaum et al., 2003). This demonstrates that the BLA facilitates stimulus-outcome encoding in the lOFC and enables new contingencies to be represented alongside those learned in the past. In contrast, generating or updating outcome expectancies in the BLA is dependent on inputs from the lOFC (Saddoris et al., 2005; Lucantonio et al., 2015).

Pathway specific manipulations have revealed distinct roles for lOFC→BLA and BLA→lOFC projections in the encoding and retrieval of appetitive memories. Inactivation of lOFC→BLA, but not BLA→lOFC, projections impairs cue-induced reinstatement of drug seeking (Arguello et al., 2017). While this could reflect disrupted retrieval of either a Pavlovian or instrumental association with the drug, it could also reflect a deficit in learning the new association between lever pressing and the delivery of the cue. An account favoring the latter would be consistent with findings that activation of lOFC→BLA projections are needed to encode

the need-state dependent incentive value of a reward, but are not needed for its retrieval to motivate reward seeking (Malvaez et al., 2019). Inactivation of lOFC→BLA projections also has no effect on the retrieval of distinct stimulus-outcome associations (Lichtenberg et al., 2017). In contrast, inactivation of BLA→lOFC projections impairs the ability to use cues within the environment to selectively motivate instrumental action during outcome-specific PIT or infer the value of an associated reward following outcome-specific devaluation (Lichtenberg et al., 2017). Collectively, these findings suggest the lOFC is needed to link the current state (internal or explicit) to outcomes that are available, whereas BLA→lOFC projections are needed later to access memories of those specific outcomes when they are not readily observable to guide adaptive choice.

VTA dopamine in associative learning: model-free vs model-based

A long and rich history implicates the activation of midbrain dopamine neurons in mediating associative learning. While recording single unit activity in primates, Schultz et al. discovered that dopamine neurons signal a prediction error – a phasic response encoding the discrepancy between what is expected and what occurs. Unexpected rewards coincide with a spike in dopamine neuron activity, which transitions to a preceding cue as learning progresses (Ljungberg et al., 1992; Schultz et al., 1993). It was later proposed that this dopamine reward prediction error (RPE) serves as the teaching signal used in temporal-difference reinforcement learning algorithms to cache a reward's value to an antecedent stimulus (Sutton, 1988; Schultz et al., 1997; Schultz, 1998, 2016). Broadcasting RPE signals to the striatum could in turn reinforce responses coincident with the RPE through potentiation of neuronal synapses activated when the response occurred (Schultz et al., 1997; Schultz, 1998; Di Ciano et al., 2001; Reynolds et al., 2001; Glimcher, 2011; Schultz, 2016). Within this framework, dopamine's involvement in associative learning can be explained through model-free mechanisms, whereby cues imbued with cached value can evoke response policies that have led to past success without detailed representation of future rewards.

Dopamine RPEs have been observed using several methods of activity monitoring (Waelti et al., 2001; D'Ardenne et al., 2008; Lutas et al., 2019) and across several species including monkeys, rodents and humans (O'Doherty et al., 2003; Bayer and Glimcher, 2005; Pan et al., 2005). Studies of dopaminergic activity within the context of Pavlovian blocking have provided both correlative and causal evidence linking the RPE signal to associative learning. In this paradigm, acquisition of a cue-reward association (Y→US) is impaired (or blocked) if another cue (X), present in the environment at the same time, already signals reward delivery (X→US) (Kamin, 1968). Dopaminergic firing rates track the fidelity of cue-evoked reward expectation during this task, increasing upon outcome delivery when the outcome is newly predicted but not when it has already come to be expected through prior association with one of the elements in the compound stimulus. Consistent with RPE theory, "blocked" cues fail to elicit a strong dopaminergic response when presented alone and are likewise insufficient to promote a conditioned response (Waelti et al., 2001). In 2013 Steinberg et al. demonstrated that optically activating dopamine neurons upon reward delivery following the compound stimulus unblocked acquisition of otherwise occluded Pavlovian associations (Steinberg et al., 2013). Subsequently Chang et al. (2016) found that optically inhibiting dopamine neurons to emulate a negative RPE (i.e., when a reward is less than expected) was sufficient to promote Pavlovian extinction learning (Chang et al., 2016).

Results from these studies have provided compelling evidence for dopamine prediction error as a mediator of reinforcement learning. But the type of information encoded by the dopamine signal and the forms of learning that it facilitates is a topic of discussion. An emerging viewpoint suggests dopamine prediction errors enable learning an associative model of related events, not just the value of reward predictive cues (Daw et al., 2005; Nasser et al., 2017; Langdon et al., 2018; Akam and Walton, 2021; Seitz et al., 2021). Several key experimental findings favor this model-based account over a model-free framework. The first is that dopamine neurons

generate sensory prediction errors that reflect unexpected changes in the identity of a predicted outcome (Takahashi et al., 2017; Stalnaker et al., 2019) and are both necessary and sufficient for unblocking Pavlovian associations (Chang et al., 2017; Keiflin et al., 2019). Such PEs are also generated in the human midbrain (Iglesias et al., 2013; Suarez et al., 2019) and are conveyed to cortical regions to update reward identity expectations (Howard and Kahnt, 2018). Outcome identity encoding cannot be explained by a model-free value computation but is an important component of model-based associations that enable flexible decision making.

Second, dopamine PEs can be computed from inference, not just through direct experience (Bromberg-Martin et al., 2010; Sadacca et al., 2016). In a sensory preconditioning task, Sadacca et al. (2016) found that a cue (A) elicited a dopaminergic response and food-cup approach when that cue was initially associated with a second neutral stimulus (A→B) that was later conditioned to predict reward (B→US) (Sadacca et al., 2016). Cue A was never directly paired with reward nor was it ever directly associated with a reward predicting stimulus, since only later was the B→US relationship established. Thus, the cue-evoked dopamine signal did not reflect cached value learned through direct experience, but rather a model-based calculation in which value was inferred from an associative structure representing causal relationships between task events.

A model-based view of dopamine function is further supported by a third finding: dopamine PEs drive neutral stimulus-stimulus learning. Combining sensory preconditioning with Pavlovian blocking, Sharpe et al. (2017) demonstrated that optically activating dopamine neurons unblocked learning the associative relationship between neutral stimuli B and X when B was presented in compound with a neutral stimulus (A) that already predicted X. Rats that had received dopaminergic stimulation at the transition between AB→X demonstrated more appetitive food-cup approach in response to B than control animals, after X had been paired with reward (Sharpe et al., 2017). By signaling a prediction error (Maes et al., 2020), this activation

generated a teaching signal that was sufficient to promote learning the causal link between valueless stimuli and did not in itself cache value independent of reward (Sharpe et al., 2020).

Model-based and model-free strategies co-exist and the ability to alternate between them, depending on the circumstance, promotes adaptive behavior (Daw et al., 2005; Balleine et al., 2009; Keramati et al., 2011; Dolan and Dayan, 2013; Drummond and Niv, 2020). Take, for example, the task of getting home from work. Often it is advantageous to use a model-free strategy in which a set route is selected based on previous experience indicating that route is an efficient way to get to the desired destination. This can save cognitive effort, but it can come at the cost of being inflexible and may be disadvantageous when circumstances change. If, for instance, you know there is major construction happening along your usual path, using a model-based strategy to mentally simulate alternative routes would clearly be the better option. It appears that in the brain, model-based and model-free processes operate in parallel through distinct neural circuits (Daw et al., 2005; Balleine et al., 2009; Balleine and O'Doherty, 2009; Gläscher et al., 2010; Dolan and Dayan, 2013; Dayan and Berridge, 2014; Lucantonio et al., 2014). A reconciliation of how dopamine contributes to each of these processes may thus require a closer examination of different dopamine pathways. While the dopaminergic circuits involved in model-free learning and decision-making strategies have been extensively investigated (Berns et al., 2001; Di Ciano et al., 2001; O'Doherty et al., 2003; Day et al., 2007; Lex and Hauber, 2008; Hart et al., 2014; Tian et al., 2016; Menegas et al., 2017; Aggarwal et al., 2020), much less is known about the projections that contribute to model-based learning.

VTA dopamine projections to the BLA and emotional learning

Dopaminergic neurons in the VTA project to the BLA, which expresses both D1 and D2 type dopamine receptors (Fallon and Ciofi, 1992; Maltais et al., 2000; Breton et al., 2019). Local circuit activity, neurotransmission and synaptic plasticity in the BLA is shaped by modulatory effects of dopamine acting on these receptor subtypes (Lee et al., 2017). The neuromodulatory effects of

dopamine are critical for enhanced neuronal plasticity observed in the BLA as a result of appetitive and aversive conditioning (Grace and Rosenkranz, 2002; Lutas et al., 2022). As such, dopaminergic modulation of BLA plasticity has been proposed to be a key contributor to affective learning and likely underlies the causal link between dopamine and associative memory established by pharmacological manipulations. Experiments that directly infuse dopamine receptor antagonists into the BLA implicate both D1, and to a lesser extent, D2 receptor activation in the acquisition of conditioned fear (Nader and LeDoux, 1999; Greba and Kokkinidis, 2000; Greba et al., 2001; Takahashi et al., 2010; Heath et al., 2015). While the expression of conditioned fear is also diminished by D2 antagonists locally infused in the BLA (de Oliveira et al., 2011; de Souza Caetano et al., 2013), studies showing similar effects from D1 antagonists are difficult to interpret as they also target the central amygdala (Lamont and Kokkinidis, 1998; Guarraci et al., 1999a; Guarraci et al., 1999b). Dopamine release, measured by microdialysis, is elevated in the BLA as a result of aversive conditioning, with further enhancement from pretreatment with methamphetamine (Suzuki et al., 2002). Bulk calcium imaging, which offers better temporal resolution, reveals heightened activation of VTA_{DA}→BLA projections shifts from an unconditioned aversive stimulus to an antecedent cue as training progresses (Lutas et al., 2019). Critically, optically inhibiting these projections at the time of foot shock during fear conditioning sessions reveals activity upon experience of the aversive US is necessary for the acquisition of cued and contextual fear memories (Tang et al., 2020).

Though more extensively studied within the context of aversive memory, dopaminergic inputs to the BLA also support appetitive learning. Dopaminergic tone at D1 and D2 receptors in this region mediates fear extinction learning (Hikind and Maroun, 2008; Shi et al., 2017; Salinas-Hernández and Duvarci, 2021), which is thought to engage appetitive motivational process (Konorski, 1967; Solomon and Corbit, 1974) and recruits reward circuitry (Kim et al., 2006; Felsenberg et al., 2018; Zhang et al., 2020). Modulation of risky decision making also directly

links dopamine to reward processing. One study found that blockade of BLA D1 receptors resulted in less risky choice following a large reward. D1 agonists bidirectionally modulated risky choice depending on whether reward probabilities were high or low to produce optimal decision making. In contrast, stimulating D2 receptors increased sensitivity to negative feedback in risk prone animals (Larkin et al., 2016). These findings suggest that dopaminergic action in the BLA, perhaps primarily at D1 receptors, facilitates positive encoding of rewarding events to enable adaptive pursuit of those rewards in the future.

Dopaminergic inputs to the BLA promote associative reward learning. Encoding cue-reward associations and filtering out task-irrelevant behaviors is dependent on the engagement of D1 and D2 receptors, respectively (Tye et al., 2010; Touzani et al., 2013). Dopamine release in the BLA is elevated during appetitive Pavlovian conditioning (Harmer and Phillips, 1999) and a shift of $VTA_{DA} \rightarrow$BLA activation from the delivery of a reward to a predictive cue parallels the development of conditioned appetitive responses (Lutas et al., 2019). This temporal shift is consistent with a PE signal that can drive model-free or model-based learning. Attentional models of reinforcement learning suggest unsigned prediction errors, derived from the absolute value of signed PEs, determine the associability of a cue. That is, attention is allocated towards cues that result in larger errors to facilitate encoding the relationship with associated outcomes (Pearce and Hall, 1980). Signaling of unexpected events in BLA neurons conforms closely to predictions made by this model (Roesch et al., 2012) and is dependent on prediction errors conveyed from VTA dopamine neurons (Esber et al., 2012). Despite these findings, whether and how dopaminergic projections modulate BLA activity to facilitate outcome-specific, model-based appetitive memories is still an open question.

Chapter 2: A bidirectional corticoamygdala circuit for the encoding and retrieval of detailed reward memories

ABSTRACT

Adaptive reward-related decision making often requires accurate and detailed representation of potential available rewards. Environmental reward-predictive stimuli can facilitate these representations, allowing one to infer which specific rewards might be available and choose accordingly. This process relies on encoded relationships between the cues and the sensory-specific details of the reward they predict. Here we interrogated the function of the basolateral amygdala (BLA) and its interaction with the lateral orbitofrontal cortex (lOFC) in the ability to learn such stimulus-outcome associations and use these memories to guide decision making. Using optical recording and inhibition approaches, Pavlovian cue-reward conditioning, and the outcome-selective Pavlovian-to-instrumental transfer (PIT) test in male rats, we found that the BLA is robustly activated at the time of stimulus-outcome learning and that this activity is necessary for sensory-specific stimulus-outcome memories to be encoded, so they can subsequently influence reward choices. Direct input from the lOFC was found to support the BLA in this function. Based on prior work, activity in BLA projections back to the lOFC was known to support the use of stimulus-outcome memories to influence decision making. By multiplexing optogenetic and chemogenetic inhibition we performed a serial circuit disconnection and found that the lOFC→BLA and BLA→lOFC pathways form a functional circuit regulating the encoding (lOFC→BLA) and subsequent use (BLA→lOFC) of the stimulus-dependent, sensory-specific reward memories that are critical for adaptive, appetitive decision making.

INTRODUCTION

To make good decisions we must accurately anticipate the potential outcomes (e.g., rewarding events) that might be available in our current situation, or state. When these outcomes are not readily observable, we can infer their availability from predictive environmental stimuli (e.g., restaurant logos on a food-delivery app). Pavlovian *stimulus-outcome associative memories* enable such cues to trigger representations of their associated outcomes, thus facilitating the state-dependent outcome expectations that influence decision making (Balleine and Dickinson, 1998b; Delamater, 2012; Fanselow and Wassum, 2015). Often our decisions require detailed information about the available outcomes (e.g., flavor, nutritional content, texture). For example, when deciding between items of similar valence (e.g., to have pizza or sushi for dinner). To enable such decisions, stimulus-outcome memories can be quite rich, including the sensory-specific, identifying details of the predicted reward (Delamater and Oakeshott, 2007; Fanselow and Wassum, 2015). Failure to properly encode or use such memories can lead to poor reward-related choices, a hallmark feature of myriad psychiatric diseases. Yet much is unknown of the neural circuits that support stimulus-outcome memory.

One potential hub for stimulus-outcome memory is the basolateral amygdala (BLA) (Wassum and Izquierdo, 2015). Long known for its function in emotional learning, the BLA is thought to link predictive stimuli with valence and to relay that valence for adaptive behavior (e.g., approach/avoidance) (Baxter and Murray, 2002; Janak and Tye, 2015; Tye, 2018; Pignatelli and Beyeler, 2019). But the BLA does more than valence. Mounting evidence, primarily collected with lesion and inactivation strategies, suggests the BLA mediates appetitive behaviors that require a rich sensory-specific representation of the expected reward. For example, the BLA is needed for reward-predictive cues to bias choice between two distinct rewards (Hatfield et al., 1996; Blundell et al., 2001; Corbit and Balleine, 2005; Ostlund and Balleine, 2008). Although the BLA's function in the *expression* of such behaviors has been established, temporal limitations of BLA lesions preclude interpretations of BLA function in stimulus-outcome *learning*. The BLA is known to be

essential for the learning of cued fear (Muller et al., 1997; Sengupta et al., 2018), but behavioral limitations of these studies preclude understanding of whether the BLA is involved in encoding the sensory-specific details of the outcome. Thus, it remains unknown whether the BLA is involved in encoding the sensory-specific stimulus-outcome memories that enable adaptive choices, or if the BLA primarily functions to assign general valence to a cue. Moreover, little is known of the endogenous activity or circuit function underlying any potential role for the BLA in the formation of appetitive stimulus-outcome memories.

To address these gaps in knowledge, here we used optical recording and inhibition approaches in male rats to examine the BLA's function in the encoding of stimulus-outcome memories for two unique food rewards. To assess the extent of stimulus-outcome memory encoding, we used the outcome-selective Pavlovian-to-instrumental transfer (PIT) test to measure the ability of a reward-paired stimulus to trigger a sensory-specific representation of its predicted reward and thus bias reward-seeking choice (Kruse et al., 1983; Colwill and Motzkin, 1994; Gilroy et al., 2014; Corbit and Balleine, 2016).

RESULTS

BLA neurons respond to rewards and cues during appetitive Pavlovian stimulus-outcome learning.

We first asked whether and when the BLA is active during the encoding of stimulus-outcome memories (Figure 2-1a). To condition cues that set the 'state' for a specific reward's availability and engender a sensory-specific representation of that reward, we used a dual food outcome Pavlovian conditioning task. Each of two, 2-min auditory conditional stimuli (CSs; white noise and tone) were associated with intermittent delivery of 1 of 2 distinct food rewards (sucrose solution or food pellets; e.g., white noise-sucrose/tone-pellet). This conditioning has been shown to engender the encoding of detailed, sensory-specific stimulus-outcome memories as measured by the cue's ability to subsequently promote instrumental choice for the specific predicted reward during a PIT test (Ostlund and Balleine, 2008; Malvaez et al., 2015; Lichtenberg and Wassum,

2016; Lichtenberg et al., 2017), as well as the sensitivity of the conditional food-port approach response to sensory-specific devaluation of the predicted reward (Lichtenberg et al., 2017) or degradation of the stimulus-outcome contingency (Ostlund and Balleine, 2008). Food-deprived, male rats (N = 11) received 8 Pavlovian conditioning sessions. During each session each cue was presented 4 times (variable intertrial interval, average = 3 min) for 2 min, during which its associated reward was intermittently delivered on average every 30 s. Rats demonstrated simple Pavlovian conditioning by gradually increasing their goal approach responses (entries into the food-delivery port) during the cue probe periods (after cue onset, before reward delivery) across training (Figure 2-1h; Training: $F_{(2.4,24.3)} = 13.18$, $P < 0.0001$; see also Figure 2-6).

To characterize the endogenous activity of BLA neurons during the encoding of appetitive stimulus-outcome memories, we used fiber photometry to image the fluorescent activity of the genetically encoded calcium indicator GCaMP6f (Chen et al., 2013) each day during Pavlovian conditioning (Figure 2-1b-d). GCaMP6f was expressed preferentially in principal neurons based on expression of calcium/calmodulin-dependent protein kinase, CaMKII (Butler et al., 2011; Tye et al., 2011). Data from the 8 training sessions were binned into 5 conditioning phases, session 1, session 2, sessions 3/4, 5/6, and 7/8. Thus, data from the last six sessions were averaged across 2-session bins. As can be seen in the representative examples (Figure 2-1e; see also Figure 2-7), or group-averaged traces (Figure 2-1f-g), BLA neurons were robustly activated by both cue onset and reward retrieval (first food-port entry after reward delivery) throughout Pavlovian conditioning. Across training, both the cues and rewards caused a similar elevation in the peak calcium response (Figure 2-1i; Event v. baseline: $F_{(0.4,3.9)} = 36.02$, $P = 0.007$; Training: $F_{(2.8,28.1)} = 4.29$, $P = 0.01$; Event type (CS/US) and interactions between factors, lowest $P = 0.18$) and area under the calcium curve (AUC; Figure 2-1j; Event v. baseline: $F_{(0.3,3.4)} = 35.23$, $P = 0.01$, Training, Event type, and interactions between factors, lowest $P = 0.23$; see also Figure 2-8). Analysis of each event relative to its immediately preceding baseline period confirmed that BLA neurons were robustly activated by CS onset as reflected in the peak calcium response (CS: $F_{(1,10)} = 7.25$, $P =$

0.02; Training: $F_{(2.5, 24.5)} = 1.88$, $P = 0.17$; CS x Training: $F_{(1.2, 12.4)} = 0.54$, $P = 0.51$) and AUC (CS: $F_{(1,10)} = 6.28$, $P = 0.03$; Training: $F_{(1.9,19.3)} = 0.40$, $P = 0.67$; CS x Training: $F_{(1.2,11.7)} = 0.17$, $P = 0.73$), as well as at reward retrieval during the cue [(Peak, Reward: $F_{(1,10)} = 16.82$, $P = 0.002$; Training: $F_{(1.9,19.4)} = 3.41$, $P = 0.06$; Reward x Training: $F_{(1.7,16.8)} = 0.88$, $P = 0.42$) (AUC, Reward: $F_{(1,10)} = 15.21$, $P = 0.003$; Training: $F_{(1.6,15.7)} = 2.13$, $P = 0.16$; Reward x Training: $F_{(1.5,14.8)} = 1.25$, $P = 0.30$)]. The same BLA reward response could also be detected when the data were aligned to reward delivery (Figure 2-9). There were no significant BLA activity changes detected in response to food-port entries absent reward (Figure 2-10), indicating that reward retrieval responses resulted from reward experience rather than the act of entering the food port. Thus, BLA neurons are active at the most critical time for the encoding of stimulus-outcome memories, when the reward is experienced during the cue (i.e., the stimulus-outcome pairing).

It was surprising that responses to the cues were present on the first conditioning session, particularly in light of evidence that BLA responses to both appetitive and aversive cues increase across learning (Tye et al., 2008; Johansen et al., 2010; Lutas et al., 2019; Crouse et al., 2020). This could reflect a non-associative, novelty response to either or both the tone or white noise presentation. To examine this and, thus, evaluate whether the BLA cue responses later in training were due to stimulus-outcome learning, we repeated the experiment in a separate group of naïve rats, but this time omitted the reward delivery during the Pavlovian conditioning (Figure 2-2a-c; $N = 6$). Instead, the rewards were delivered unpaired with the cues several hours after each session in a distinct context. Like presentation of the reward-predictive cues, presentation of either the tone or white noise stimulus unpaired with reward ($CS_{Ø}$) robustly activated BLA neurons during the first session, but, in contrast to the reward-predictive cues, this effect habituated over sessions (Figure 2-2d). Both tone and noise elicited a similar elevation in the peak calcium response that was largest on session 1 and diminished with subsequent days of exposure (Figure 2-2e; Session x $CS_{Ø}$: $F_{(4,20)} = 3.25$, $P = 0.03$; $CS_{Ø}$ presence: $F_{(0.4,2.1)} = 4.84$, $P = 0.13$; $CS_{Ø}$ type (white noise v. tone): $F_{(0.3,1.5)} = 7.03$, $P = 0.12$; Session: $F_{(2.3,11.7)} = 3.27$, $P = 0.07$; Session x $CS_{Ø}$ type: $F_{(4,20)} =$

1.42, P = 0.26; $CS_{Ø}$ x $CS_{Ø}$ type: $F_{(0.5,2.3)}$ = 9.69, P = 0.07; Session x $CS_{Ø}$ x $CS_{Ø}$ type: $F_{(0.6,3.2)}$ = 0.80, P = 0.37). The effect was similar when quantified using area under the calcium curve (Figure 2-2f; Session x $CS_{Ø}$: $F_{(4,20)}$ = 2.65, P = 0.06; $CS_{Ø}$ presence: $F_{(0.5,2.4)}$ = 5.07, P = 0.12; $CS_{Ø}$ type: $F_{(0.3,1.4)}$ = 4.81, P = 0.14; Session: $F_{(2.6,12.8)}$ = 1.55, P = 0.25; Session x $CS_{Ø}$ type: $F_{(4,20)}$ = 1.14, P = 0.37; $CS_{Ø}$ x $CS_{Ø}$ type: $F_{(0.5,2.4)}$ = 10.43, P = 0.06; Session x $CS_{Ø}$ x $CS_{Ø}$ type: $F_{(0.7,3.7)}$ = 1.81, P = 0.24). To check whether the decline of the $CS_{Ø}$ response was due simply to signal degradation over time, following the last $CS_{Ø}$ session we recorded BLA calcium responses to unpredicted reward delivery. Rewards were capable of robustly activating the BLA (Figure 2-2g-i; Peak, t_5 = 2.93, P = 0.03; AUC, t_5 = 4.07, P = 0.01). This positive control indicates that the decline of the BLA $CS_{Ø}$ response was due to stimulus habituation, not signal degradation. Thus, the BLA response to cue presentation during early Pavlovian conditioning likely reflects a non-associative novelty effect that habituates with subsequent exposure, indicating that the BLA responses to the reward-predictive cues later in training (Figure 2-1) largely result from the association with reward.

BLA neuron activity is necessary during outcome experience to encode appetitive Pavlovian stimulus-outcome memories.

We found that BLA neurons are robustly activated at the time at which stimulus-reward memories can be formed: when the reward is experienced during a predictive cue. We next asked whether this activity is necessary for such learning and, if so, whether it is necessary for encoding sensory-specific stimulus-outcome memories (Figure 2-3a). We expressed the inhibitory opsin archaerhodopsin T (ArchT; N = 9) or eYFP control (N = 10) in BLA, primarily, principal neurons (Figure 2-3b-d) to allow green light (532nm, ~10mW) to transiently hyperpolarize and inhibit the activity of these cells (Figure 2-11). Rats were again given 8 Pavlovian conditioning sessions during which each of 2 distinct, 2-min auditory CSs was paired with intermittent delivery of one specific food reward (8 of each CS/session). During each Pavlovian conditioning session, we optically inhibited the activity of BLA neurons during each cue. We restricted inhibition to 5 s concurrent with the delivery and retrieval of each food reward because this is the time at which

the stimulus-outcome pairing occurs and when we found the BLA to be endogenously active (Figure 2-1). Optical inhibition of BLA neurons at reward experience during Pavlovian conditioning did not impede the development of the Pavlovian conditional goal-approach response to the cue sampled prior to reward delivery (Figure 2-3e; Training: $F_{(3.8,64.9)} = 17.53$, $P < 0.0001$; Virus (eYFP v. ArchT): $F_{(1,17)} = 0.19$, $P = 0.67$; Virus x Training: $F_{(7,119)} = 1.28$, $P = 0.26$; see also Figure 2-12a). This general conditional response at the shared food port, however, does not require that the subjects have learned the sensory-specific details of the predicted reward. To test for such stimulus-outcome memory encoding, we gave subjects instrumental conditioning followed by a PIT test. Both were conducted without any manipulation. During instrumental conditioning, rats were trained that two different actions (left or right lever press) each earned one of the unique food rewards (e.g., left press→sucrose/right press→pellets; Figure 2-12b). At the PIT test both levers were present, but lever pressing was not rewarded. Each CS was presented 4 times (also without accompanying reward), with intervening CS-free baseline periods, to assess its influence on action performance and selection in the novel choice scenario. Because the cues are never associated with the instrumental actions, this test assesses the ability to, upon cue presentation, retrieve a memory of the specific predicted reward and use it to motivate choice of the action known to earn the same unique reward (Kruse et al., 1983; Colwill and Motzkin, 1994; Gilroy et al., 2014; Corbit and Balleine, 2016). If subjects had encoded detailed stimulus-outcome memories during Pavlovian conditioning, then the CS should cause them to increase presses selectively on the lever that, during training, earned the *same* outcome as predicted by that cue. Controls showed this outcome-specific PIT effect (Figure 2-3f). Conversely, the cues were not capable of influencing lever-press choice in the group for which the BLA was inhibited at the time of outcome experience during Pavlovian conditioning (Figure 2-3f; Virus x Lever: $F_{(1,17)} = 5.10$, $P = 0.04$; Virus: $F_{(1,17)} = 1.41$, $P = 0.25$; Lever (Same v. Different): $F_{(1,17)} = 3.84$, $P = 0.07$; see also Figure 2-12c). As in training, during this PIT test the conditional goal-approach response was similar between groups (Figure 2-3g; $t_{17} = 0.94$, $P = 0.36$; see also Figure 2-12d). Thus, BLA

neuronal activity is not needed for the learning that supports general conditional approach responses, but is necessary, specifically at the time of outcome experience, to link the sensory-specific details of the outcome to a predictive cue. Such encoding is critical for that cue to subsequently guide decision making.

An alternative possibility is that the total amount of inhibition compromised BLA activity more broadly. That is, that BLA activity *per se* rather than specifically at the time of stimulus-outcome pairing mediates the encoding of stimulus-outcome memories. To rule this out, we repeated the experiment in a new cohort of naïve rats in which we matched the frequency and duration of inhibition to the experimental group, but delivered it during baseline pre-CS periods during Pavlovian conditioning. This inhibition had no effect on the subsequent influence of the cues on instrumental choice behavior during the PIT test (Figure 2-13), confirming that BLA activity specifically at the time of stimulus-outcome pairing mediates the encoding of detailed stimulus-outcome memories.

lOFC→ BLA projections are necessary for encoding Pavlovian stimulus-outcome memories.

We found that activity in BLA neurons at the time of reward delivery/experience mediates encoding of the relationship between that specific rewarding event and the environmental stimulus that predicts it. We next asked which BLA input might facilitate this function. The orbitofrontal cortex (OFC) is a prime candidate. The OFC sends dense glutamatergic innervation to the BLA (Aggleton et al., 1980; Carmichael and Price, 1995; Price, 2007; Heilbronner et al., 2016; Lichtenberg et al., 2017; Malvaez et al., 2019) and is itself implicated in appetitive learning (Murray and Izquierdo, 2007; Ostlund and Balleine, 2007a; Baltz et al., 2018; Rudebeck and Rich, 2018). BLA inputs from the lateral (lOFC), rather than medial OFC subregion, have previously been shown to be involved in learning information about a reward (i.e., its incentive value) (Malvaez et al., 2019), but are not required for retrieving appetitive memories (Lichtenberg et al., 2017; Malvaez et al., 2019). Thus, this pathway might play a critical role specifically in *forming*

stimulus-outcome associative memories. To evaluate this, we used pathway-specific optical inhibition to ask whether activity in lOFC→BLA projections mediates the encoding of stimulus-outcome memories (Figure 2-4a). We expressed ArchT (N = 8) or eYFP control (N = 8) in lOFC neurons and detected expression in lOFC axons and terminals in the BLA in the vicinity of implanted optical fibers (Figure 2-4b-d). Green light (532nm, ~10mW) was used to inhibit lOFC axons and terminals in the BLA (Figure 2-14). Subjects received Pavlovian conditioning, as above, and inhibition was again restricted to 5 s during the delivery and retrieval of each reward during each cue. Similar to inhibition of BLA neurons, optical inhibition of lOFC→BLA projection activity during stimulus-outcome pairing did not affect the development of the Pavlovian conditional goal-approach response (Figure 2-4e; Training: $F_{(3.9,54.3)}$ = 7.84, P < 0.0001; Virus: $F_{(1,14)}$ = 0.22, P = 0.65; Virus x Training: $F_{(7,98)}$ = 0.43, P = 0.88; see also Figure 2-15a) or its expression during the PIT test (Figure 2-4g; t_{14} = 0.49, P = 0.63; see also Figure 2-15). It did, however, attenuate encoding of sensory-specific stimulus-outcome memories as evidenced by the subjects' inability to later use those memories to allow cue presentation to bias choice behavior during the PIT test (Figure 2-4f; Virus x Lever: $F_{(1,14)}$ = 6.49, P = 0.02; Virus: $F_{(1,14)}$ = 0.04, P = 0.85; Lever: $F_{(1,14)}$ = 7.10, P = 0.02; see also Figure 2-15c). Thus, activity in lOFC→BLA projections regulates the encoding of detailed, sensory-specific stimulus-outcome memories. Together, with prior evidence that inactivation of lOFC→BLA projections does not disrupt the *expression* of outcome-selective PIT (Lichtenberg et al., 2017), these data suggest that activity in lOFC→BLA projections mediates the encoding, but not retrieval of stimulus-outcome memories.

lOFC→ BLA→lOFC is a stimulus-outcome memory circuit.

Collectively, the data show that the BLA, with help from direct lOFC input, mediates the encoding of the detailed cue-reward memories that enable the cues to trigger the sensory-specific reward outcome representations that influence decision making. The lOFC-BLA circuit is bidirectional. The BLA sends dense excitatory projections back to the lOFC (Morecraft et al., 1992; Lichtenberg et al., 2017; Barreiros et al., 2021). Activity in these projections mediates the representation of

expected outcomes in the lOFC (Schoenbaum et al., 2003; Rudebeck et al., 2013; Rudebeck et al., 2017) and the use of stimulus-outcome memories to guide choice (Lichtenberg et al., 2017). But it remains unknown whether BLA→lOFC projection activity enables the use of the associative information that is learned via activation of lOFC→BLA projections. That is, whether lOFC→BLA→lOFC is a functional stimulus-outcome memory encoding and retrieval circuit or whether lOFC→BLA and BLA→lOFC projections tap in to independent, parallel information streams. Indeed, stimulus-outcome memories are highly complex including multifaceted information about outcome attributes (e.g., value, taste, texture, nutritional content, category, probability, timing, etc.) and related consummatory and appetitive responses (Delamater and Oakeshott, 2007). Therefore, we next asked whether the lOFC→BLA and BLA→lOFC pathways form a functional stimulus-outcome memory encoding and retrieval circuit, i.e., whether the sensory-specific associative information that requires lOFC→BLA projections to be encoded also requires activation of BLA→lOFC projections to be used to guide decision making, or whether these are independent, parallel pathways, tapping into essential but independent streams of information.

To arbitrate between these possibilities, we multiplexed optogenetic and chemogenetic inhibition to perform a serial circuit disconnection. We disconnected lOFC→BLA projection activity during stimulus-outcome learning from BLA→lOFC projection activity during the retrieval of these memories at the PIT test (Figure 2-5a). For the disconnection group (N = 10), we again expressed ArchT bilaterally in lOFC neurons (Figure 2-5b-d) to allow expression in lOFC axons and terminals in the BLA. This time, we implanted the optical fiber only unilaterally in the BLA (Figure 2-5b-d), so that green light (532nm, ~10mW), delivered again during Pavlovian conditioning for 5 s during the delivery and retrieval of each reward during each cue, would inhibit both the ipsilateral and contralateral lOFC input to the BLA of only one hemisphere. In these subjects, we also expressed the inhibitory designer receptor human M4 muscarinic receptor (hM4Di) unilaterally in the BLA of the hemisphere opposite to the optical fiber and in that same

hemisphere placed a guide cannula over the lOFC near hM4Di-expressing BLA axons and terminals (Figure 2-5b-d). This allowed us to infuse the hM4Di ligand clozapine-*n*-oxide (CNO; 1 mM in 0.25 μl) prior to the PIT test to unilaterally inhibit BLA terminals in the lOFC, which are largely ipsilateral (Lichtenberg et al., 2017), in the hemisphere opposite to that for which we had inhibited lOFC→BLA projection activity during Pavlovian conditioning. Thus, we optically inhibited the lOFC→BLA stimulus-outcome learning pathway in one hemisphere at each stimulus-outcome pairing during Pavlovian conditioning, and chemogenetically inhibited the putative BLA→lOFC retrieval pathway in the opposite hemisphere during the PIT test in which stimulus-outcome memories must be used to guide choice. If BLA→lOFC projection activity mediates the retrieval of the sensory-specific associative memory that requires activation of lOFC→BLA projections to be encoded, then we will have bilaterally disconnected the circuit, attenuating encoding in one hemisphere and retrieval in the other, thereby disrupting the ability to use the stimulus-outcome memories to guide choice behavior during the PIT test. If, however, these pathways mediate parallel information streams, i.e., independent components of the stimulus-outcome memory, the expression of PIT should be intact because one of each pathway is undisrupted to mediate its individual component during each phase. The control group received identical procedures with the exception that viruses lacked ArchT and hM4Di (N = 8). To control for unilateral inhibition of each pathway without disconnecting the circuit, a second control group (N = 8) received the same procedures as the experimental contralateral ArchT/hM4Di disconnection group, except with BLA hM4Di and the lOFC guide cannula in the same hemisphere as the optical fiber used to inactivate lOFC axons and terminals in the BLA (Figure 2-16). Thus, during the PIT test for this group the BLA→lOFC pathway was chemogenetically inactivated in the same hemisphere in which the lOFC→BLA pathway had been optically inactivated during Pavlovian conditioning, leaving the entire circuit undisrupted in the other hemisphere. These control groups did not differ on any measure and so were collapsed into a single control group [(Pavlovian training, Training: $F_{(2.2,31.3)} = 12.96$, $P < 0.0001$; Control group type: $F_{(1,14)} = 0.02$, $P =$

0.89; Group x Training: $F_{(7.98)} = 0.76$, $P = 0.62$) (PIT Lever presses, Lever: $F_{(1,14)} = 14.68$, $P = 0.002$; Control group type: $F_{(1,14)} = 0.38$, $P = 0.55$; Group x Lever: $F_{(1,14)} = 0.43$, $P = 0.52$) (PIT Food-port entries, $t_{14} = 0.72$, $P = 0.48$)]. See also Figure 2-17 for disaggregated control data.

We found evidence that activity in lOFC→BLA projections mediates the encoding of the sensory-specific stimulus-outcome memory that is later used to allow cues to guide choice via activation of BLA→lOFC projections. As with the bilateral inhibition experiments, the control and disconnection groups both developed a Pavlovian conditional goal-approach response with training (Figure 2-5e; Training: $F_{(2.8,68.1)} = 28.13$, $P < 0.0001$; Group (Combined control group v. Contralateral ArchT/hM4Di- disconnection): $F_{(1,24)} = 0.46$, $P = 0.51$; Group x Training: $F_{(7,168)} = 0.44$, $P = 0.88$; see also Figure 2-17a), which was similarly expressed during the PIT test (Figure 2-5g; $t_{24} = 0.11$, $P = 0.91$; see also Figure 2-17d). But disconnection of lOFC→BLA projection activity during stimulus-outcome learning from BLA→lOFC projection activity during the PIT test attenuated the ability to use such memories to guide choice behavior (Figure 2-5f; Group x Lever: $F_{(1,24)} = 5.57$, $P = 0.03$; Group: $F_{(1,24)} = 0.47$, $P = 0.50$; Lever: $F_{(1,24)} = 1.39$, $P = 0.21$; see also Figure 2-17c). Whereas in the control group cue presentation significantly biased choice towards the action earning the same predicted reward, this outcome-specific PIT effect did not occur in the disconnection group. Rather, during the cues rats in the disconnection group showed a non-discriminate elevation in pressing on both levers (Figure 2-17c). Thus, disconnection of lOFC→BLA projection activity during stimulus-outcome learning from BLA→lOFC projection activity during the retrieval of this information attenuated the ability to use stimulus-outcome memories to bias choice behavior, indicating that the lOFC and BLA form a bidirectional circuit for the encoding (lOFC→BLA) and use (BLA→lOFC) of appetitive stimulus-outcome memories.

DISCUSSION

Using fiber photometry bulk calcium imaging, cell-type and pathway-specific optogenetic inhibition, multiplexed optogenetic and chemogenetic inhibition, Pavlovian conditioning, and the outcome selective PIT test, we explored the function of the BLA and its interaction with the lOFC

in the ability to learn detailed cue-reward memories and use them to guide decision making. Such memories are critical to the ability to use environmental cues to infer which specific rewards are likely to be available in the current state and, thus, to choose adaptively. We found that the BLA is robustly activated at the time of stimulus-outcome pairing and that this activity is necessary for sensory-specific, appetitive associative memories to be encoded, so that they can later influence decision making. We also found that this BLA activity is not necessary for the appetitive learning that supports general conditional goal-approach behavior, which does not require a detailed stimulus-outcome memory. lOFC input to the BLA supports its function in encoding stimulus-outcome memories and BLA projections back to the lOFC mediate the use of these memories to guide decision making. Thus, the lOFC→BLA→lOFC circuit regulates the encoding and subsequent use of the state-dependent and sensory-specific reward memories that are critical for decision making between two appetitive choices.

BLA neurons were found to be robustly activated at the time of stimulus-reward pairing as well as at cue onset, consistent with prior evidence that the BLA is activated by both rewards (Schoenbaum et al., 1998; Sugase-Miyamoto and Richmond, 2005; Fontanini et al., 2009; Roesch et al., 2010; Malvaez et al., 2019; Crouse et al., 2020) and their predictors (Muramoto et al., 1993; Schoenbaum et al., 1998, 1999; Sugase-Miyamoto and Richmond, 2005; Paton et al., 2006; Tye and Janak, 2007; Belova et al., 2008; Tye et al., 2008; Malvaez et al., 2015; Beyeler et al., 2016; Beyeler et al., 2018; Lutas et al., 2019; Crouse et al., 2020). Interestingly, the cues triggered a transient elevation in BLA activity at their onset, rather than a sustained elevation throughout their 2-min duration, perhaps suggesting that such activity reflects the state change, rather than the state *per se*. Both the cue and reward responses were present from the first conditioning session and persisted throughout training. That we detected cue responses on the first day of training before associative learning had occurred is, perhaps, unexpected and likely due to the novelty of the auditory stimuli during early training (Bordi and LeDoux, 1992; Bordi et al., 1993; Romanski et al., 1993; Cromwell et al., 2005). Indeed, we found that presentation of identical

auditory stimuli unpaired with reward activated BLA neurons during the first session, much like the reward-predictive cues, but, in contrast to the reward-predictive cues, this response habituated over subsequent sessions. Thus, BLA cue responses later in training result from appetitive associative learning. Whereas we detected reward responses throughout training, prior data have demonstrated a shift in BLA responses from the reward to predictive events (Crouse et al., 2020) and little response to rewards in the absence of learning (Malvaez et al., 2015). The persistent reward response detected here likely results from the uncertainty of reward timing during the cues, which set the context for the intermittent availability of one specific reward. Another possibility is that it relates to the learning of two unique cue-reward contingencies, which was not the case in prior tasks. Nonetheless, the data show the BLA to be robustly activated at the time of stimulus-reward pairing in a task known to engender the encoding of detailed, sensory-specific stimulus-outcome memories.

We also found the BLA to be necessary, specifically at the time of stimulus-reward pairing, to encode the detailed stimulus-outcome memories. This is consistent with evidence that either pre- or post-training BLA lesion or pre-test inactivation disrupts appetitive conditional behaviors that rely on a sensory-specific, stimulus-outcome memory in rodents (Hatfield et al., 1996; Blundell et al., 2001; Corbit and Balleine, 2005; Ostlund and Balleine, 2008; Malvaez et al., 2015; Lichtenberg and Wassum, 2016; Lichtenberg et al., 2017; Derman et al., 2020; Morse et al., 2020) and in primates (Málková et al., 1997; Murray and Izquierdo, 2007). Leveraging the temporal resolution of optogenetics, we demonstrated that BLA principal neurons mediate the *encoding* of such memories, and specifically that activity at the time of reward experience during a cue is critical. Inhibiting the BLA during reward experience attenuated the animal's ability to link that specific rewarding event to the associated cue, disrupting the encoding of the sensory-specific stimulus-outcome memories to the extent that animals were unable to later use those memories to guide choice behavior. Future work is needed to reveal the precise information content encoded by BLA neurons during reward experience that renders their function necessary in the formation

of stimulus-outcome memories, though BLA neurons will respond selectively to unique food rewards (Liu et al., 2018), which could support the generation of sensory-specific reward memories. Whether BLA cue responses are also important for encoding stimulus-outcome memories is another important question exposed by the current results.

Although BLA activity during stimulus-outcome pairing was critical for encoding a detailed, outcome-specific, appetitive cue-reward memory, it was not necessary for the learning underlying the development a non-specific Pavlovian conditional goal-approach response, consistent with data collected with BLA lesions or inactivation (Hatfield et al., 1996; Everitt et al., 2000; Parkinson et al., 2000; Corbit and Balleine, 2005; Malvaez et al., 2015; Morse et al., 2020). Although influenced by positive outcome valence, such responses do not require a rich sensory-specific representation of the predicted reward. Thus, BLA neurons appear not to be required to reinforce an appetitive Pavlovian response policy. Rather, the BLA mediates the encoding of the association between a cue and the specific reward it predicts, which includes encoding of the sensory-specific features of the reward. Optical stimulation of BLA neurons will, however, augment conditional goal-approach responses (Servonnet et al., 2020), suggesting BLA activation is capable of influencing such appetitive conditional behaviors.

Input from the lOFC was found to facilitate the BLA's function in mediating the encoding of stimulus-outcome memories. This expands upon previous findings that pre-training lOFC lesions disrupt behaviors that require a sensory-specific stimulus-outcome memory (Pickens et al., 2003; Izquierdo et al., 2004; Pickens et al., 2005; Machado and Bachevalier, 2007; Ostlund and Balleine, 2007b; Scarlet et al., 2012; Rhodes and Murray, 2013), that the lOFC is active during cue-reward learning (Schoenbaum et al., 1998; Wallis and Miller, 2003; Paton et al., 2006; Takahashi et al., 2013; Miller et al., 2018; Constantinople et al., 2019), and that encoding of expected outcomes in the BLA requires an intact lOFC (Saddoris et al., 2005; Lucantonio et al., 2015). Our data add to this literature by revealing the causal contribution of the direct lOFC→BLA pathway, specifically at the time of stimulus-outcome pairing, to the formation of detailed,

outcome-specific, appetitive associative memories. Indeed, lOFC neurons respond to rewarding events during learning to signal reward expectations that may support learning in downstream structures, such as the BLA (Stalnaker et al., 2007; Stalnaker et al., 2018). Prior evidence also indicates that activity in lOFC→BLA projections drives the encoding of the incentive value of a specific rewarding event (Malvaez et al., 2019). Such incentive value is dependent upon one's current physiological state (e.g., food has high value when hungry, but low when sated). Thus, lOFC→BLA projections may be responsible for linking states, defined by internal physiological and external predictive cues, to the specific rewarding events with which they are associated. The precise information content conveyed by lOFC→BLA projections and how it is used in the BLA is a critical question for follow-up investigation.

We also discovered that the lOFC and BLA form a bidirectional circuit for the encoding and use of appetitive stimulus-outcome memories. The BLA has been implicated in appetitive decision making (Wellman et al., 2005; Ostlund and Balleine, 2008; Johnson et al., 2009; Izquierdo et al., 2013; Costa et al., 2016; Orsini et al., 2017; Costa et al., 2019; Stolyarova et al., 2019) and has been shown in non-human primates to interact with the lOFC in that regard (Baxter et al., 2000; Fiuzat et al., 2017). We previously found that BLA activity correlates with and regulates the ability to use sensory-specific, appetitive, stimulus-outcome memories to guide choice behavior (Malvaez et al., 2015). This function is mediated via direct BLA→lOFC projections, but does not require activation of lOFC→BLA projections (Lichtenberg et al., 2017). Here, using a serial disconnection procedure, we found that during reward choice BLA→lOFC projection activity mediates the use of the sensory-specific associative information that is learned via activation of lOFC→BLA projections. Thus, lOFC→BLA→lOFC is a functional circuit for the encoding (lOFC→BLA) and subsequent use (BLA→lOFC) of sensory-specific reward memories to inform decision making. Interestingly, the serial disconnection disrupted the outcome-specificity of PIT but, unlike bilateral BLA or lOFC→BLA inhibition during learning, allowed the cues to non-discriminately excite instrumental activity. This could have resulted from incomplete

disconnection. But it may indicate that lOFC→BLA projections facilitate the encoding of a broader set of information than that being transmitted back to the lOFC by BLA→lOFC projection activity during choice. BLA→lOFC projections mediate use of the sensory-specific components of the reward memory needed to allow animals to know during a cue which specific reward is predicted and thus which action to select, but lOFC→BLA projections may facilitate the encoding of additional features of the memory, including those capable of promoting food- or reward-seeking activity more broadly. The encoding of such information would have been disrupted by bilateral lOFC→BLA or BLA inactivation during learning, but in the disconnection experiment could have been learned in the hemisphere that did not receive lOFC→BLA inactivation and subsequently retrieved via an alternate BLA pathway. Indeed, BLA→lOFC are not the only amygdala projections involved in reward memory (Corbit et al., 2013; Parkes and Balleine, 2013; Beyeler et al., 2016; Fisher et al., 2020; Kochli et al., 2020; Morse et al., 2020).

lOFC activity in both humans and non-human animals can encode the features of an expected reward (Pritchard et al., 2005; van Duuren et al., 2007; Klein-Flügge et al., 2013; McDannald et al., 2014; Howard et al., 2015; Lopatina et al., 2015; Suzuki et al., 2017; Howard and Kahnt, 2018; Zhou et al., 2019b) and the lOFC has been proposed to be critical for using this information to guide decision making (Delamater, 2007; Keiflin et al., 2013; Rudebeck and Murray, 2014; Wilson et al., 2014a; Rich and Wallis, 2016; Sharpe and Schoenbaum, 2016; Rudebeck and Rich, 2018; Groman et al., 2019; Bradfield and Hart, 2020). This might especially be the case in novel situations (Gardner and Schoenbaum, 2021). The PIT test is a novel choice scenario in which the subjects must use the cues to represent the sensory-specific features of the predicted reward, infer which reward is most likely to be available and, therefore, which action will be the most beneficial. lOFC→BLA projection activity, perhaps via relaying reward expectation (Stalnaker et al., 2007; Stalnaker et al., 2018), regulates the associative learning that may allow subsequent activity in BLA→lOFC projections to promote the representation of a specific predicted reward in the lOFC to enable decision making. The precise information content

conveyed by each component of the lOFC-BLA circuit and how it is used in the receiving structure is a critical follow-up question that will require a cellular resolution investigation of the activity of each pathway. Another critical question is whether this circuitry similarly mediates appetitive associative learning and its influence on decision making in females. The exclusion of female subjects is a clear limitation of this study, though females do show similar performance in the task used here and also require the BLA and lOFC for its performance (Ostlund and Balleine, 2007b, 2008). Whether this lOFC-BLA architecture also underlies sensory-specific aversive memory is also a question ripe for further exploration.

The BLA, via input from the lOFC, helps to link environmental cues to the specific rewards they predict and, via projections back to the lOFC, to allow the cues to access those representations to influence decision making. An inability to either properly encode reward memories or to use such memories to inform decision making can lead to ill-informed motivations and decisions. This is characteristic of the cognitive symptoms underlying many psychiatric diseases, including substance use disorder. The OFC-BLA circuit is known to be altered by addictive substances (Arguello et al., 2017) and to be dysfunctional in myriad psychiatric illnesses (Ressler and Mayberg, 2007; Goldstein and Volkow, 2011; Passamonti et al., 2012; Liu et al., 2014; Sladky et al., 2015). Thus, these data may also aid our understanding and treatment of substance use disorders and other mental illnesses marked by disruptions to decision making.

MATERIALS AND METHODS

Subjects.

Male, Long Evans rats aged 8-10 weeks at the start of the experiment (Charles River Laboratories, Wilmington, MA) were group housed (2/cage) in a temperature (68-79°F) and humidity (30-70%) regulated vivarium prior to surgery and then subsequently housed individually to preserve implants. Rats were provided with water *ad libitum* in the home cage and were maintained on a food-restricted 12-14 g daily diet (Lab Diet, St. Louis, MO) to maintain ~85-90% free-feeding body weight. Rats were handled for 3-5 days prior to the onset of each experiment. Separate groups of

naïve rats were used for each experiment. Experiments were performed during the dark phase of a 12:12 hr reverse dark/light cycle (lights off at 7AM). All procedures were conducted in accordance with the NIH Guide for the Care and Use of Laboratory Animals and were approved by the UCLA Institutional Animal Care and Use Committee.

Surgery.

Standard surgical procedures, described previously (Malvaez et al., 2015; Lichtenberg et al., 2017; Malvaez et al., 2019), were used for all surgeries. Rats were anesthetized with isoflurane (4–5% induction, 1–3% maintenance) and a nonsteroidal anti-inflammatory agent was administered pre- and post-operatively to minimize pain and discomfort.

Fiber photometry recordings. Surgery occurred prior to onset of behavioral training. Rats (*N* = 11) were infused bilaterally with adeno-associated virus (AAV) expressing the genetically encoded calcium indicator GCaMP6f under control of the calcium/calmodulin-dependent protein kinase (CaMKII) promoter (pENN.AAV5.CAMKII.GCaMP6f.WPRE.SV40, Addgene, Watertown, MA) to drive expression preferentially in principal neurons. Virus (0.5 µl) was infused a rate of 0.1 µl/min into the BLA [AP: -2.7 (*N* = 5) or -3.0 (*N* = 6); ML: ± 5.0; DV: -8.6 mm from bregma] using a 28-gauge injector. Injectors were left in place for an additional 10 minutes to ensure adequate diffusion and to minimize off-target spread along the injector tract. Optical fibers (200 µm diameter, 0.37 numerical aperture (NA), Neurophotometrics, San Diego, CA) were implanted bilaterally 0.2 mm dorsal to the infusion site to allow subsequent imaging of GCaMP fluctuations in BLA neurons. These procedures were replicated in a separate group of subjects (*N* = 6) that served as unpaired CS$_{\emptyset}$ control. Behavioral training commenced approximately 3-4 weeks after surgery to allow sufficient expression in BLA neurons.

Optogenetic inhibition of BLA. Prior to the onset of behavioral training, rats were randomly assigned to a viral group and were infused bilaterally with AAV encoding either the inhibitory opsin archaerhodopsin T (ArchT; *N* = 9; rAAV5-CAMKIIa-eArchT3.0-eYFP, University of North Carolina Vector Core, Chapel Hill, NC) or the enhanced yellow fluorescent protein control (eYFP; *N* = 10; rAAV5-CAMKIIa-eYFP, University of North Carolina Vector Core) under control of the CaMKII promoter. Virus (0.5 µl) was infused at a rate of 0.1 µl/min into the BLA (AP: -2.8; ML: ±5.0; DV: -8.6 mm from bregma) using a 28-gauge injector. Injectors were left in place for an additional 10 minutes. Optical fibers (200 µm core, 0.39 NA, Thorlabs, Newton, NJ) held in ceramic ferrules (Kientec Systems, Stuart, FL) were implanted bilaterally 0.6 mm dorsal to the injection site to allow subsequent light delivery to ArchT- or eYFP-expressing BLA neurons. Identical surgical procedures were used for a separate yoked inhibition control group (*N* = 7). A third group (*N* = 5) also received bilateral infusion of rAAV5-CAMKIIa-eArchT3.0-eYFP into the BLA, without fiber implants, for subsequent *ex vivo* electrophysiological validation of optical inhibition of BLA neurons. Experiments commenced 3 weeks after surgery to allow sufficient expression in BLA neurons.

Optogenetic inhibition of lOFC→BLA projections. Prior to the onset of behavioral training, rats were randomly assigned to a viral group and were infused with AAV encoding either the inhibitory opsin ArchT (*N* = 8; rAAV5-CAMKIIa-eArchT3.0-eYFP) or eYFP control (*N* = 8; rAAV5-CAMKIIa-eYFP). Virus (0.3 µl) was infused at a rate of 0.1 µl/min bilaterally into the lOFC (AP: +3.3; ML: ±2.5; DV: -5.4 mm from bregma) using a 28-gauge injector tip. Injectors were left in place for an additional 10 minutes. Optical fibers (200 µm core, 0.39 NA) held in ceramic ferrules were implanted bilaterally in the BLA (AP: -2.7; ML: ± 5.0; DV: -8.0 mm from bregma) to allow subsequent light delivery to ArchT- or eYFP-expressing axons and terminals in the BLA. A separate group (*N* = 4) also received bilateral infusion of rAAV5-CAMKIIa-eArchT3.0-eYFP into the lOFC, without fiber implants, for subsequent *ex vivo* electrophysiological validation of optical

inhibition of lOFC terminals in the BLA. Experiments began 7-8 weeks following surgery to allow axonal transport to the BLA.

Multiplexed optogenetic inhibition lOFC→BLA projections and chemogenetic inhibition of BLA→lOFC projections for serial circuit disconnection. Prior to the onset of behavioral training, rats were randomly assigned to viral group. The disconnection group (*N* = 10) was infused with AAV encoding the inhibitory opsin ArchT (rAAV5-CAMKIIa-eArchT3.0-eYFP; 0.3 µl) bilaterally at a rate of 0.1 µl/min into the lOFC (AP: +3.3; ML: ±2.5; DV: -5.4 mm from bregma) using a 28-gauge injector tip. Injectors were left in place for an additional 10 minutes. An optical fiber (200 µm core, 0.39 NA) held in a ceramic ferrule was implanted unilaterally (hemisphere counterbalanced across subjects) in the BLA (AP: -2.7; ML: ±5.0; DV: -7.7 mm from dura) to allow subsequent light delivery to both the ipsilateral and contralateral ArchT-expressing axons and terminals in the BLA of only one hemisphere. During the same surgery, in the hemisphere contralateral to optical fiber placement, a second AAV was infused unilaterally at a rate of 0.1 µl/min into the BLA (AP: -3.0; ML: ±5.1; DV: -8.6 from bregma) to drive expression of the inhibitory designer receptor *human M4 muscarinic receptor* (hM4Di; pAAV8-hSyn-hM4D(Gi)-mCherry, Addgene; 0.5 µl). A 22-gauge stainless-steel guide cannula was implanted unilaterally above the lOFC (AP: +3.0; ML: ±3.2: DV: -4.0) of the BLA-hM4Di hemisphere to target the hM4D(Gi)-expressing axonal terminals, which are predominantly ipsilateral. This allowed subsequent optical inhibition of lOFC terminals in the BLA of one hemisphere and chemogenetic inhibition of BLA terminals in the lOFC of the other hemisphere, thus disconnecting the putative lOFC→BLA→lOFC circuit. Surgical procedures were identical for the fluorophore-only control group (*N* = 8), except with AAVs encoding only eYFP (lOFC; rAAV5-CAMKIIa-eYFP) and mCherry (BLA; pAAV8-hSyn-mCherry). A separate ipsilateral control group received the same surgical procedures as the experimental contralateral ArchT/hM4Di group, but with BLA pAAV8-hSyn-hM4D(Gi)-mCherry and lOFC guide cannula placed in the same hemisphere as the BLA

optical fiber. Experiments began 7-8 weeks following surgery to allow sufficient viral expression and axonal transport. Two subjects became ill before testing and, thus, were excluded from the experiment (Contralateral ArchT/hM4Di, $N = 1$; Ipsilateral ArchT/hM4Di, $N = 1$).

Behavioral Procedures.

Apparatus. Training took place in Med Associates conditioning chambers (East Fairfield, VT) housed within sound- and light-attenuating boxes, described previously (Malvaez et al., 2015; Collins et al., 2019; Malvaez et al., 2019). For optogenetic manipulations, the chambers were outfitted with an Intensity Division Fiberoptic Rotary Joint (Doric Lenses, Quebec, QC, Canada) connecting the output fiber optic patch cords to a laser (Dragon Lasers, ChangChun, JiLin, China) positioned outside of the chamber.

Each chamber contained two retractable levers that could be inserted to the left and right of a recessed food-delivery port (magazine) in the front wall. A photobeam entry detector was positioned at the entry to the food port. Each chamber was equipped with a syringe pump to deliver 20% sucrose solution in 0.1 ml increments through a stainless-steel tube into one well of the food port and a pellet dispenser to deliver 45-mg purified chocolate food pellets (Bio-Serv, Frenchtown, NJ) into another well. Both a tone and white noise generator were attached to individual speakers on the wall opposite the levers and food-delivery port. A 3-watt, 24-volt house light mounted on the top of the back wall opposite the food-delivery port provided illumination and a fan mounted to the outer chamber provided ventilation and external noise reduction. Behavioral procedures were similar to that we have described previously (Malvaez et al., 2015; Lichtenberg and Wassum, 2016; Lichtenberg et al., 2017)

Magazine conditioning. Rats first received one day of training to learn where to receive the sucrose and food pellet rewards. This included two separate sessions, separated by approximately

1 hr, order counterbalanced, one with 30 non-contingent deliveries of sucrose (60 s intertrial interval, ITI) and one with 30 food pellet deliveries (60 s ITI).

Pavlovian conditioning. Rats then received 8 sessions of Pavlovian conditioning (1 session/day on consecutive days) to learn to associate each of two auditory conditional stimuli (CSs; 80-82 db, 2 min duration), tone (1.5 kHz) or white noise, with a specific food reward, sucrose (20%, 0.1 ml/delivery) or purified chocolate pellets (45 mg; Bio-Serv). CS-reward pairings were counterbalanced at the start of each experiment. For half the subjects, tone was paired with sucrose and noise with pellets, with the other half receiving the opposite arrangement. Each session consisted of 8 tone and 8 white noise presentations, with the exception of the fiber photometry experiments, in which rats received 4 of each CS/session to reduce session time and, thus, minimize the effects of photobleaching. During each 2 min CS the associated reward was delivered on a 30 s random-time schedule, resulting in an average of 4 stimulus-reward pairings per trial. For the fiber photometry experiments, there was a minimum 15 s probe period after CS onset before the first reward delivery to allow us to dissociate signal fluctuations due to CS onset from those due to reward delivery/retrieval. CSs were delivered pseudo-randomly with a variable 2-4 min ITI (mean = 3 min).

Procedures were identical for the unpaired $CS_{Ø}$ control fiber photometry experiment, except no rewards were delivered during Pavlovian training. Subjects in this experiment instead received rewards in their home cage several hours after the $CS_{Ø}$ sessions. On the day following the last $CS_{Ø}$ session, these subjects received one session with non-contingent, unpredicted deliveries of sucrose and food pellets, each delivered on a 30 s random-time schedule during 4, 2-min periods (variable 2-4 min ITI, mean = 3 min), resulting in an average of 16 deliveries of each outcome.

Instrumental conditioning. Rats were then given 11 days, minimum, of instrumental conditioning. They received two separate training sessions per day, one with the left lever and one with the right lever, separated by at least 1 hr. Each action was reinforced with a different outcome (e.g., left press-chocolate pellets / right press-sucrose solution; counterbalanced with respect to the Pavlovian contingencies). Each session terminated after 30 outcomes had been earned or 45 min had elapsed. Actions were continuously reinforced on the first day and then escalated ultimately to a random-ratio 20 schedule of reinforcement.

Outcome-selective Pavlovian-to-instrumental transfer test. Following Pavlovian and instrumental conditioning, rats received an outcome-selective Pavlovian-to-instrumental transfer (PIT) test. On the day prior to the PIT test, rats were given a single 30-min extinction session during which both levers were available but pressing was not reinforced to establish a low level of responding. During the PIT test, both levers were continuously present, but pressing was not reinforced. After 5 min of lever-pressing extinction, each 2-min CS was presented separately 4 times in pseudorandom order, separated by a fixed 4-min inter-trial interval. No rewards were delivered during CS presentation.

Data collection. Lever presses and/or discrete entries into the food-delivery port were recorded continuously for each session. For both Pavlovian training and PIT test sessions, the 2-min periods prior to each CS onset served as the baseline for comparison of CS-induced elevations in lever pressing and/or food-port entries.

In vivo fiber photometry.

Fiber photometry was used to image bulk calcium activity in BLA neurons throughout each Pavlovian conditioning session. We simultaneously imaged GCaMP6f and control fluorescence in the BLA using a commercial fiber photometry system (Neurophotometrics Ltd., San Diego, CA).

Two light-emitting LEDs (470 nm: Ca2+-dependent GCaMP fluorescence; 415 nm: autofluorescence, motion artifact, Ca2+-independent GCaMP fluorescence) were reflected off dichroic mirrors and coupled via a patch cord (fiber core diameter, 200 μm; Doric Lenses) to the implanted optical fiber. The intensity of the light for excitation was adjusted to ~80 μW at the tip of the patch cord. Fluorescence emission was passed through a 535nm bandpass filter and focused onto the complementary metal-oxide semiconductor (CMOS) camera sensor through a tube lens. Samples were collected at 20 Hz, interleaved between the 415 and 470 excitation channels, using a custom Bonsai (Lopes et al., 2015) workflow. Time stamps of task events were collected simultaneously through an additional synchronized camera aimed at the Med Associates interface, which sent light pulses coincident with task events. Signals were saved using Bonsai software and exported to MATLAB (MathWorks, Natick, MA) for analysis. Recordings were collected unilaterally from the hemisphere with the strongest fluorescence signal in the 470 channel at the start of the experiment, which was kept consistent throughout the remainder of the experiment. Animals were habituated to the optical tether during the magazine conditioning sessions, but no light was delivered.

Optogenetic inhibition of BLA neurons.

Optogenetic inhibition was used to attenuate the activity of ArchT-expressing BLA neurons at the time of stimulus-outcome pairing during each CS during each Pavlovian conditioning session. Animals were habituated to the optical tether (200 μm, 0.22 NA, Doric) during the magazine conditioning sessions, but no light was delivered. During each Pavlovian conditioning session, green light (532nm; 10 mW) was delivered to the BLA via a laser (Dragon Lasers, ChangChun) connected through a ceramic mating sleeve (Thorlabs) to the ferrule implanted on the rat. Light was delivered continuously for 5 seconds concurrent with each reward delivery. If the reward was retrieved (first food-port entry after reward delivery) while the light was still being delivered (i.e., within 5 s of reward delivery), then the light delivery was extended to 5 s from the time of the

retrieval. If the reward was retrieved after the laser had gone off, then the retrieval entry triggered an additional 5 s continuous illumination. To control for the overall amount of inhibition, a separate control group received green light during the 2-min preCS baseline periods with the same number, duration, and pattern as the experimental group. Light effects were estimated to be restricted to the BLA based on predicted irradiance values (https://web.stanford.edu/group/dlab/cgi-bin/graph/chart.php). Following Pavlovian conditioning, rats proceeded through instrumental conditioning and the PIT test, as above. Light was not delivered during these subsequent phases of the experiment.

Optogenetic inhibition of lOFC→BLA projections.

Optogenetic inhibition was used to attenuate the activity of ArchT-expressing lOFC→BLA terminals at the time of stimulus-outcome pairing during each CS during each Pavlovian conditioning session. Procedures were identical to those for BLA inhibition above. Green light (532 nm; 10 mW) was delivered to the BLA continuously for 5 seconds concurrent with each reward delivery and/or retrieval during Pavlovian conditioning.

Multiplexed optogenetic inhibition of lOFC→BLA projections during Pavlovian conditioning and chemogenetic inhibition of BLA→lOFC projections during the Pavlovian-to-instrumental transfer test for serial circuit disconnection.

We multiplexed optogenetic inhibition of lOFC→BLA projection activity during stimulus-outcome pairing during Pavlovian conditioning with chemogenetic inhibition of BLA→lOFC projection activity during the PIT test to perform a serial circuit disconnection and ask whether activity in lOFC→BLA projections mediates the encoding of the stimulus-outcome memory that is later retrieved via activation of BLA→lOFC projections (Lichtenberg et al., 2017). That is, whether lOFC→BLA→lOFC is a functional circuit for the encoding (lOFC→BLA) and subsequent use for guiding decision making (BLA→lOFC) of appetitive, sensory-specific, stimulus-outcome

memories. To achieve the serial circuit disconnection, in the experimental group, we optically inactivated ipsilateral and contralateral lOFC input to the BLA of only one hemisphere during stimulus-outcome pairing during Pavlovian conditioning, and then chemogenetically inactivated predominantly ipsilateral (Lichtenberg et al., 2017) BLA axons and terminals in the lOFC of the other hemisphere during the PIT test. This leaves one of each pathway undisrupted to mediate the stimulus-outcome learning (lOFC→BLA) and retrieval (BLA→lOFC), but if lOFC→BLA→lOFC forms a functional stimulus-outcome memory circuit, then we will have disconnected the circuit in each hemisphere.

Optogenetic inhibition of lOFC→BLA projections during Pavlovian conditioning. Optogenetic inhibition was used to attenuate the activity of ArchT-expressing lOFC→BLA terminals of one hemisphere at the time of stimulus-outcome pairing (reward delivery and retrieval) during each CS during each Pavlovian conditioning session. Procedures were identical to those described above, except that green light (532nm; 10 mW) was delivered unilaterally to the BLA continuously for 5 seconds concurrent with each reward delivery and retrieval during Pavlovian conditioning.

Chemogenetic inhibition of BLA→lOFC projections during the Pavlovian-to-instrumental transfer test. Chemogenetic inhibition was used to inactivate hM4Di-expressing BLA axons and terminals in the lOFC of one hemisphere during the PIT test. For the contralateral ArchT/hM4Di group, chemogenetic inhibition occurred in the hemisphere opposite to the one that received optical inhibition of lOFC→BLA projections during learning, thus achieving the disconnection. In a separate ipsilateral control group, the chemogenetic inhibition occurred on the same side as optical inhibition of lOFC→BLA projections during learning, leaving the entire circuit undisrupted in one hemisphere, while controlling for unilateral inhibition of each pathway. We selected chemogenetic inhibition so it could be multiplexed with optogenetic inhibition and to allow inhibition throughout the duration of the PIT test. CNO (Tocris Bioscience, Sterling Heights,

MI) was dissolved in artificial CSF to 1 mM and 0.25 μL was intracranially infused over 1 minute into the lOFC as previously described (Lichtenberg et al., 2017). Injectors were left in place for at least 1 additional min to allow for drug diffusion. The PIT test commenced within 5-10 min following infusion. CNO dose was selected based on evidence of both its behavioral effectiveness and ability to attenuate the activity of hM4Di-expressing BLA terminals in the lOFC (Lichtenberg et al., 2017). We have also demonstrated that this dose of CNO when infused into the lOFC has no effect on reward-related behavior in the absence of the hM4Di transgene (Lichtenberg et al., 2017).

Ex vivo electrophysiology.

Whole-cell patch clamp recordings were used to validate the efficacy of optical inhibition of BLA principal neuron activity and lOFC terminal activity in the BLA. Recordings were performed in brain slices from ~3-4 month old rats 3-4 (BLA cell body inhibition) or 7-8 (lOFC→BLA inhibition) weeks following surgery. To prepare brain slices, rats were deeply anesthetized with isoflurane and perfused transcardially with an ice-cold, oxygenated NMDG-based slicing solution containing (in mM): 30 $NaHCO_3$, 20 HEPES, 1.25 NaH_2PO_4, 102 NMDG, 40 glucose, 3 KCl, 0.5 $CaCl_2$-$2H_2O$, 10 $MgSO_4$-H_2O (pH adjusted to 7.3-7.35, osmolality 300-310 mOsm/L). Brains were extracted and immediately placed in ice-cold, oxygenated NMDG slicing solution. Coronal slices (350 μm) were cut using a vibrating microtome (VT1000S; Leica Microsystems, Germany), transferred to an incubating chamber containing oxygenated NMDG slicing solution warmed to 32-34 °C, and allowed to recover for 15 min before being transferred to an artificial cerebral spinal fluid (aCSF) solution containing (in mM): 130 NaCl, 3 KCl, 1.25 NaH_2PO_4, 26 $NaHCO_3$, 2 $MgCl_2$, 2 $CaCl_2$, and 10 glucose) oxygenated with 95% O_2, 5% CO_2 (pH 7.2-7.4, osmolality 290-310 mOsm/L, 32-34°C). After 15 min, slices were moved to room temperature and allowed to recover for ~30 additional min prior to recording. All recordings were performed using an upright microscope (Olympus BX51WI, Center Valley, PA) equipped with differential interference

contrast optics and fluorescence imaging (QIACAM fast 1394 monochromatic camera with Q-Capture Pro software, QImaging, Surrey, BC, Canada). Patch pipettes (3-5 MΩ resistance) contained a Cesium methanesulfonate-based internal recording solution (in mM): 125 Cs-methanesulfonate, 4 NaCl, 1 MgCl2, 5 MgATP, 9 EGTA, 8 HEPES, 1 GTP-Tris, 10 phosphocreatine, and 0.1 leupeptin; pH 7.2 with CsOH, 270-280 mOsm). Biocytin (0.2%, Sigma-Aldrich, St. Louis, MO) was included in the internal recording solution for subsequent postsynaptic cell visualization and identification. Recordings were obtained using a MultiClamp 700B Amplifier (Molecular Devices, Sunnyvale, CA) and the pCLAMP 10.3 acquisition software.

Validation of BLA principal neuron optogenetic inhibition. Whole-cell patch clamp recordings in current-clamp mode were obtained from BLA principal neurons expressing ArchT-eYFP (N = 12 cells, 5 subjects). Visible eYFP-expressing cell bodies were identified in the BLA for recordings. After breaking through the membrane, recordings were obtained from cells while injecting suprathreshold depolarizing current (1 s). Current injection intensities that resulted in 8-15 action potentials were selected for recordings (100-800 pA). Electrode access resistances were maintained at <30 MΩ. Green light (535 nm, 1 s pulse, 0.25-1 mW; CoolLED Ltd, Andover, UK) was delivered through the epifluorescence illumination pathway using Chroma Technologies filter cubes to activate ArchT and inhibit BLA cell bodies. The number of action potentials recorded in ArchT-expressing cells injected with suprathreshold current were recorded both prior to and after green light illumination.

Validation of lOFC terminal optogenetic inhibition in the BLA. Whole-cell patch-clamp recordings were collected in voltage-clamp mode. Visible eYFP-expressing axons and terminals were identified in the BLA and recordings were obtained from postsynaptic BLA neurons located only in highly fluorescent regions. After breaking through the membrane, recordings were obtained while holding the membrane potential at -70 mV. Electrode access resistances were

maintained at <30 MΩ. Spontaneous excitatory postsynaptic currents (sEPSCs) were recorded in the presence of the $GABA_A$ receptor antagonist bicuculline (10 μM). Fifteen seconds of baseline recordings of sEPSCs were obtained prior to exposure to green light. Following baseline measurements, recordings of sEPSCs were obtained during continuous exposure to green light (535 nm, 0.5 mW) for 15 s. Spontaneous EPSC events were analyzed offline using the automatic detection protocol within the MiniAnalysis software (Synaptosoft, version 6.0), and then were checked manually blinded to light condition.

Histology.

Following the behavioral experiments, rats were deeply anesthetized with Nembutal and transcardially perfused with phosphate buffered saline (PBS) followed by 4% paraformaldehyde (PFA). Brains were removed and post-fixed in 4% PFA overnight, placed into 30% sucrose solution, then sectioned into 30-40 μm slices using a cryostat and stored in PBS or cryoprotectant. eYFP fluorescence was used to confirm ArchT expression in lOFC and BLA cell bodies. mCherry expression was used to confirm hM4D(Gi) in BLA cell bodies. Immunofluorescence was used to confirm expression of ArchT-eYFP in lOFC axons and terminals in the BLA. Floating coronal sections were washed 3 times in 1x PBS for 30 min and then blocked for 1–1.5 hr at room temperature in a solution of 3% normal goat serum and 0.3% Triton X-100 dissolved in PBS. Sections were then washed 3 times in PBS for 15 min and incubated in blocking solution containing chicken anti-GFP polyclonal antibody (1:1000; Abcam, Cambridge, MA) with gentle agitation at 4°C for 18–22 hr. Sections were next rinsed 3 times in PBS for 30 min and incubated with goat anti-chicken IgY, Alexa Fluor 488 conjugate (1:500; Abcam) at room temperature for 2 hr. Sections were washed a final 3 times in PBS for 30 min. Immunofluorescence was also used to confirm expression of hM4Di-mCherry in BLA axons and terminals in the lOFC. The signal for axonal expression of hM4D(Gi)-mCherry in terminals in the lOFC was immunohistochemically amplified following procedures described previously (Lichtenberg et al., 2017). Briefly, floating

coronal sections were rinsed in PBS and blocked for 1–2 hr at room temperature in a solution of 10% normal goat serum and 0.5% Triton X-100 dissolved in PBS and then incubated in blocking solution containing rabbit anti-DsRed polyclonal antibody (1:1000; Takara Bio, Mountain View, CA) with gentle agitation at 4°C for 18–22 hr. Sections were next rinsed in blocking solution and incubated with goat anti-rabbit IgG, Alexa Fluor 594 conjugate (1:500; Invitrogen, Waltham, MA) for 2 hr. Slices were mounted on slides and coverslipped with ProLong Gold mounting medium with DAPI. Images were acquired using a Keyence BZ-X710 microscope (Keyence, El Segundo, CA) with a 4x,10x, and 20x objective (CFI Plan Apo), CCD camera, and BZ-X Analyze software or a Zeiss apotome confocal microscope (Zeiss, Oberkochen, Germany) and Zeiss Zen Blue software (Zeiss). Subjects with off-target viral, fiber, and/or cannula placements were removed from the dataset (Fiber photometry: $N = 2$; Fiber photometry $CS_{\emptyset}$ control $N = 0$; BLA ArchT: $N = 2$; BLA ArchT yoked control: $N = 1$; Contralateral disconnection, $N = 6$; Ipsilateral control $N = 7$).

Data analysis.

Behavioral analysis. Behavioral data were processed with Microsoft Excel (Microsoft, Redmond, WA). Left and/or right lever presses and/or entries into the food-delivery port were collected continuously for each training and test session. Acquisition of the Pavlovian conditional food-port approach response was assessed by computing an elevation ratio of the rate of entries into the food-delivery port (entries/min) during the CS prior to reward delivery (CS-probe) relative to 2-min baseline periods immediately prior to CS onset [(CS probe entry rate)/(CS probe entry rate + preCS entry rate)]. Data were averaged across trials for each CS and then averaged across the two CSs. We also compared the rate of food-port entries between the CS probe and the preCS baseline periods (see Figures 2-6a, 2-12a, 2-15a, 2-17a). Press rates on the last day of instrumental training were averaged across levers and compared between groups to test for any differences in the acquisition of lever press responding during instrumental training. No significant group differences were detected in any of the experiments (see Figures 2-6b, 2-12b, 2-15b, 2-17b). For

the PIT test, lever pressing during the 2-min baseline periods immediately prior to the onset of each CS was compared with that during the 2-min CS periods. For both the baseline and CS periods, lever pressing was separated for presses on the lever that, during training, earned the same outcome as the presented cue (i.e., preCS-Same and CS-Same presses) versus those on the other available lever (i.e., preCS-Different and CS-Different presses). To evaluate the influence of CS presentation on lever pressing, we computed an elevation ratio for each lever [(CS-Same presses)/(CS-Same presses + preCS-Same presses)] and [(CS-Different presses)/(CS-Different presses + preCS-Different presses)]. In all cases, there were no significant differences in baseline presses between levers in the absence of the CSs (Lever: lowest $P = 0.33$, $F_{1,14} = 1.02$), and no effect of group on baseline lever pressing (Group: lowest $P = 0.54$, $F_{2,23} = 0.63$; Group x Lever lowest $P = 0.21$, $F_{1,14} = 1.71$). To evaluate the influence of CS presentation on food-port entries, i.e., the conditional goal-approach responses, we also computed an elevation ratio [(CS entries)/(CS entries + preCS entries)]. Data were averaged across trials for each CS and then averaged across the two CSs. We also compared the rate of pressing on each lever and, separately, food-port entries between the CS and preCS baseline periods (see Figures 2-6c-d, 2-12c-d, 2-15c-d, 2-17c-d).

Fiber photometry data analysis. Data were pre-processed using a custom-written pipeline in MATLAB (MathWorks, Natick, MA). Data from the 415 nm isosbestic control channel were used to correct for motion artifacts and photobleaching. Using least-squares linear regression, the 415 signal was fit to the 470 signal. Change in fluorescence ($\Delta F/F$) at each time point was calculated by subtracting the fitted 415 signal from the 470 signal and normalizing to the fitted 415 data [(470-fitted 415)/fitted 415)] (See Figure 2-7). The $\Delta F/F$ data were then Z-scored [($\Delta F/F$ - mean $\Delta F/F$)/std($\Delta F/F$)]. Using a custom MATLAB workflow, Z-scored traces were then aligned to CS onset, reward delivery, reward retrieval (first food-port entry after reward delivery), and food-port entries without reward present during the CS probe period (after CS before first reward delivery) during the CS for each trial. Peak magnitude and AUC were calculated on the Z-scored

trace for each trial using 3-s pre-event baseline and 3-s post-event windows. Data were averaged across trials and then across CSs. Session data were excluded if no transient calcium fluctuations were detected on the 470 nm channel above the isosbestic channel or if poor linear fit was detected due to excessive motion artifact. To examine the progression in BLA activity across training, we compared data across conditioning sessions 1, 2, 3/4, 5/6, and 7/8. Data from the mid and latter training sessions were averaged across bins of 2 training sessions. Subjects without reliable data from at least one session per bin were excluded (CS+ $N = 5$; $CS_{\emptyset}$ $N = 1$). We were able to obtain reliable imaging data from all of the 8 training sessions from $N = 8$ of the 11 total final subjects that received CS-reward pairing (see Figure 2-8).

Ex vivo electrophysiology. The number of action potentials evoked by suprathreshold current injection was compared before and during exposure to green light to confirm the inhibitory effect of ArchT in BLA principal neurons. To assess the effect of ArchT activation in lOFC→BLA terminals, the frequency of sEPSCs was compared before and during green light exposure.

Statistical analysis. Datasets were analyzed by two-tailed, paired and unpaired Student's *t* tests, one-, two-, or three-way repeated-measures analysis of variance (ANOVA), as appropriate (GraphPad Prism, GraphPad, San Diego, CA; SPSS, IBM, Chicago, IL). Post hoc tests were corrected for multiple comparisons using the Bonferroni method. All data were tested for normality prior to analysis with ANOVA and the Greenhouse-Geisser correction was applied to mitigate the influence of unequal variance between conditions. Alpha levels were set at $P<0.05$.

Rigor and reproducibility.

Group sizes were estimated *a priori* based on prior work using male Long Evans rats in this behavioral task (Malvaez et al., 2015; Lichtenberg and Wassum, 2016; Lichtenberg et al., 2017) and to ensure counterbalancing of CS-reward and Lever-reward pairings. Investigators were not

blinded to viral group because they were required to administer virus. All behaviors were scored using automated software (MedPC). Each primary experiment included at least 1 replication cohort and cohorts were balanced by viral group, CS-reward and Lever-reward pairings, hemisphere etc. prior to the start of the experiment.

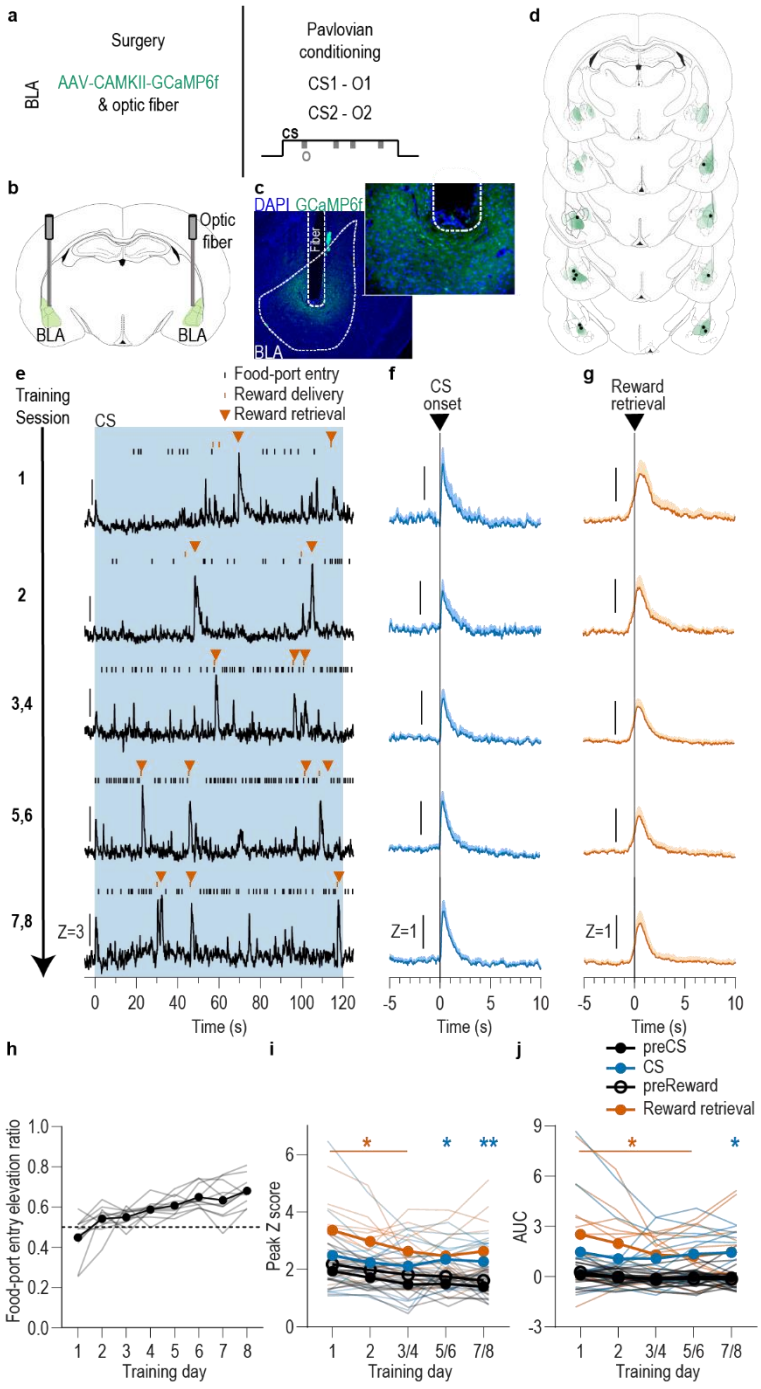

Figure 2-1: BLA neurons are activated during stimulus-outcome learning.

(a) Procedure schematic. CS, conditional stimulus (white noise or tone); O, outcome (sucrose solution or food pellet). **(b)** Schematic of fiber photometry approach for imaging bulk calcium activity in BLA neurons. **(c)** Representative fluorescent image of GCaMP6f expression and fiber placement in the BLA. (d) Schematic representation of GCaMP6f expression and placement of optical fiber tips in BLA for all subjects. Brain slides from (Paxinos and Watson, 1998). **(e)** Representative examples of GCaMP6f fluorescence changes (Z-scored ΔF/F) in response to CS presentation (blue box), reward delivery, and reward retrieval (first food-port entry following reward delivery) across days of training. Traces from the last 6 days of training were selected from 1 of each 2-session bin. See Figure 2-7 for raw GCaMP and isosbestic signal fluctuations. **(f-**

g) Trial-averaged GCaMP6f fluorescence changes (Z-scored ΔF/F) in response to CS onset (f; blue) or reward retrieval during the CS (g; orange) across days of training. Shading reflects between-subjects s.e.m. Data from the last six sessions were averaged across 2-session bins (3/4, 5/6, and 7/8). **(h)** Elevation [(CS probe entry rate)/(CS probe entry rate + preCS entry rate)] in food-port entries during the CS probe period (after CS onset, before first reward delivery), averaged across trials and across the 2 CSs for each day of Pavlovian conditioning. Gray lines represent individual subjects. **(i-j)** Trial-averaged quantification of maximal (i; peak) and area under the GCaMP Z-scored ΔF/F curve (j; AUC) during the 3-s period following CS onset or reward retrieval compared to equivalent baseline periods immediately prior to each event. Thin light lines represent individual subjects. $N = 11$ (see Figure 2-8 for data from $N = 8$ subjects with longitudinal data from each session). $^{*}P < 0.05$, $^{**}P < 0.01$ relative to pre-event baseline.

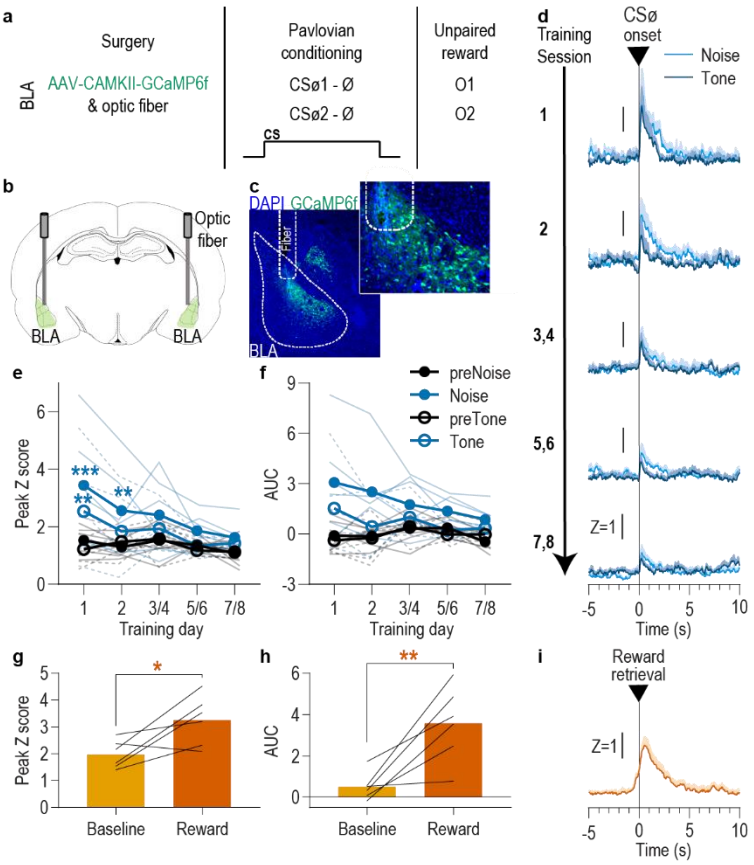

Figure 2-2: BLA neurons are only transiently activated by stimuli if they are not paired with reward.

(a) Procedure schematic. CSø, neutral stimulus; Ø, no reward outcome; O, outcome (sucrose solution or food pellet). **(b)** Schematic of fiber photometry approach for imaging bulk calcium activity in BLA neurons. **(c)** Representative fluorescent image of GCaMP6f expression and fiber placement in the BLA. **(d)** Trial-averaged GCaMP6f fluorescence change (Z-scored ΔF/F) in response to noise and tone CSø onset across days. Shading reflects between-subjects s.e.m.. **(e-f)** Trial-averaged quantification of maximal (e; peak) and area under the GCaMP Z-scored ΔF/F curve (f; AUC) during the 3 s following noise and tone CSø onset compared to equivalent baseline periods immediately prior to each event. Thin light lines represent individual subjects (solid = Noise, dashed = Tone). **(g-h)** Trial-averaged quantification of maximal (g; peak) and area under the GCaMP Z-scored ΔF/F curve (h; AUC) during the 3 s following retrieval of the unpaired reward compared to equivalent baseline period immediately prior reward retrieval. Lines represent individual subjects. **(i)** Trial-averaged GCaMP6f fluorescence (Z-scored ΔF/F) in response to unpaired reward, averaged across reward type. Shading reflects between-subjects s.e.m.. $N = 6$. *$P < 0.05$, ** $P < .01$ relative to pre-event baseline.

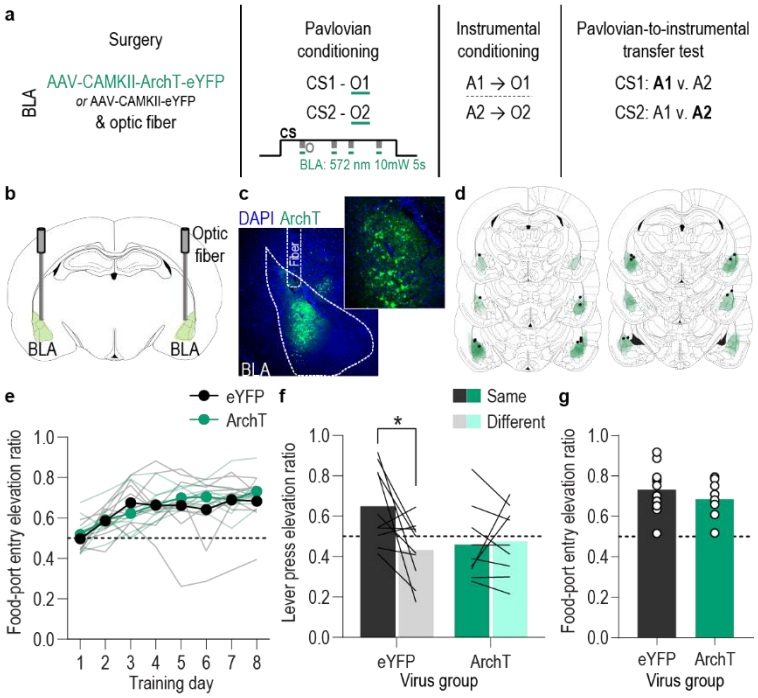

Figure 2-3: Optical inhibition of BLA neurons during stimulus-outcome pairing attenuates the encoding of stimulus-outcome memories.

(a) Procedure schematic. CS, conditional stimulus (white noise or tone); O, outcome (sucrose solution or food pellet); A, action (left or right lever press). **(b)** Schematic of optogenetic strategy for bilateral inhibition of BLA neurons. **(c)** Representative fluorescent image of ArchT-eYFP expression and fiber placement in the BLA. **(d)** Schematic representation of ArchT-eYFP expression and placement of optical fiber tips in BLA for all subjects. **(e)** Elevation [(CS probe entry rate)/(CS probe entry rate + preCS entry rate)] in food-port entries during the CS probe period (after CS onset, before first reward delivery), averaged across trials and CSs for each day of Pavlovian conditioning. Thin light lines represent individual subjects. **(f)** Elevation in lever presses on the lever that earned the same outcome as the presented CS (Same; [(presses on Same lever during CS)/(presses on Same lever during CS + Same presses during preCS)], averaged across trials and across CSs), relative to the elevation in responding on the alternate lever (Different; [(presses on Different lever during CS)/(presses on Different lever during CS + Different presses during preCS)], averaged across trials and across CSs) during the PIT test. Lines represent individual subjects. **(g)** Elevation in food-port entries to CS presentation (averaged across trials and CSs) during the PIT test. Circles represent individual subjects. ArchT, $N = 9$; eYFP, $N = 10$. $^*P < 0.05$.

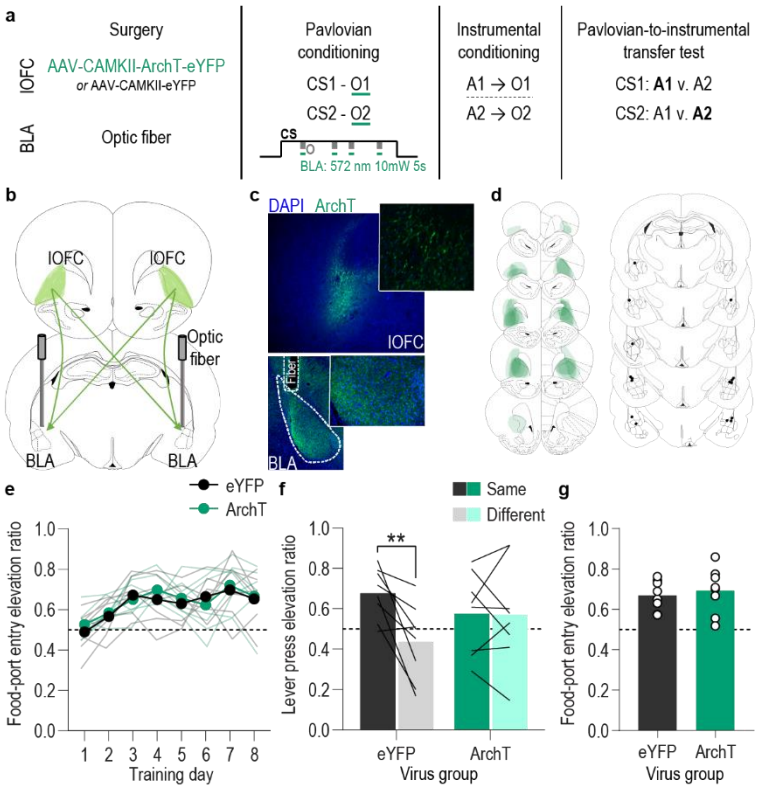

Figure 2-4: Optical inhibition of lOFC terminals in the BLA during stimulus-outcome pairing attenuates the encoding of stimulus-outcome memories.

(a) Procedure schematic. CS, conditional stimulus (white noise or tone); O, outcome (sucrose solution or food pellet); A, action (left or right lever press). **(b)** Schematic of optogenetic strategy for bilateral inhibition of lOFC axons and terminals in the BLA. **(c)** Top: Representative fluorescent image of ArchT-eYFP expression in lOFC cell bodies. Bottom: Representative image of fiber placement in the vicinity of immunofluorescent ArchT-eYFP-expressing lOFC axons and terminals in the BLA. **(d)** Schematic representation of ArchT-eYFP expression in lOFC and placement of optical fiber tips in BLA for all subjects. **(e)** Elevation [(CS probe entry rate)/(CS probe entry rate + preCS entry rate)] in food-port entries during the CS probe period (after CS onset, before first reward delivery), averaged across trials and CSs for each day of Pavlovian conditioning. Thin light lines represent individual subjects. **(f)** Elevation in lever presses on the lever that earned the same outcome as the presented CS (Same; [(presses on Same lever during CS)/(presses on Same lever during CS + Same presses during preCS)], averaged across trials and across CSs), relative to the elevation in responding on the alternate lever (Different; [(presses on Different lever during CS)/(presses on Different lever during CS + Different presses during preCS)], averaged across trials and across CSs) during the PIT test. Lines represent individual subjects. **(g)** Elevation in food-port entries to CS presentation (averaged across trials and CSs) during the PIT test. Circles represent individual subjects. ArchT, $N = 8$; eYFP, $N = 8$. $^{**}P < 0.01$.

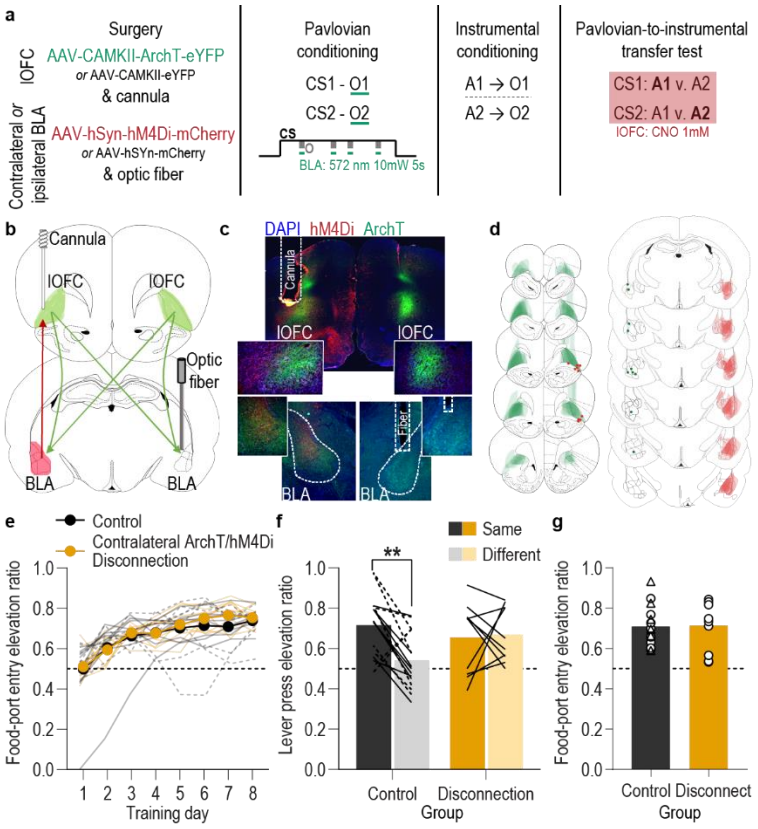

Figure 2-5: Serial disconnection of lOFC→BLA projections during stimulus-outcome pairing from BLA→lOFC projections during Pavlovian-to-instrumental transfer test disrupts stimulus-outcome memory.

(a) Procedure schematic. CS, conditional stimulus (white noise or tone); O, outcome (sucrose solution or food pellet); A, action (left or right lever press); CNO, clozapine-*n*-oxide. **(b)** Schematic of multiplexed optogenetic/chemogenetic inhibition strategy for unilateral optical inhibition of lOFC→BLA projections during Pavlovian conditioning and contralateral, unilateral, chemogenetic inhibition of BLA→lOFC projections during the PIT test. **(c)** Top: Representative fluorescent image of bilateral ArchT-eYFP expression in lOFC cells bodies and unilateral expression of hM4Di-mCherry in BLA axons and terminals in the lOFC in the vicinity of implanted guide cannula. Bottom: Representative image of unilateral BLA fiber placement in the vicinity of immunofluorescent ArchT-eYFP expressing lOFC axons and terminals (right) and unilateral expression of hM4Di-mCherry in BLA cell bodies in the contralateral hemisphere (left). **(d)** Schematic representation of bilateral ArchT-eYFP expression and unilateral cannula placement in lOFC and unilateral hM4Di expression and placement of optical fiber tips in the contralateral BLA for all Contralateral group subjects. Fibers are shown in left and cannula placement in the right hemisphere, but fiber/cannula hemisphere arrangement was counterbalanced across subjects. See Figure 5- Figure Supplement 1 for histological verification of ipsilateral control. **(e)** Elevation [(CS probe entry rate)/(CS probe entry rate + preCS entry rate)] in food-port entries during the CS probe period (after CS onset, before first reward delivery), averaged across trials and CSs for each day of Pavlovian conditioning. Thin light lines represent individual subjects (Contralateral eYFP/mCherry (solid lines) and Ipsilateral ArchT/hM4Di (dashed lines) collapsed into a single control group). **(f)** Elevation in lever presses on the lever that earned the same outcome as the presented CS (Same; [(presses on Same lever during CS)/(presses on Same lever during CS + Same presses during preCS)], averaged across trials and across CSs), relative to the elevation in responding on the alternate lever (Different; [(presses on Different lever during CS)/(presses on Different lever during CS + Different presses during preCS)], averaged across trials and across CSs) during the PIT test. Lines represent individual subjects. **(g)** Elevation in food-port entries to CS presentation (averaged across trials and CSs) during the PIT test. Data points represent

individual subjects, triangles indicate ipsilateral control subjects. Control, $N = 16$; Contralateral disconnection group, $N = 10$. $^{**}P < 0.01$.

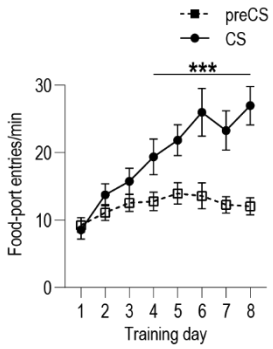

Figure 2-6: Food-port entry rate during Pavlovian conditioning for BLA fiber photometry GCaMP6f imaging experiment.

Food-port entry rate (entries/min) during the CS probe period (after CS onset, before first reward delivery), averaged across trials and across the 2 CSs for each day of Pavlovian conditioning. Rats increased food-port approach responses to the CS across training (CS x Training: $F_{(7,70)} = 15.31$, $P < 0.0001$; CS: $F_{(1,10)} = 48.30$, $P < 0.0001$; Training: $F_{(7,70)} = 10.42$, $P < 0.0001$). *** $P < 0.0001$, relative to preCS.

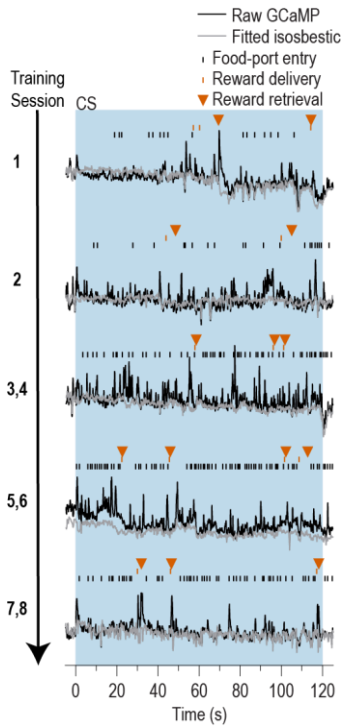

Figure 2-7: Representative examples of raw GCaMP6f and isosbestic fluorescent changes in response to cue presentation and reward delivery and retrieval across days of training.

Raw GCaMP6f (470 nm channel) fluorescence and corresponding fitted fluorescent trace from the isosbestic (415 nm) channel.

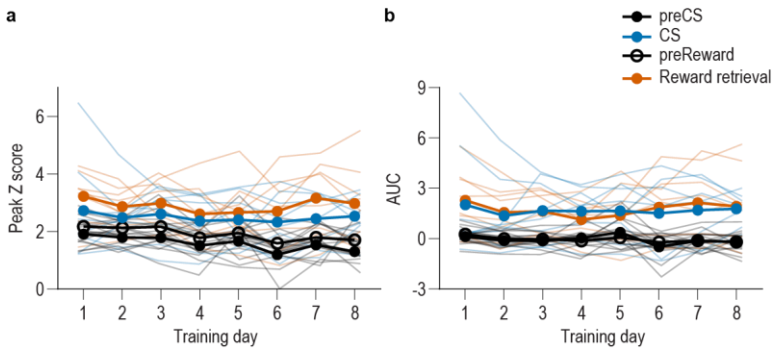

Figure 2-8: BLA neurons are activated during stimulus-outcome learning across each of the 8 Pavlovian conditioning sessions.

(a-b) Trial-averaged quantification of maximal (a; peak) and area under the GCaMP Z-scored ΔF/F curve (b; AUC) during the 3 s following CS onset or reward retrieval compared to equivalent baseline periods immediately prior to each event from the $N = 8$ subjects for which we were able to obtain reliable recordings from each of the 8 Pavlovian conditioning sessions. Thin light lines represent individual subjects. Both CS and reward retrieval caused a similar elevation in the peak calcium response (Event v. baseline $F_{(0.3,1.9)} = 28.14$, $P = 0.03$; Training, Event type (CS/US), and all other interactions between factors, lowest $P = 0.12$) and area under the calcium curve (AUC; Event v. baseline $F_{(0.2,1.2)} = 40.57$, $P = 0.04$, Training, Event type (CS/US), and all other interactions between factors, lowest $P = 0.21$) across training. Analysis of each event relative to its immediately preceding baseline period confirmed that BLA neurons were robustly activated by both the onset of the CS as reflected in the peak calcium response (CS: $F_{(1,7)} = 9.95$, $P = 0.02$; Training: $F_{(3.0,21.3)} = 1.58$, $P = 0.22$; CS x Training: $F_{(1.5,10.7)} = 0.43$, $P = 0.61$) and AUC (CS: $F_{(1,7)} = 9.01$, $P = 0.02$; Training: $F_{(2.3,16.0)} = 0.56$, $P = 0.60$; CS x Training: $F_{(1.5,10.2)} = 0.30$, $P = 0.68$), as well as at reward retrieval during the CS [(Peak, Reward: $F_{(1,7)} = 12.22$, $P = 0.01$; Training: $F_{(3.5,24.1)} = 1.18$, $P = 0.34$; Reward x Training: $F_{(2.5,17.4)} = 1.75$, $P = 0.20$) AUC, Reward: $F_{(1,7)} = 13.73$, $P = 0.008$; Training: $F_{(2.4,17.1)} = 1.19$, $P = 0.34$; Reward x Training: $F_{(3.0,21.3)} = 2.46$, $P = 0.09$)].

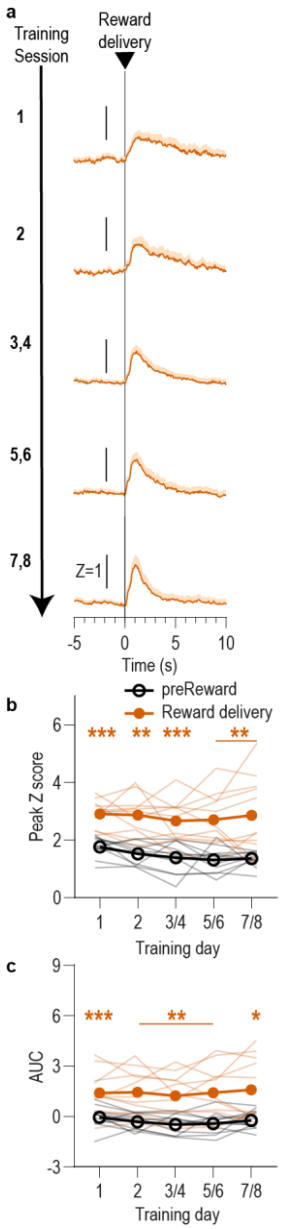

Figure 2-9: BLA reward responses aligned to reward delivery during Pavlovian conditioning.

We detected a robust BLA response to reward retrieval during CS presentation during Pavlovian conditioning. This response was also detected when the data were aligned to reward delivery, which was signaled by the subtle but audible click of the pellet dispenser or sound of the sucrose pump. After initial training, reward retrieval often immediately followed reward delivery. **(a)** Trial-averaged GCaMP6f fluorescence (Z-scored ΔF/F) in response to reward delivery during the CS across days of training. Shading reflects between-subjects s.e.m. Data from the last six training sessions were averaged across 2-session bins (3/4, 5/6, and 7/8). **(b)** Trial-averaged quantification of maximal (peak) GCaMP Z-scored ΔF/F during the 3-s period following reward delivery compared to the equivalent baseline period 3 s prior to reward delivery. Thin light lines represent individual subjects. **(c)** Trial-averaged quantification of area under the GCaMP Z-scored ΔF/F curve (AUC) during the 3 s period following reward delivery compared to the equivalent baseline period. Across training, reward delivery caused a robust elevation in the peak calcium response (Reward delivery: $F_{(1,10)} = 57.73$, $P < 0.0001$; Training: $F_{(2.5,\ 24.8)} = 1.29$, $P = 0.30$; Reward delivery x Training: $F_{(1.8,\ 18.1)} = 0.43$, $P = 0.64$) and area under the calcium curve (Reward delivery: $F_{(1,10)} = 36.44$, $P =$

0.0001; Training: $F_{(2.0, 19.7)} = 0.51$, $P = 0.60$; Reward delivery x Training: $F_{(1.8,17.7)} = 0.39$, $P = 0.66$). N = 11. *$P < 0.05$, **$P < 0.01$, ***$P < 0.001$ relative to pre-event baseline.

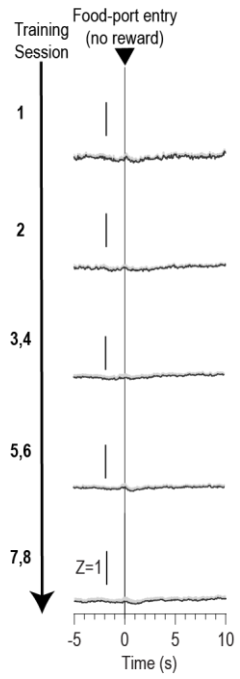

Figure 2-10: Food-port entries during the CS in the absence of reward do not trigger a BLA response.

We detected a robust elevation in BLA calcium activity in response to reward retrieval during CS presentation during Pavlovian conditioning. To determine the extent to which the action of entering the food-delivery port influenced this response, we examined BLA calcium activity in response to food-port entries during the CS probe period (after CS onset, before first reward delivery). Trial-averaged GCaMP6f fluorescence (Z-scored ΔF/F) in response to food-port entries during the CS across days of training. Shading reflects between-subjects s.e.m. Data plotted on the same scale as Figure 1 and 1-4 to facilitate comparison. Data from the last six training sessions were averaged across 2-session bins (3/4, 5/6, and 7/8). N = 11.

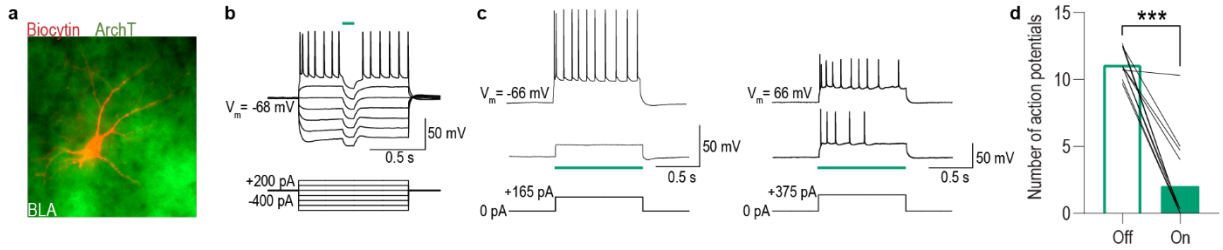

Figure 2-11: Green light activation of ArchT hyperpolarizes and attenuates the firing of BLA cells.

(a) Confocal image of biocytin-filled BLA cell (red) expressing ArchT-eYFP. **(b)** Current-clamp recording of an ArchT-expressing BLA cell responding to hyperpolarizing and depolarizing current injections. When illuminated with green light (535 nm, 100 ms pulse, 0.5 mW), activation of ArchT hyperpolarizes the cell membrane resulting in the absence of action potential firing at suprathreshold membrane potentials. This hyperpolarization of the cell membrane occurs only during green light luminescence. **(c)** Representative recordings from 2 ArchT-expressing BLA cells when injected with a suprathreshold pulse of current (165 or 375 pA 1 s; bottom) with green light off (top) or on (middle). **(d)** Summary of the number of action potentials recorded in ArchT-expressing BLA cells (N = 12 cells/5 subjects) injected with a suprathreshold amount of current before (Off) and during (On) green light illumination (median = 1 mW, range = 0.25-1). Current injection intensities that resulted in 8-15 action potentials were selected for recordings (median = 275 pA, range 100-800 pA, duration = 1 s). Number of action potentials was averaged across 3 sweeps/condition. Green light activation of ArchT in BLA cells reduced action potential firing in all cells and abolished (>97% reduction) it in most cells. The average number of action potentials recorded during green light exposure was significantly lower than the control no-light period (t_{11} = 9.25, P < 0.0001). Lines represent individual cells. ***P < 0.001.

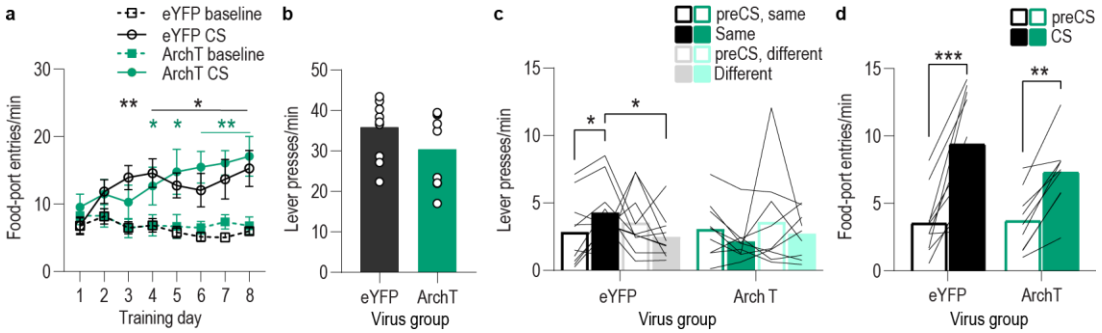

Figure 2-12: Food-port entry and press rates during Pavlovian conditioning and PIT test for BLA optical inhibition experiment.

(a) Food-port entry rate (entries/min) during CS probe period (after CS onset, before first reward delivery), averaged across trials and across CSs for each day of Pavlovian conditioning. There was no effect of BLA inhibition during reward retrieval on the development of this Pavlovian conditional goal-approach response (CS x Training: $F_{(3.4,57.8)} = 16.44$, $P < 0.0001$; CS: $F_{(1,17)} = 46.73$, $P < 0.0001$; Virus: $F_{(1,17)} = 0.17$, $P = 0.68$; Training: $F_{(2.3,38.5)} = 2.37$, $P = 0.10$; Virus x Training: $F_{(7,119)} = 1.55$, $P = 0.16$; Virus x CS: $F_{(1,17)} = 0.0009$, $P = 0.98$; Virus x Training x CS: $F_{(7,119)} = 1.63$, $P = 0.13$). $^{*}P < 0.05$, $^{**}P < 0.01$ relative to pre-CS. **(b)** Lever press rate (presses/min) averaged across levers and across the final 2 days of instrumental conditioning. There was no significant difference in press rate between the control group and the group that received BLA inhibition during Pavlovian conditioning ($t_{17} = 1.44$, $P = 0.17$). Circles represent individual subjects. **(c).** Lever press rate (presses/min) on the lever earning the same outcome as the presented CS (averaged across trials and CSs), relative to the press rate on the alternate lever (Different) during the PIT test. Planned comparisons (Levin et al., 1994), based on the significant interaction and post hoc effect detected in Figure 3f, showed that for the eYFP control group CS presentation significantly increased responding on the lever that earned the same reward as that predicted by the presented CS relative to the preCS baseline period ($t_9 = 3.11$, $P = 0.01$). The CSs did not significantly alter responses on the different lever in the control group ($t_9 = 1.35$, $P = 0.21$). For the ArchT group, the CSs were not capable of significantly altering lever pressing relative to the baseline period (Same: $t_8 = 2.13$, $P = 0.07$; Different: $t_8 = 0.77$, $P = 0.46$). Lines represent individual subjects. **(d)** Food-port entry rate during CS presentation (averaged across trials and CSs) during the PIT test. For both groups CS presentation triggered a similar elevation in this goal-approach behavior (CS: $F_{(1,17)} = 59.41$, $P < 0.0001$; Virus: $F_{(1,17)} = 0.63$, $P = 0.44$; Virus x CS: $F_{(1,17)} = 3.42$, $P = 0.08$). Lines represent individual subjects. $^{*}P < 0.05$, $^{***}P < 0.001$.

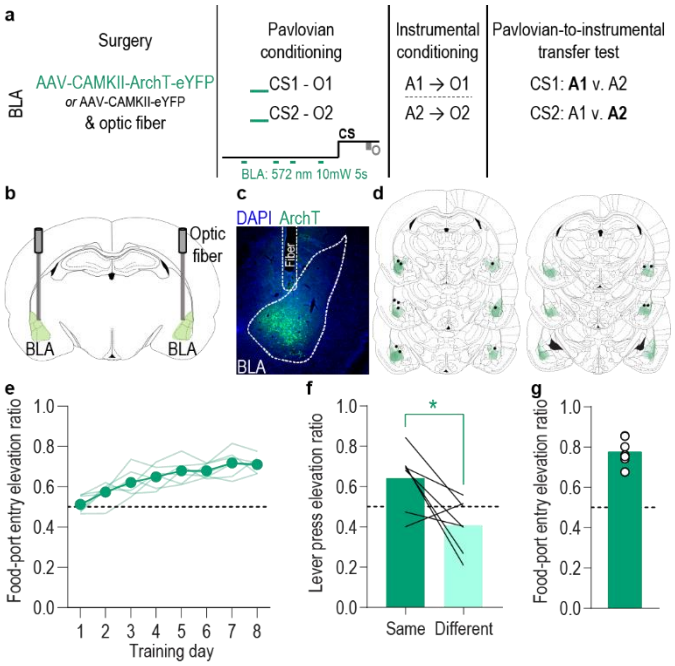

Figure 2-13: Inhibition of BLA neurons unpaired with reward delivery does not disrupt the encoding of stimulus-outcome memories.

We found that inhibition of BLA neurons specifically at the time of outcome experience during each CS during Pavlovian conditioning attenuated subjects' encoding of the sensory-specific stimulus-outcome memories, as evidenced by their inability to later use those memories to guide choice behavior during a PIT test. To control for the total amount of BLA inhibition during Pavlovian conditioning, we repeated the BLA inhibition experiment in a separate group of subjects matching the frequency and duration of inhibition to the experimental group (Figure 3), but delivering it during the baseline, 2-min pre-CS periods. We selected this period for control inhibition to maintain proximity to the CS period but avoid inhibition during the CS at periods in which the rat might be expecting, checking for, and/or retrieving reward, events that were not possible for us to time. **(a)** Procedure schematic. CS, conditional stimulus; O, outcome (sucrose solution or food pellet); A, action (left or right lever press). **(b)** Schematic of optogenetic strategy for inhibition of BLA neurons. **(c)** Representative fluorescent image of ArchT-eYFP expression and fiber placement in the BLA. **(d)** Schematic representation of ArchT-eYFP expression and placement of optical fiber tips in BLA for all subjects. **(e)** Elevation [(CS probe entry rate)/(CS probe entry rate + preCS entry rate)] in food-port entries during CS probe period (after CS onset, before first reward delivery), averaged across trials and CSs for each day of Pavlovian conditioning. Optical inhibition of BLA neurons unpaired with reward delivery did not affect development of the Pavlovian conditional goal-approach response (Training: $F_{(3.4,20.6)} = 16.83$, $P < 0.0001$). Thin light lines represent individual subjects. **(f)** Elevation in lever presses on the lever that earned the same outcome as the presented CS (Same; [(presses on Same lever during CS)/(presses on Same lever during CS + Same presses during preCS)], averaged across trials and across CSs), relative to the elevation in responding on the alternate lever (Different; [(presses on Different lever during CS)/(presses on Different lever during CS + Different presses during preCS)], averaged across trials and CSs) during the PIT test. Inhibition of BLA neurons unpaired with reward delivery during the Pavlovian conditioning sessions did not affect the subsequent ability of the CSs to bias instrumental choice behavior during the PIT test ($t_6 = 2.88$, $P = 0.03$). Lines represent individual subjects. **(g)** Elevation in food-port entries to CS presentation (averaged across trials and CSs) during the PIT test. The CSs were also capable of elevating food-port entries above baseline during the PIT test. Circles represent individual subjects. $N = 7$. $^*P < 0.05$, corrected post hoc comparison.

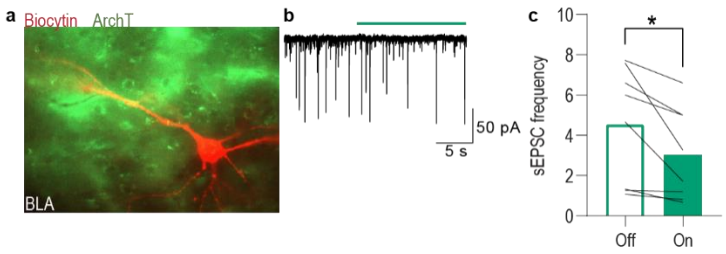

Figure 2-14: Green light activation of ArchT-expressing lOFC terminals reduces spontaneous activity in BLA neurons

(a) Confocal image of biocytin-filled BLA neuron (red) in the vicinity of ArchT-eYFP-expressing lOFC axons and terminals. **(b)** Representative recording of spontaneous excitatory postsynatic currents (sEPSCs) in a BLA neuron before and during green light (535 nm, 0.5 mW, 15 s; green bar) activation of ArchT in lOFC axonal processes. **(c)** Average change in sEPSC frequency in BLA cells induced by green light activation of ArchT-expressing lOFC axons and terminals in the BLA for the subset (N = 8 cells/4 subjects) of total cells (N = 12) that displayed a reduction in sEPSC frequency during light. Of the remaining 4 cells, 2 showed no change in sEPSC frequency during light and 2 show an increase in frequency. Optical inhibition of lOFC terminals in the BLA resulted in a reduction in the spontaneous activity of these BLA cells (t_7 = 2.92, P = 0.02). Lines represent individual cells. *P < 0.05.

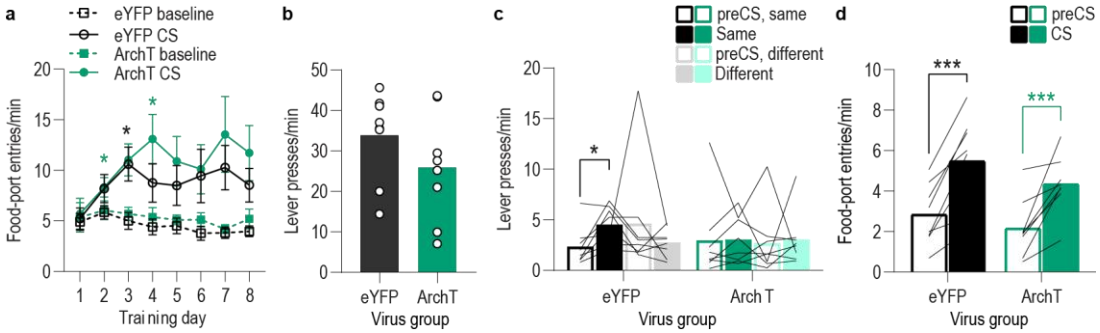

Figure 2-15: Food-port entry and press rates during Pavlovian conditioning and PIT test for lOFC→BLA optical inhibition experiment.

(a) Food-port entry rate (entries/min) during CS probe period (after CS onset, before first reward delivery), averaged across trials and CSs for each day of Pavlovian conditioning. There was no effect of inhibition of lOFC→BLA projection activity during reward delivery on the development of this Pavlovian conditional goal-approach response (CS x Training: $F_{(3.5,49.1)} = 5.50$, $P = 0.002$; CS: $F_{(1,14)} = 27.94$, $P = 0.0001$; Virus: $F_{(1,14)} = 0.82$, $P = 0.38$; Training: $F_{(2.0,28.3)} = 1.88$, $P = 0.17$; Virus x Training: $F_{(7,98)} = 0.48$, $P = 0.85$; Virus x CS: $F_{(1,14)} = 0.40$, $P = 0.54$; Virus x Training x CS: $F_{(7,98)} = 0.62$, $P = 0.74$). $^{*}P < 0.05$, $^{**}P < 0.01$ relative to pre-CS. **(b)** Lever press rate (presses/min) averaged across levers and across the final 2 days of instrumental conditioning. There was no significant difference in press rate between the control group and the group that received inhibition of lOFC→BLA projection activity during Pavlovian conditioning ($t_{14} = 1.29$, $P = 0.22$). Circles represent individual subjects. **(c).** Lever press rate (presses/min) on the lever that earned the same outcome as the presented CS (averaged across trials and across CSs), relative to the press rate on the alternate lever (Different) during the PIT test. Planned comparisons, based on the significant interaction and post hoc effect detected in Figure 4f, showed that for the eYFP group CS presentation significantly increased responding on the lever that earned the same reward as that predicted by the presented CS relative to the preCS baseline period ($t_7 = 3.16$, $P = 0.02$). The CSs did not significantly alter responses on the different lever in the control group ($t_7 = 1.05$, $P = 0.33$). For the ArchT group, the CSs were not capable of significantly altering lever pressing relative to the baseline period (Same: $t_7 = 0.07$, $P = 0.95$; Different: $t_7 = 0.22$, $P = 0.83$). Lines represent individual subjects. **(d)** Food-port entry rate during CS presentation (averaged across trials and across CSs) during the PIT test. For both groups CS presentation triggered a similar significant elevation in this goal-approach behavior (CS: $F_{(1,14)} = 49.96$, $P < 0.0001$; Virus: $F_{(1,14)} = 1.35$, $P = 0.26$; Virus x CS: $F_{(1,14)} = 0.44$, $P = 0.52$). Lines represent individual subjects. $^{*}P < 0.05$, $^{***}P < 0.001$.

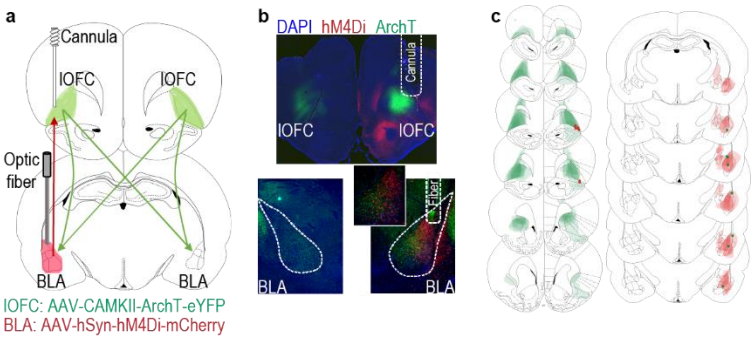

Figure 2-16: Histological verification for unilateral, ipsilateral lOFC→BLA/BLA→lOFC inhibition subjects.

(a) Schematic of multiplexed optogenetic/chemogenetic inhibition strategy for unilateral optical inhibition of lOFC→BLA projections during Pavlovian conditioning and ipsilateral, unilateral, chemogenetic inhibition of BLA→lOFC projections during the PIT test. **(b)** Top: Representative fluorescent image of ArchT-eYFP expression in lOFC cells bodies and unilateral expression of hM4Di-mCherry in BLA axons and terminals in the lOFC in the vicinity of implanted guide cannula. Bottom: Representative image of fiber placements in the vicinity of immunofluorescent ArchT-eYFP expression in lOFC axons and terminals in the BLA and unilateral expression of hM4Di-mCherry in BLA cell bodies in that same hemisphere. **(c)** Schematic representation of bilateral ArchT-eYFP expression and unilateral cannula placement in lOFC and unilateral, ipsilateral hM4Di expression and placement of optical fiber tips in BLA for all subjects. All fibers and cannula are shown in left hemisphere, but inhibited hemisphere was counterbalanced across subjects.

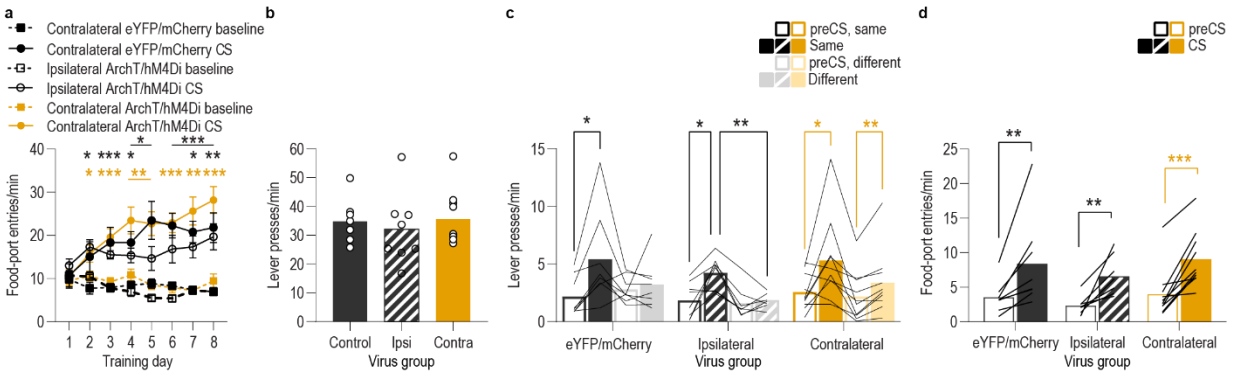

Figure 2-17: Food-port entry and press rates during Pavlovian conditioning and PIT test for lOFC→BLA/BLA→lOFC serial disconnection experiment.

(a) Food-port entry rate (entries/min) during CS probe period (after CS onset, before first reward delivery), averaged across trials and CSs for each day of Pavlovian conditioning. There was no effect of unilateral lOFC→BLA inhibition during reward delivery on the development of this Pavlovian conditional goal-approach response in either the disconnection or ipsilateral control group (CS x Training: $F_{(3.4,78.6)}$ = 23.07, P < 0.0001; CS: $F_{(1,23)}$ = 131.7, P < 0.0001; Virus group: $F_{(2,23)}$ = 1.42, P = 0.26; Training: $F_{(3.7,85.4)}$ = 3.95, P = 0.007; Virus x Training: $F_{(7.4,85.43)}$ = 2.24, P = 0.04; Virus x CS: $F_{(2,23)}$ = 1.19, P = 0.32; Virus x Training x CS: $F_{(6.8,78.6)}$ = 1.36, P = 0.24). ** < 0.05, **P < 0.01, ***P < 0.001, relative to preCS (top, eYFP/mCherry; middle, ipsilateral ArchT/hM4Di; bottom, contralateral ArchT/hM4Di). **(b)** Lever press rate (presses/min) averaged across levers and across the final 2 days of instrumental conditioning. There was no significant difference in press rate between the control groups and the disconnection group ($F_{(2,23)}$ = 0.30, P = 0.75). Circles represent individual subjects. **(c).** Lever press rate (presses/min) on the lever that earned the same outcome as the presented CS (averaged across trials and across CSs), relative to the press rate on the alternate lever (Different) during the PIT test. Planned comparisons, based on the results detected in Figure 5f, showed that for the contralateral eYFP/mCherry control subjects CS presentation significantly increased responding on the action earning the same reward as that predicted by the presented cue relative to the preCS baseline period (t_7 = 3.30, P = 0.01). The CSs did not significantly alter responses on the different lever in this group (t_7 = 0.58, P = 0.58). For the ipsilateral ArchT/hM4Di control subjects, CS presentation increased responding on the Same action relative to both the preCS baseline period (t_7 = 3.43, P = 0.01) and to the different action during the CS (t_7 = 4.51, P = 0.003). The CSs also did not significantly alter responses on the different lever in this control group (t_7 = 0.67, P = 0.52). For the Disconnection (contralateral ArchT/hM4Di) group, the CSs caused a non-discriminate increase in lever pressing relative to the baseline period on both levers (Same: t_9 = 2.54, P = 0.03; Different: t_9 = 3.92, P = 0.004). Lines represent individual subjects. **(d)** Food-port entry rate during CS presentation (averaged across trials and across CSs) during the PIT test. For all groups, CS presentation triggered a similar significant elevation in this goal-approach behavior (CS: $F_{(1,23)}$ = 47.67, P < 0.0001; Virus: $F_{(2,23)}$ = 0.86, P = 0.44; Virus x CS: $F_{(2,23)}$ = 0.14, P = 0.87). Lines represent individual subjects. Contra, contralateral. *P < 0.05, **P < 0.01, ***P < 0.001.

Chapter 3: Dopamine projections to the basolateral amygdala mediate the encoding of outcome-specific reward memories

ABSTRACT

To make adaptive decisions, we must accurately anticipate potential outcomes (e.g., rewarding events) that might be available. This is facilitated by environmental cues, which we use to retrieve detailed reward memories that enable the predictions and inferences critical for decision making. Although canonically thought to only cache value to predictive cues, emerging evidence suggests ventral tegmental area (VTA) dopamine might also be involved in learning the relationship between a cue and the specific reward it predicts. Our goal here was to explore dopamine's putative role in such model-based learning and to reveal the projection through which this function is achieved. One candidate projection target is the basolateral amygdala (BLA). We recently demonstrated that BLA principal neurons mediate the encoding of sensory-specific stimulus-reward memories. Using optical imaging and manipulation methods coupled with Pavlovian cue-reward conditioning and the outcome-specific Pavlovian-to-instrumental transfer task, we found VTA dopamine projections to the BLA to be both necessary and sufficient for linking stimuli to the unique rewards they predict, enabling the use of these rich associative memories to inform decision making. Thus, these data reveal a pathway through which dopamine achieves its function in model-based learning and, more broadly, they expose a critical circuit that drives the rich associative learning necessary for adaptive decision making.

INTRODUCTION

Adaptive decision making requires accurate and detailed representation of potential available rewards. Predictive cues facilitate these mental simulations, allowing one to infer which specific rewards might be available and choose accordingly. This process relies on encoded relationships between the cues and the sensory-specific, identifying features of the rewards they predict, referred to as stimulus-outcome memories (Delamater, 2012; Fanselow and Wassum, 2015). For instance, pizza and doughnut boxes outside the seminar room are cues that let you know which specific food items are available. Such memories contribute to an 'internal model' of the relationships between environmental events that is critical for the predictions and inferences that underlie flexible, advantageous decision making. Studies indicate ventral tegmental dopamine neurons (VTA_{DA}) can provide a teaching signal that facilitates learning essential elements of this model (Wunderlich et al., 2012; Sadacca et al., 2016; Nasser et al., 2017; Sharpe et al., 2017; Langdon et al., 2018; Sharpe et al., 2020), including the identity of outcomes predicted by external cues (Chang et al., 2017; Keiflin et al., 2019). But the projections through which dopamine mediates detailed associative learning is unknown.

One likely candidate is the basolateral amygdala (BLA). VTA dopamine neurons directly project to the BLA (Fallon and Ciofi, 1992; Brinley-Reed and McDonald, 1999), which is itself a crucial hub for sensory-specific cue-reward memories (Corbit and Balleine, 2005; Malvaez et al., 2015; Lichtenberg and Wassum, 2016; Lichtenberg et al., 2017; Morse et al., 2020; Lichtenberg et al., 2021; Sias et al., 2021). Dopaminergic inputs to the BLA influence Pavlovian fear conditioning (Nader and LeDoux, 1999; Greba and Kokkinidis, 2000; Greba et al., 2001; Pezze and Feldon, 2004; de Oliveira et al., 2011; de Souza Caetano et al., 2013; Tang et al., 2020), but few studies have investigated the function of this innervation in the context of appetitive learning (See et al., 2001; Esber et al., 2012; Lutas et al., 2019) and nothing is known regarding the contribution of VTA_{DA}→BLA projections to encoding outcome-specific reward memories. Therefore, here we used optical recordings of BLA dopamine and optical manipulations of

VTA_{DA}→BLA activity to evaluate the role of this pathway in forming the association between predictive cues and the unique features of their associated outcomes.

RESULTS

BLA neurons are active during stimulus-outcome learning

We recently demonstrated that BLA principal neurons are activated during detailed stimulus-outcome learning when unique food rewards were delivered intermittently throughout 2 min auditory cues (Sias et al., 2021). Work from others shows that, with learning, dopamine neurons shift responding from an initially unexpected outcome to a cue that precedes it (Schultz et al., 1993; Schultz et al., 1997). Thus, to investigate the potential involvement of VTA_{DA}→BLA projections in stimulus-outcome learning, we first wanted to confirm our prior results using a delayed conditioning task, where cues precede the delivery of distinct outcomes (Figure 3-1c). Food deprived male and female rats received 8 sessions of Pavlovian conditioning. During each session, 2, 30 sec auditory conditional stimuli (white noise and click) were presented 8 times each (variable ITI, mean = 2.5 min) and each terminated in the delivery of one of two distinct food rewards (sucrose or grain pellets; e.g. white noise→sucrose/click→pellets). Rats developed a Pavlovian conditional response, increasing their entries into the food-delivery port during CS presentation (before reward delivery) relative to a CS-free baseline period (preCS) across training (Figure 3-1d; Training: $F_{(3.30, 23.10)} = 4.85$, $P = 0.008$; CS period (preCS vs CS): $F_{(1, 7)} = 80.33$, $P < 0.0001$; Training x CS period: $F_{(2.44, 17.07)} = 7.97$, $P = 0.002$).

To characterize the endogenous activity of BLA neurons during the encoding of appetitive, outcome-specific Pavlovian memories, we used fiber photometry to image the fluorescent activity of the genetically encoded calcium indicator GCaMP6f (Chen et al., 2013) each day during Pavlovian conditioning (Figure 3-1a-c). GCaMP6f was expressed preferentially in principal neurons based on expression of calcium/calmodulin-dependent protein kinase, CaMKII (Butler et al., 2011; Tye et al., 2011). Data from the eight training sessions were binned into five conditioning phases, session 1, session 2, sessions 3/4, 5/6, and 7/8. Thus, data from the last six

sessions were averaged across two-session bins. Group-averaged traces (Figure 3-1f; Figure 3-2) reveal that BLA neurons were robustly activated both at cue onset and at cue offset, when the outcome was delivered. Both cue onset and outcome delivery caused an elevation in peak calcium response, which varied across training and was greater for outcome delivery relative to CS onset (Figure 3-1e; Event (preCS/CS onset/outcome delivery): $F_{(1.39, 9.71)} = 58.63$, $P < 0.0001$; Training x Event: $F_{(2.52, 17.61)} = 3.94$, $P = 0.03$; Training $F_{(1.71, 11.97)} = 2.29$, $P = 0.15$; see also Figure 3-2). Thus, the BLA is activated by critical events during stimulus-outcome learning, with activation being particularly robust upon reward delivery, an essential period for linking cues to the sensory-specific features of the outcomes they predict.

Dopamine is released in the BLA during stimulus-outcome learning

We next sought to investigate whether and when dopamine is released in the BLA during detailed stimulus-outcome learning. To monitor endogenous dopamine activity, we imaged the fluorescent activity of the GPCR-activation-based-DA (GRABDA) sensor (Sun et al., 2020), expressed in the BLA, each day of Pavlovian conditioning (Figure 3-3a-c). Male and female rats received 8 Pavlovian condition sessions as described above and developed a Pavlovian conditional response across training (Figure 3-3d; Training: $F_{(4.75, 38.02)} = 2.76$, $P = 0.03$; CS period (preCS vs CS): $F_{(1, 8)} = 44.00$, $P = 0.0002$; Training x CS period: $F_{(2.77, 22.15)} = 14.69$, $P < 0.0001$). Data from the eight training sessions were binned into five conditioning phases, session 1, session 2, sessions 3/4, 5/6, and 7/8. Group-averaged traces (Figure 3-3f; Figure 3-4) reveal that BLA neurons were activated both at cue onset and at the time of outcome delivery. Outcome delivery caused an elevation in peak calcium response present across training; elevations were also detected for CS onset, though to a lesser degree (Figure 3-3e; Training: $F_{(2.14, 17.14)} = 1.07$, $P = 0.37$; Event (preCS/CS onset/outcome delivery): $F_{(1.89, 15.08)} = 16.07$, $P = 0.0002$; Training x Event: $F_{(3.79, 30.35)} = 0.84$, $P = 0.51$; see also Figure 3-4). This indicates that dopamine is released into the BLA most prominently when outcomes are delivered, a critical window for learning during which BLA neurons are also activated.

VTA_{DA}→BLA projections are necessary for encoding detailed Pavlovian stimulus-outcome memories

BLA principal neurons are activated during a time when stimulus-outcome memories can be formed and when dopamine is also released into the BLA: when reward is delivered following a predictive cue. We next asked whether activation of VTA_{DA}→BLA projections coincident with delivery of a unique food reward is also necessary for encoding sensory-specific stimulus-outcome memories (Figure 3-5d). Prior to training, we expressed the inhibitory opsin archaerhodopsin T (ArchT) or tdTomato control in VTA_{DA} neurons of Th-cre^{+} rats and implanted optic fibers over ArchT-expressing terminals in the BLA to transiently inactivate these projections upon delivery of green light (532nm; 10Mw; Figure 3-5a-c). Rats then received 11 days of instrumental conditioning, without manipulation, where both groups learned that two actions (left or right lever press) each earned one of two distinct food rewards (e.g. left press→sucrose/right press→pellets; Figure 3-5d-e; Last 2 days averaged press rates: $t_{(19)} = 0.07$, $P = 0.94$). In the following 8 Pavlovian conditioning sessions, each 30 sec auditory CS was presented 8 times and terminated in the delivery of one of the unique food rewards experienced during instrumental conditioning. VTA_{DA}→BLA projections were optically inhibited upon delivery of food reward during each session. We restricted optical inhibition to 3 sec concurrent with the delivery each food reward because this is the time at which the stimulus-outcome pairing occurs and when we detected robust BLA neuronal activation and dopamine release in the BLA (Figure 3-1 and 3-3). Optical inhibition of VTA_{DA}→BLA projections during Pavlovian conditioning did not disrupt collection of the earned reward (Figure 3-6). It also did not impede the development of a Pavlovian conditional goal approach response (Figure 3-5f; Training: $F_{(1.47, 27.98)} = 1.19$, $P = 0.31$; Virus (tdTomato vs ArchT): $F_{(1,19)} = 0.05$, $P = 0.83$; CS period: $F_{(1,19)} = 10.34$, $P = 0.005$; Training x Virus: $F_{(7,133)} = 1.23$, $P = 0.29$; Training x CS period: $F_{(4.09, 77.71)} = 5.73$, $P = 0.0004$; Virus x CS period: $F_{(1,19)} = 1.04$, $P = 0.32$; Training x Virus x CS period: $F_{(7,133)} = 0.75$, $P = 0.63$). This general conditional response at the shared food port, however, does not require that the subjects have

learned the sensory-specific details of the predicted reward. To test for such stimulus-outcome memory encoding, we gave subjects an outcome-specific Pavlovian to Instrumental Transfer test, conducted without any manipulation. During the test both levers were present, but lever pressing was not rewarded. Each CS was presented four times (also without accompanying reward), with intervening CS-free baseline periods, to assess its influence on action performance and selection in the novel choice scenario. Because the cues are never directly associated with the instrumental actions, this test assesses the ability to upon cue presentation, retrieve a representation of the specific predicted reward and use it to motivate choice of the action known to earn the same unique outcome (Kruse et al., 1983; Colwill and Motzkin, 1994; Corbit and Balleine, 2016). If subjects had encoded detailed stimulus-outcome memories during Pavlovian conditioning, then the CS should cause them to increase presses selectively on the lever that, during training, earned the *same* outcome as predicted by that cue. Controls showed this outcome-specific PIT effect. Conversely, the cues were not capable of adaptively biasing lever-press choice in the group for which VTA_{DA}→BLA projections were inhibited at the time of outcome delivery during Pavlovian conditioning (Figure 3-5g; Virus: $F_{(1, 19)} = 0.93$, $P = 0.35$; Lever (Same vs Different): $F_{(1, 19)} = 3.36$, $P = 0.08$; CS period (CS vs preCS): $F_{(1, 19)} = 22.02$, $P = 0.0002$; Virus x Lever: $F_{(1, 19)} = 0.12$, $P = 0.73$; Virus x CS period: $F_{(1, 19)} = 0.37$, $P = 0.55$; Lever x CS period: $F_{(1, 19)} = 0.25$, $P = 0.62$; Virus x Lever x CS period: $F_{(1, 19)} = 2.63$, $P = 0.12$). Whereas in controls the presence of the CS increased pressing for the lever associated with the same outcome (CS: Same), respective to the preCS baseline period, but not for the lever associated with the alternative outcome (CS: Different), the opposite pattern was observed for subjects that had received VTA_{DA}→BLA inhibition. Quantifying CS-induced changes in press rate as an elevation ratio similarly revealed a selective elevation in responses for the Same lever relative to the Different lever, which was only present in controls (Figure 3-5h; Virus x Lever: $F_{(1, 19)} = 9.22$, $P = 0.007$; Virus: $F_{(1, 19)} = 0.33$, $P = 0.57$; Lever: $F_{(1, 19)} = 0.45$, $P = 0.51$). As in training, during this PIT test the conditional goal-approach response was similar between groups (Figure 3-5i; Virus x CS period: $F_{(1, 19)} = 0.008$, $P = 0.93$; Virus: $F_{(1, 19)} =$

1.15, $P = 0.30$; CS period: $F_{(1, 19)} = 15.18$, $P = 0.001$). Thus, activation of VTA_{DA}→BLA projections is not needed for the learning that supports general conditional approach, but is necessary, specifically at the time of outcome delivery, to link the sensory-specific details of the outcome to a predictive cue. Such encoding is critical for that cue to subsequently guide decision making.

Optical stimulation of VTA_{DA}→BLA projections is sufficient to drive encoding of sensory-specific stimulus-outcome memories

The finding that VTA_{DA}→BLA projections are necessary for encoding sensory-specific stimulus-outcome memories suggest activity in these projections may also be sufficient for driving such encoding. To address this, we first adapted a Pavlovian blocking protocol (Rescorla, 1999), that would allow us to determine if stimulating these projections can rescue sensory-specific stimulus-outcome learning in circumstances where this learning is prevented (Figure 3-7a). Prior to behavioral training, rats were assigned to either a Pavlovian blocking or no-blocking control group. All rats received 11 days of instrumental conditioning, where they learned that two actions each earnt a specific food reward (sucrose or grain pellets; Figure 3-7b; $t_{(30)} = 1.03$, $P = 0.31$). All subjects then received 12 sessions of Pavlovian conditioning. During each session, rats in the blocking group were conditioned to 2, 30 sec visual stimuli (house light and flashing stimulus light), each terminating in the delivery of 1 of the 2 food outcomes (e.g., house light→sucrose/flashing light→pellet). Each visual CS was presented 16 times per session (mean ITI = 2.5 min). No-blocking controls were conditioned to a third visual stimulus (outside lights; 30 sec duration), which was presented 32 times per session (mean ITI = 2.5 min) and terminated in the delivery of one food outcome on half of the trials and the other food outcome in the remaining half. Subjects acquired Pavlovian conditional responses to the visual CSs (Figure 3-7c; Training: $F_{(2.71, 81.41)} = 4.29$, $P = 0.01$; Group (blocking vs control): $F_{(1, 30)} = 0.56$, $P = 0.46$; CS period: $F_{(1, 30)} = 186.2$, $P < 0.0001$; Training x Group: $F_{(11, 330)} = 1.77$, $P = 0.06$; Training x CS period: $F_{(4.55, 136.4)} = 30.77$, $P < 0.0001$; Group x CS period: $F_{(1, 30)} = 0.22$, $P = 0.64$; Session x Group x CS period: $F_{(11, 330)} = 0.98$, $P = 0.47$). In subsequent conditioning sessions, the house light

and flashing light CSs were each paired with one of two distinct auditory stimuli (e.g., white noise or click) to form 2 distinct compound stimuli (e.g., house light+white noise/flashing light+click). All subjects received 4 compound conditioning sessions, where each compound stimulus (30 sec duration) was presented 8 times and terminated in the delivery of one of the distinct food rewards. This was the outcome paired with the visual stimulus in initial Pavlovian conditioning for subjects in the blocking condition. Compound stimulus-outcome pairings were counterbalanced across controls. All subjects demonstrated Pavlovian conditional goal-approach responses to the compound cues (Figure 3-7d; Training: $F_{(1.32, 39.71)} = 0.01$, $P = 0.96$; Group: $F_{(1, 30)} = 0.35$, $P = 0.56$; CS period: $F_{(1,30)} = 173.6$, $P < 0.0001$; Training x Group: $F_{(3, 90)} = 0.12$, $P = 0.95$; Training x CS period: $F_{(2.50, 75.01)} = 0.50$, $P = 0.65$; Group x CS period: $F_{(1, 30)} = 0.51$, $P = 0.48$; Training x Group x CS period: $F_{(3, 90)} = 0.89$, $P = 0.45$). When both elements of a compound stimulus are novel, reinforcement engenders encoding of each of these elements (Kamin, 1968). In controls, because both the visual and auditory stimuli were newly experienced during compound training, subjects should have learned the auditory stimulus-outcome associations. For subjects, in the blocking group, however, the previously encoded visual stimulus-outcome memories should have blocked learning the auditory cues. To specifically assess acquisition of the unique auditory stimulus-outcome relationships, rats were given a PIT test in which action selection was evaluated in the presence of the auditory cues presented alone. Animals in the blocking group were impaired in their ability to use the auditory cues to adaptively guide choice (Figure 3-7e; Group: $F_{(1, 30)} = 0.59$, $P = 0.45$; Lever (Same vs Different): $F_{(1,30)} = 0.06$, $P = 0.81$; CS period (preCS vs CS): $F_{(1,30)} = 29.11$, $P < 0.0001$; Group x Lever: $F_{(1, 30)} = 2.09$, $P = 0.16$; Group x CS period: $F_{(1, 30)} = 4.54$, $P = 0.04$; Lever x CS period: $F_{(1,30)} = 6.24$, $P = 0.02$; Group x Lever x CS period: $F_{(1, 30)} = 0.81$, $P = 0.38$). Whereas controls selectively biased responses towards the action that had earnt the same outcome predicted by each auditory cue, subjects in the blocking group exhibited non-selective, increased pressing on both levers. Assessment of CS-induced elevations in performance confirmed adaptive responding in controls, which was absent in the blocking group (Figure 3-7f;

Lever: $F_{(1, 30)} = 4.35$, P = 0.046; Group: $F_{(1, 30)} = 3.99$, P = 0.055; Group x Lever: $F_{(1, 30)} = 1.57$, P = 0.22). Despite disrupted PIT performance in the blocking condition, expression of conditional goal-approach was preserved (Figure 3-7g; CS period: $F_{(1, 30)} = 154.7$, $P < 0.0001$; Group x CS period: $F_{(1, 30)} = 0.06$, $P = 0.80$; Group: $F_{(1, 30)} = 0.10$, $P = 0.75$).

Using this blocking procedure as a platform, we next asked whether stimulating VTA_{DA}→BLA projections would be sufficient to rescue, or unblock, encoding of sensory-specific stimulus-outcome memories (Figure 3-8a-d). We expressed the excitatory opsin channelrhodopsin (ChR2) or eYFP control in VTA_{DA} neurons of Th-cre rats (Figure 3-8a-b) and implanted optical fibers over the BLA (Figure 3-8c) to allow us to, in ChR2-expressing subjects, transiently stimulate VTA_{DA} axons and terminals in the BLA. Rats first received instrumental conditioning, without manipulation, to learn two action-reward relationships (e.g. left press→sucrose/right press→pellets; Figure 3-8e; $t_{(22)} = 1.39$, $P = 0.18$). They then received visual cue Pavlovian conditioning, also manipulation-free. All subjects received blocking conditions and, thus, during this conditioning had two distinct visual cues each paired with a unique food reward (e.g., house light→sucrose/flashing light→pellet). Both groups similarly developed Pavlovian conditional goal-approach responses with training (Figure 3-8f; Training: $F_{(2.60, 57.21)} = 7.22$, $P = 0.0006$; Virus (Chr2 vs eYFP): $F_{(1, 22)} = 0.67$, $P = 0.42$; CS period: $F_{(1, 22)} = 264.7$, $P < 0.0001$; Training x Virus: $F_{(11, 242)} = 0.47$, $P = 0.92$; Training x CS period: $F_{(4.15, 91.32)} = 25.86$, $P < 0.0001$; Virus x CS period: $F_{(1, 22)} = 2.24$, $P = 0.15$; Training x Virus x CS period: $F_{(11, 242)} = 0.86$, $P = 0.58$). Rats next received compound conditioning during which the each of the visual cues was presented concurrent with an auditory cue for 30 sec terminating in the delivery of the same reward the visual cue had predicted previously (e.g., house light + white noise→sucrose/flashing light + clicker→pellet; 8 of each compound cue/session). During each compound training session, VTA_{DA}→BLA projections were optically stimulated (473 nm; 20 Hz, 10 mW, 3 sec) at the time of outcome delivery. We selected this time period because it is when the stimulus-outcome pairing and, thus, learning can occur. VTA_{DA}→BLA stimulation had no effect on collection of the reward

(Figure 3-9). It also did not affect goal-approach responses to the compound cue (Figure 3-8g; Training: $F_{(1.35, 29.67)} = 6.43$, $P = 0.01$; Virus: $F_{(1, 22)} = 0.88$, $P = 0.36$; CS period: $F_{(1, 22)} = 232.1$, $P < 0.0001$; Training x Virus: $F_{(3, 66)} = 1.01$, $P = 0.40$; Training x CS period: $F_{(2.28, 50.21)} = 9.06$, $P = 0.0002$; Virus x CS period: $F_{(1, 22)} = 0.54$, $P = 0.47$; Training x Virus x CS period: $F_{(3, 66)} = 1.07$, $P = 0.37$). To ask whether rats had encoded an outcome-specific stimulus-outcome memory, they received a PIT test with the auditory cues, without manipulation. We replicated the blocking of outcome-specific stimulus-outcome memories in the eYFP controls, such that they were unable to use the auditory cues to guide their choice behavior. Stimulation of VTA_{DA}→BLA projections during compound training did, however, drive the encoding of outcome-specific stimulus-outcome memories as evidence by the rats ability to use the auditory cues to know which reward was predicted and press on the associated lever (Figure 3-8h; Virus: $F_{(1, 22)} = 0.14$, $P = 0.72$; Lever (Same vs Different): $F_{(1, 22)} = 0.001$, $P = 0.97$; CS period: $F_{(1, 22)} = 7.45$, $P = 0.01$; Virus x Lever: $F_{(1, 22)} = 1.57$, p =0.22; Virus x CS period: $F_{(1, 22)} = 1.24$, $P = 0.28$; Lever x CS period: $F_{(1, 22)} = 1.57$, $P = 0.0002$; Virus x Lever x CS period: $F_{(1, 22)} = 4.48$, $P = 0.046$). Auditory CSs induced greater elevations in performance for actions that had earnt the same outcome predicted by that CS relative to actions that had earnt the other outcome, in subjects that had received VTA_{DA}→BLA stimulation during compound conditioning (Figure 3-8i; Virus x Lever: $F_{(1, 22)} = 5.72$, $P = 0.03$; Virus: $F_{(1, 22)} = 3.29$, $P = 0.08$; Lever: $F_{(1, 22)} = 20.82$, $P = 0.0002$). As in compound conditioning, both groups showed similar conditional goal-approach responses to the cues (Figure 3-8j; Virus x CS period: $F_{(1, 22)} = 1.65$, $P = 0.21$; Virus: $F_{(1, 22)} = 0.08$, $P = 0.77$; CS period: $F_{(1, 22)} = 36.10$, $P < 0.0001$), indicating that optical stimulation of VTA_{DA}→BLA projections did not strengthen the reinforcement of a general conditional response policy. To determine if VTA_{DA}→BLA activation was itself reinforcing, all rats were given two sessions of intracranial self-stimulation. We found that while both groups initially nose poked for 1 sec of blue light delivery to these projections (473nm; 10mW; 20Hz) in the first session, rats expressing ChR2 showed no differences between the number of active (light delivery) and inactive nose pokes (no light) during the second session

(Figure 3-10). Thus, activation of VTA_{DA}→BLA projections is sufficient to drive the encoding of outcome-specific stimulus-outcome memories, but does not, at these stimulation parameters, support reinforcement.

DISCUSSION

These data demonstrate that VTA_{DA}→BLA projections are essential for encoding detailed stimulus-outcome memories, identifying these projections as critical contributors to an internal model of related environmental events that enables adaptive decision making. We found dopamine is released in the BLA at the time of stimulus-outcome pairing, when BLA neurons are also robustly activated and when learning occurs. Activity in VTA_{DA}→BLA projections during this time was necessary for encoding the sensory-specific details of cue-reward memories but was not needed for the development of a Pavlovian goal-approach response policy. Stimulation of VTA_{DA}→BLA projections was sufficient to rescue encoding of outcome-specific cue-reward memories in a novel Pavlovian blocking paradigm but did not enhance Pavlovian goal-approach nor was it inherently reinforcing.

BLA neuron activity and dopamine release in the BLA was elevated upon delivery of unique food outcomes and at the onset of cues that predict them. We observed that CS responses were present on the first day of training. These responses likely reflect the initial novelty of the stimuli early in training, which habituates in the absence of reward (Bordi and LeDoux, 1992; Ljungberg et al., 1992; Bordi et al., 1993; Bunzeck and Düzel, 2006; Sias et al., 2021). Although subjects were pre-exposed to the cues before Pavlovian conditioning, the number of presentations were minimal and may have been insufficient to completely habituate these responses given the robust salience of the auditory stimuli (Schultz, 1998; Hersman et al., 2020). Unlike early in training, cue-evoked activations observed in later conditioning sessions result from associative learning (Muramoto et al., 1993; Schultz et al., 1997; Schoenbaum et al., 1999; Saddoris et al., 2005; Paton et al., 2006; Day et al., 2007; Cone et al., 2016; Sadacca et al., 2016; Lutas et al., 2019; Sias et al., 2021). Dopamine release and neuronal activity in the BLA were also robustly and

consistently activated by rewards throughout training. Although this seemingly contrasts previous reports of neuronal (Belova et al., 2007) and dopaminergic (Lutas et al., 2019) BLA activity attenuating in response to rewards reliably predicted by a preceding stimulus, it in part replicates our previous findings that BLA neurons are persistently activated by unique rewards delivered randomly throughout a cue. These differences may arise from some uncertainty in the timing of reward delivery, which in our delayed conditioning task occurred after a prolonged 30 sec CS and happened intermittently during the CS in the task we used previously. Alternatively, it could relate to the encoding of the unique stimulus-outcome contingencies. BLA and VTA dopamine neurons encode information about an outcome's identity (Takahashi et al., 2017; Liu et al., 2018; Stalnaker et al., 2019), the maintenance of which may promote goal-directed behavior (Courtin et al., 2022). Regardless, these data show that dopamine release coincides with neuronal activation in the BLA during stimulus-outcome pairing in a task that promotes the encoding of detailed associative reward memories. The precise information conveyed by these dopamine responses and whether they directly influence neuronal activation in the BLA during detailed Pavlovian learning are important questions open to investigation.

We found that BLA dopamine release coinciding with reward delivery was necessary for encoding detailed Pavlovian memories. Optically inhibiting VTA_{DA}→BLA projections at the time of reward during Pavlovian conditioning attenuated the animals' ability to encode the sensory-specific details of stimulus-outcome memories to the extent that they were unable to use this information to adaptively inform decision making during the outcome-specific PIT test. A prevailing theory of dopamine's function in associative learning suggests dopamine provides a teaching signal to cache value of future rewarding events to a predictive cue (Schultz, 1998). Thus, while it is possible that inhibiting these projections disrupted learning the outcomes' value, this is unlikely the primary factor driving our results. Neither CS-motivated instrumental action nor Pavlovian conditional food-port approach was generally suppressed during the PIT test in animals that received VTA_{DA}→inhibition during training, contrary to what might be expected if purely

value-driven learning was impaired. Instead, these results arise from an inability to link specific stimuli to the identifying features of the outcomes they predict. We also found inactivating VTA_{DA}→BLA projections had no impact on the acquisition of a Pavlovian conditional response during learning, which does not necessitate encoding outcome-specific information. Consistent with this, the learning underlying the development of this behavior is not dependent on the BLA itself (Hatfield et al., 1996; Sias et al., 2021) and dopamine's involvement in mediating conditioned responses has been shown to be circuit specific (Saunders et al., 2018). Thus, the necessity of VTA→BLA projections in encoding detailed stimulus-outcome memories, but not the development of a Pavlovian response policy, may reflect a specialized function for dopamine within this target region.

Adapting a Pavlovian blocking paradigm from (Rescorla, 1999), we showed that detailed stimulus-outcome memories can be blocked by previously learnt Pavlovian associations. Encoding two distinct auditory stimulus-outcome associations during compound conditioning was prevented by concurrent presentations of visual stimuli when those stimuli were already predictive of the same food rewards. A PIT test revealed subjects were unable to use the auditory cues to selectively motivate choice, suggesting that encoding the sensory specific features of the associated outcomes was blocked by previous learning. This builds upon prior work demonstrating that blocking effects are sensitive to shifts in reward identity. In 1999, Rescorla found disrupted PIT for a cue that, during compound training, was blocked by another stimulus predicting the same outcome but not for a cue that was paired with a stimulus that predicted a different outcome (Rescorla, 1999). A possible confound in these findings is that blocked learning of one cue could have altered learning about the other, unblocked cue, thus biasing the discrepancy in PIT performance. By blocking both auditory stimuli in one group and including a separate, no blocking, control group, we largely ruled out this explanation. Interestingly, we also found that the expression of Pavlovian goal-approach was unaffected by blocking. Such behaviors can be mediated by a stimulus-response strategy that was initially reinforced by a reward's value

(Fanselow and Wassum, 2015). Thus, the distinct effects we observed on cue-motivated lever pressing compared to food-port entries suggests information regarding value may be dissociable from outcome identity in blocked stimulus-outcome memories and emphasizes the need for more complex tests, such as PIT, to evaluate the nature of the disrupted learning.

Optically stimulating VTA_{DA}→BLA projections was sufficient to rescue, or unblock, encoding of sensory-specific stimulus-outcome memories, such that subjects were able to use these memories to make adaptive decisions. This is in line with previous studies demonstrating VTA dopamine neuron activity tracks (Takahashi et al., 2017; Stalnaker et al., 2019) and mediates (Chang et al., 2017; Keiflin et al., 2019) unblocking driven by changes in an outcome's identity. That stimulation of VTA_{DA}→BLA projections resulted in selective motivation for actions associated with the same outcome predicted by the auditory CS during PIT, rather than a non-selective cue-induced increase in lever pressing, suggests activating these projections did not enhance the overall perceived value of the food rewards. This is supported by the observation that stimulation did not enhance Pavlovian conditional goal-approach either during compound conditioning or at test. Furthermore, activation of these projections was not inherently reinforcing as we found that rats expressing ChR2 did not elevate nose poking for VTA_{DA}→BLA stimulation during the second session of ICSS. Elevated nose poking was comparable to eYFP controls during the first session and likely resulted from an association formed between visible light from the laser and reward delivery during compound conditioning, which extinguished by the second session. Though reinforcing effects of directly stimulating VTA dopamine neurons have been established (Crow, 1972; Witten et al., 2011), collectively our results align with findings that activating VTA dopamine neurons can also facilitate learning the associative structure between related events, independent of value (Sharpe et al., 2017). Moreover, we are the first to show that the BLA is a key target region to which dopaminergic projections can drive the link between distinct stimuli and the details of their predicted outcomes.

A critical new question is how dopaminergic innervation of the BLA facilitates sensory-specific stimulus-outcome learning. Although not tested here, dopamine likely exerts its effects through modulation of neural plasticity in the BLA. Dopamine can act on GABAergic interneurons to increase spontaneous inhibitory network activity (Lorétan et al., 2004; Kröner et al., 2005) and can also enhance LTP induction through suppression of feedforward inhibition (Bissière et al., 2003). Like dopaminergic function in the prefrontal cortex (Vander Weele et al., 2018; Stalter et al., 2020), this balance might enhance signal-to-noise by filtering out weak inputs and ensuring only the strongest are potentiated. Authors from a recent study suggest this as a potential mechanism for the emergence of distinct neuronal populations that encode opposing valence in the BLA (Lutas et al., 2019). Given that separate populations of cells in the BLA also encode unique appetitive outcomes (Liu et al., 2018; Courtin et al., 2022), it seems plausible then that through modulation of inhibitory neuron activity, VTA_{DA}→BLA projections may contribute to detailed associative learning by shaping the formation of these neuronal groups. These projections could also be influencing plasticity of principal neurons directly by increasing their excitability (Kröner et al., 2005) and/or cAMP production (Lutas et al., 2022). Future investigation into the BLA cell types dopamine directly interacts with during outcome-specific appetitive learning is warranted. Furthermore, if dopamine is shaping plasticity in the BLA during this form of learning, a second question is which excitatory inputs are potentiated as a result. One likely candidate is projections from the lateral orbital frontal cortex, which are also essential for encoding these rich associative memories (Sias et al., 2021; Costa et al., 2022).

Findings from this study have important implications for how we conceptualize dopamine's function in associative learning. While our data might seem at odds with the canonical view that dopamine signals and assigns cached value to reward predictive cues, they do not negate this interpretation but rather expand upon evidence demonstrating diversity in the range of information dopamine neurons encode (Engelhard et al., 2019). Our work and other's indicate

dopamine's contribution to learning may be multifaceted and largely shaped by the function of downstream target regions (Collins and Saunders, 2020).

METHODS

Housing.

Rats were group housed (2/cage) in a temperature (68-79°F) and humidity (30-70%) regulated vivarium prior to surgery and then subsequently housed individually to preserve implants. Rats were provided with water *ad libitum* in the home cage and were maintained on a food-restricted 12-14 g daily diet (Lab Diet, St. Louis, MO) to maintain ~85-90% free-feeding body weight. Rats were handled for 3-5 days prior to the onset of each experiment. Separate groups of naïve rats were used for each experiment. Experiments were performed during the dark phase of a 12:12 hr reverse dark/light cycle (lights off at 7AM). All procedures were conducted in accordance with the NIH Guide for the Care and Use of Laboratory Animals and were approved by the UCLA Institutional Animal Care and Use Committee.

Apparatus.

Training took place in Med Associates conditioning chambers (East Fairfield, VT) housed within sound- and light-attenuating boxes, described previously (Malvaez et al., 2015). For optogenetic manipulations, the chambers were outfitted with an Intensity Division Fiberoptic Rotary Joint (Doric Lenses, Quebec, QC, Canada) connecting the output fiber optic patch cords to a laser (Dragon Lasers, ChangChun, JiLin, China) positioned outside of the chamber. Each chamber contained 2 retractable levers that could be inserted to the left and right of a recessed food-delivery port (magazine) in the front wall. Stimulus lights were positioned above each of these levers. Chambers used for ICSS experiments also contained 2 nose poke ports on the wall opposite the magazine. A photobeam entry detector was positioned at the entry to the food port. Each chamber was equipped with a syringe pump to deliver 20% sucrose solution in 0.1 ml increments through a stainless-steel tube into one well of the food port and a pellet dispenser to deliver 45-

mg grain pellets (Bio-Serv, Frenchtown, NJ) into another well. A white noise generator was attached to a speaker on the wall opposite the levers and food-delivery port, where a clicker was also directly attached. A fan mounted to the outer chamber provided ventilation and external noise reduction. A 3-watt, 24-volt house light mounted on the top of the back wall opposite the food-delivery port provided illumination, except in Pavlovian blocking experiments where it was used as a conditional stimulus.

General histological procedures.

Following behavioral experiments, rats were deeply anesthetized with Nembutal and transcardially perfused with phosphate buffered saline (PBS) followed by 4% paraformaldehyde (PFA). Brains were removed and post-fixed in 4% PFA overnight, placed into 30% sucrose solution, then sectioned into 30 μm slices using a cryostat and stored in cryoprotectant. Slices were rinsed in a DAPI solution for 4 min (5mg/mL stock, 1:10000), washed 3 times in PBS for 15 min, mounted on slides and coverslipped with ProLong Gold mounting medium. Images were acquired using a Keyence BZ-X710 microscope (Keyence, El Segundo, CA) with a 4x,10x, and 20x objective (CFI Plan Apo), CCD camera, and BZ-X Analyze software.

Statistical analysis.

Datasets were analyzed by two-tailed, paired and unpaired Student's *t* tests, two-, or three-way repeated-measures analysis of variance (ANOVA), as appropriate (GraphPad Prism, GraphPad, San Diego, CA; SPSS, IBM, Chicago, IL). For well-established behavioral effects (PIT), multiple pairwise were used for a priori *post hoc* comparisons, as advised by ref (Levin et al., 1994) based on a logical extension of Fisher's protected least significant difference procedure for controlling familywise Type I error rates. All other *post hoc* tests were corrected for multiple comparisons using the Bonferroni method and used to clarify main and interaction effects. Greenhouse-Geisser

correction was applied to mitigate the influence of unequal variance between conditions. Alpha levels were set at $P < 0.05$.

Rigor and reproducibility.

Group sizes were estimated *a priori* based on prior work using male Long Evans rats in this behavioral task (Malvaez et al., 2015; Lichtenberg and Wassum, 2016; Lichtenberg et al., 2017) and to ensure counterbalancing of CS-reward and Lever-reward pairings. Male and Female rats were used in approximately equal numbers for each analysis, but the *N* per sex was underpowered to examine sex differences. Sex was therefore not included as a factor in statistical analyses, though individual data points are visually disaggregated by sex. Investigators were not blinded to viral group because they were required to administer virus. All behaviors were scored using automated software (MedPC). Each primary experiment included at least 1 replication cohort and cohorts were balanced by viral group, CS-reward and Lever-reward pairings, hemisphere etc. prior to the start of the experiment.

Experiment 1: Fiber photometry recordings of BLA principal neurons during Pavlovian conditioning

Subjects.

Eight experimentally naïve Male ($N = 4$) and Female ($N = 4$) wild type rats (Charles River Laboratories, Wilmington, MA) aged ~9 weeks at the time of surgery were included in this study. Subjects with misplaced optic fibers (N = 0), insufficient viral expression (N = 0), or lacking fiber photometry data of sufficient quality (N = 0) were excluded prior to analysis.

Surgery.

Surgery occurred prior to onset of behavioral training. Rats were infused bilaterally with adeno-associated virus (AAV) expressing the genetically encoded calcium indicator GCaMP6f under

control of the calcium/calmodulin-dependent protein kinase (CaMKII) promoter (pENN.AAV5.CAMKII.GCaMP6f.WPRE.SV40, Addgene, Watertown, MA) to drive expression preferentially in principal neurons. Virus (0.5 µl) was bilaterally infused into the BLA [AP: -2.9; ML: ± 5.0; DV: -8.8 mm from bregma] at a rate of 0.1ul/min using 28-gauge injectors. Injectors were left in place for an additional 10 minutes following viral infusions. Optical fibers (200 µm diameter, 0.37 numerical aperture (NA), Neurophotometrics, San Diego, CA) were implanted bilaterally 0.2 mm dorsal to the infusion site. Experiments commenced ~4 weeks after surgery to allow sufficient expression in BLA cell bodies.

Behavioral procedures

Magazine conditioning. Rats first received two days of training to learn where to receive the sucrose and food pellet rewards. Each day included two separate sessions, separated by approximately 1 hr, order counterbalanced across days, one with 30 non-contingent deliveries of sucrose (60 sec intertrial interval, ITI) and one with 30 food pellet deliveries (60 sec ITI).

Preexposure. To reduce the initial saliency of the auditory stimuli used in subsequent Pavlovian conditioning, subjects received one day of preexposure to click and white noise stimuli. Click and noise were presented pseudo-randomly for 30 second durations, 4 times each with a variable 1.5m-3min ITI (mean = 2.5 min).

Pavlovian conditioning. Rats then received 8 sessions of Pavlovian conditioning (1 session/day on consecutive days) to learn to associate each of two auditory conditional stimuli (CSs; 80-82 db, 30 sec duration), click (10 Hz) or white noise, with a specific food reward, sucrose (20%, 0.1 ml/delivery) or grain pellets (45 mg; Bio-Serv). For half the subjects, click terminated in the delivery of sucrose and noise in the delivery of pellets, with the other half receiving the opposite

arrangement. Each session consisted of 8 click and 8 white noise presentations. CSs were delivered pseudo-randomly with a variable 1.5-3 min ITI (mean = 2.5 min).

Data collection. Entries into the food-delivery port were recorded continuously for each session.

Behavioral analysis.

Behavioral data were processed with Microsoft Excel (Microsoft, Redmond, WA). Acquisition of the Pavlovian conditional food-port approach response was assessed by comparing the rate of entries into the food-delivery port (entries/min) during the 30 sec CS, prior to reward delivery, relative to the 30 sec period preceding CS onset (preCS). Data were averaged across trials for each CS and then averaged across the two CSs.

In vivo fiber photometry recordings

Fiber photometry was used to image bulk calcium activity in BLA neurons throughout each Pavlovian conditioning session. We simultaneously imaged GCaMP6f and control fluorescence in the BLA using a commercial fiber photometry system (Neurophotometrics Ltd., San Diego, CA). Two light-emitting LEDs (470nm: Ca2+-dependent GCaMP fluorescence; 415nm: autofluorescence, motion artifact, Ca2+-independent GCaMP fluorescence) were reflected off dichroic mirrors and coupled via a patch cord (fiber core diameter: 200 μm; Doric Lenses) to the implanted optical fiber. The intensity of the light for excitation was adjusted to ~80 μW at the tip of the patch cord. Fluorescence emission was passed through a 535nm bandpass filter and focused onto the complementary metal-oxide semiconductor (CMOS) camera sensor through a tube lens. Samples were collected at 20Hz interleaved between the 415 and 470 excitation channels using a custom Bonsai (Lopes et al., 2015) workflow. Time stamps of task events were collected simultaneously through an additional synchronized camera aimed at the Med Associates interface, which sent light pulses coincident with task events. Signals were saved using Bonsai

software and exported to MATLAB (MathWorks, Natick, MA) for analysis. Recordings were collected unilaterally from the hemisphere with the strongest fluorescence signal in the 470 channel at the start of the experiment. Animals were habituated to the optical tether during the magazine conditioning sessions, but no light was delivered.

Fiber photometry data analysis.

Data were pre-processed using a custom-written pipeline in MATLAB (MathWorks, Natick, MA). Data from the 415 nm isosbestic control channel were used to correct for motion artifacts and photobleaching. Using least-squares linear regression, the 415 signal was fit to the 470 signal. Change in fluorescence ($\Delta F/F$) at each time point was calculated by subtracting the fitted 415 signal from the 470 signal and normalizing to the fitted 415 data [(470-fitted 415)/fitted 415)]. The $\Delta F/F$ data were resampled to 19.5 Hz then Z-scored [($\Delta F/F$ - mean $\Delta F/F$)/std($\Delta F/F$)]. Using a custom MATLAB workflow, Z-scored traces were then aligned to CS onset for each trial. Peak magnitude was calculated on the Z-scored trace for each trial using 5 sec pre-CS baseline and 5 sec post-CS onset and post-CS offset/outcome delivery windows. Data were averaged across trials and then across CSs. Session data were excluded if no transient calcium fluctuations were detected on the 470 nm channel above the isosbestic channel or if poor linear fit was detected due to excessive motion artifact. To examine the progression in BLA activity across training, we compared data across conditioning sessions 1, 2, 3/4, 5/6, and 7/8. Thus, data from the mid and latter training sessions were averaged across bins of 2 training sessions. All subjects had reliable data from at least one session per bin and were included in analysis. We were able to obtain reliable imaging data from all the 8 training sessions from $N = 6$ of the 8 total subjects (see Figure 3-2).

Histology.

GFP fluorescence was used to confirm expression of GCaMP in BLA cell bodies.

Experiment 2: Fiber photometry recordings of dopamine activity in the BLA during Pavlovian conditioning

Subjects.

Nine experimentally naïve Male (*N* = 5) and Female (*N* = 4) Long Evans rats (Th-cre$^-$ littermates, *N* = 6; Charles River Laboratories, *N* = 3) aged 9-11 weeks at the time of surgery were used in this study. Subjects with misplaced optic fibers (N = 0), insufficient viral expression (N = 0), or lacking fiber photometry data of sufficient quality (N = 2) were excluded prior to analysis.

Surgery.

Surgery occurred prior to onset of behavioral training. Rats were infused bilaterally with AAV encoding the GPCR-activation-based-DA (GRABDA) sensor (pAAV9-hsyn-GRAB_DA2h, Addgene). Virus (0.3ul) was infused bilaterally into the BLA [AP: -2.7; ML: ±5.0; DV: -8.7mm (Males) or -8.6mm (Females) from bregma]. 5 minutes later, viral injectors were dorsally repositioned in the BLA and a second viral infusion (0.3ul) of GrabDA was administered [DV: -8.4mm (Males) or -8.3mm (Females)]. Optical fibers (400 um diameter, 0.37 NA, Neurophotometrics) were implanted bilaterally 0.2 mm dorsal to the first infusion site. Virus was infused at a rate of 0.1ul/min using 28-gauge injectors and injectors were left in place for an additional 10 minutes after the second set of infusions. Experiments commenced ~4 weeks after surgery to allow sufficient expression in the BLA.

Behavioral procedures

Behavioral procedures were identical to Experiment 1.

Behavioral analysis

Behavioral analysis was identical to Experiment 1.

In vivo fiber photometry recordings.

Details of the system (Neurophotometrics) used to image GCaMP6f and record task events in Experiment 1 were the same for recordings of GrabDA fluorescence in the BLA. 470nm excitation light was adjusted to ~80-100μW at the tip of the patch cord (fiber core diameter: 400 um; Doric Lenses) and samples from 470nm excitation were collected at 20Hz. Samples collected using the 415nm excitation channel were not used. Recordings were collected unilaterally from the hemisphere with the strongest fluorescence signal in the 470 channel at the start of the experiment. Animals were habituated to the optical tether during the magazine conditioning sessions, but no light was delivered.

Fiber photometry data analysis.

Data were pre-processed using a custom-written pipeline in MATLAB (MathWorks, Natick, MA). To account for attenuation in fluorescence resulting from photobleaching across the session, the 470 signal was divided by a second order exponential fitted to the raw data. The data were then resampled to 19.5 Hz and Z-scored. Peak magnitude was calculated on the Z-scored trace using 5 sec peri-event windows as described in Experiment 1. We compared data across conditioning sessions 1, 2, 3/4, 5/6, and 7/8. Session data were excluded if artifactual signal due to excessive motion or patch cord twisting was detected for at least half of the trials. Subjects without reliable data from at least one session per bin were excluded (N = 2). We were able to obtain reliable imaging data from all of the 8 training sessions from N = 7 of the 9 total subjects (see Figure 3-4).

Immunohistochemistry.

Immunofluorescence was used to confirm expression of GrabDA in the BLA. Floating coronal sections were washed 3 times in 1x PBS for 30 min and then blocked for 1–1.5 hr at room temperature in a solution of 3% normal goat serum and 0.3% Triton X-100 dissolved in PBS.

Sections were then washed 3 times in PBS for 15 min and incubated in blocking solution containing chicken anti-GFP polyclonal antibody (1:1000; Abcam, Cambridge, MA) with gentle agitation at 4°C for 18–22 hr. Sections were next rinsed 3 times in PBS for 30 min and incubated with goat anti-chicken IgY, Alexa Fluor 488 conjugate (1:500; Abcam) in blocking solution at room temperature for 2 hr. Sections were washed a final 2 times in PBS for 10 min.

Experiment 3: VTA_{DA}→BLA terminal inhibition during Pavlovian conditioning

Subjects.

Twenty-one experimentally naïve Male (*N* = 11) and Female (*N* = 10) transgenic Long Evans rats carrying a TH-dependent Cre expressing system (Th-cre^{+}; hemizygous) aged approximately 10 weeks at the time of surgery were used in this study. Subjects with misplaced optic fibers (N = 3) or lacking viral expression (N = 0) were excluded prior to analysis.

Surgery.

Prior to the onset of behavioral training, Th-cre+ rats were randomly assigned to a viral group and were infused bilaterally with a cre-dependent AAV encoding either the inhibitory opsin archaerhodopsin T (ArchT; Females: N = 5; Males: N = 6; AAV5-FLEX-CAG-ArchT-tdTomato, Addgene) or a tdTomato fluorescent protein control (tdTomato; Females: N = 5; Males: N = 5; AAV5-FLEX-CAG-ArchT-tdTomato, University of North Carolina Vector Core, Chapel Hill, NC). Virus (0.2 µl) was infused bilaterally at a rate of 0.1 µl/min into the VTA (AP: -5.3; ML: ±0.7; DV: -8.3 mm from bregma) using a 28-gauge injector. Injectors were left in place for an additional 10 minutes following infusion. Optical fibers (200 µm core, 0.39 NA, Thorlabs, Newton, NJ) held in ceramic ferrules (Kientec Systems, Stuart, FL) were implanted bilaterally in the BLA [AP: -2.7; ML: ±5.0; DV: -8.2] to allow subsequent light delivery to ArchT- or tdTomato-expressing axon terminal in the BLA. Experiments commenced 4-5 weeks after surgery to allow sufficient expression in VTA→BLA terminals at the time of manipulation (7-9 weeks after surgery).

Behavioral procedures.

Magazine conditioning. Procedures were exactly as described in Experiment 1.

Instrumental conditioning. After magazine conditioning, rats were then given 11 days, minimum, of instrumental conditioning. They received 2 separate training sessions per day, one with the left lever and one with the right lever, separated by at least 1 hr. Each action was reinforced with a different food outcome (e.g., left press-grain pellets/right press-sucrose solution). Lever-outcome pairings were counterbalanced at the start of the experiment within each viral group. Each session terminated after 20 outcomes had been earned or 45 min had elapsed. Actions were continuously reinforced on the first day and then escalated ultimately to a random-ratio 20 schedule of reinforcement.

Pavlovian conditioning. Rats then received 8 sessions of Pavlovian conditioning as described in Experiment 1. CS-reward pairings were counterbalanced within groups and with respect to instrumental lever-outcome pairings.

Instrumental retraining and extinction. Following Pavlovian conditioning rats received one day of instrumental retraining which followed the procedures described above. Lever pressing during each session was reinforced on an RR20 schedule. After this, subjects received one day of instrumental extinction consisting of a single 30-min session during which both levers were available but pressing was not reinforced to establish a low level of responding.

Outcome-specific Pavlovian-to-instrumental transfer tests. Rats next received an outcome-selective Pavlovian-to-instrumental transfer (PIT) test. During the PIT test, both levers were continuously present, but pressing was not reinforced. After 5 min of lever-pressing extinction, each 30-sec CS was presented separately 4 times, separated by a fixed 2.5-min inter-trial interval.

Within each group, half of the subjects received presentation of the click followed by the noise in alternating order (i.e CNCNCNCN) and the other half received noise presented first (NCNCNCNC). No rewards were delivered following CS presentation.

Rats next received two days of instrumental retraining. Lever pressing was reinforced on an RR10 schedule for the first day of retraining and on an RR20 schedule for the second day. Rats then received one day of Pavlovian retraining. Lever-outcome and CS-outcome pairings were kept the same as initial conditioning. After retraining, rats were given a second PIT test where, following 10 min of lever pressing extinction, each CS was presented 4 times, the order of which was counterbalanced with respect to the first PIT test. Levers were present throughout the test and no rewards were delivered.

Data collection. Lever presses and/or discrete entries into the food-delivery port were recorded continuously for each session. For Pavlovian training and PIT test sessions, the 30-sec periods prior to each CS onset served as the baseline for comparison of CS-induced elevations in lever pressing and/or food-port entries.

Behavioral analysis.

Behavioral data were processed with Microsoft Excel (Microsoft, Redmond, WA). Press rates on the last 2 days of instrumental training were averaged across levers then across days and compared between groups to test for any differences in the acquisition of lever press responding. Acquisition of the Pavlovian conditional food-port approach response was assessed by comparing the rate of entries into the food-delivery port (entries/min) during the 30 sec CS, prior to reward delivery, relative to the 30 sec period prior to CS onset (preCS). To determine the effect of optically inhibiting $VTAD_A \rightarrow$BLA projections on reward collection during compound training, entry rates during the 30 sec period following reward delivery were compared to the 30 sec preCS baseline window. Data were averaged across trials for each CS and then averaged across the two CSs. For

PIT tests, entry rates into the food-port during the 30 sec CSs were compared to the baseline 30 sec preCS periods. Data were averaged across trials for each CS and then averaged across the two CSs. Lever press rates (presses/min) during the 30 sec baseline periods immediately prior to the onset of each CS were compared with that during the 30 sec CS periods. For both the baseline and CS periods, lever pressing was separated for presses on the lever that, during training, earned the same outcome as the presented cue (i.e., preCS: Same and CS: Same presses) versus those on the other available lever (i.e., preCS: Different and CS: Different presses). Data was separated into Same vs Different presses for each CS, averaged across trials, then averaged across CSs. To examine how the presence of the CS changed lever pressing behavior, we also computed an elevation ratio for each lever [(CS: Same presses)/(CS: Same presses + preCS: Same presses)] and [(CS: Different presses)/(CS: Different presses + preCS: Different presses)]. Food-delivery port entry rates, lever press rates, and elevation ratios were averaged across PIT tests.

Optogenetic inhibition of VTA_{DA}→BLA projections.

Optogenetic inhibition was used to attenuate the activity of ArchT-expressing VTA_{DA}→BLA terminals at the time of stimulus-outcome pairing during each CS during each Pavlovian conditioning session. Animals were habituated to the optical tether (200 μm, 0.22 NA, Doric) for at least the last two days of instrumental conditioning, but no light was delivered. During each Pavlovian conditioning session, green light (532nm; 10 mW) was delivered to the BLA via a laser (Dragon Lasers, ChangChun) connected through a ceramic mating sleeve (Thorlabs) to the ferrule implanted on the rat. Light was delivered continuously for 3 seconds concurrent with each reward delivery. If the reward was retrieved (first food-port entry after reward delivery) while the light was still being delivered (i.e., within 3 sec of reward delivery), then the light delivery was extended by 3 sec from the time of the retrieval. If the reward was retrieved after the laser had gone off, then the retrieval entry triggered an additional 3 sec continuous illumination. Light effects were estimated to be restricted to the BLA based on predicted irradiance values

(https://web.stanford.edu/group/dlab/cgi-bin/graph/chart.php). Following Pavlovian conditioning, rats proceeded to the PIT tests as described above, during which they were tethered to the optical patch cords, but no light was delivered. The same light delivery parameters were used during Pavlovian retraining in between PIT tests, but light was not delivered at any other phase of training or test.

Immunohistochemistry.

tdTomato fluorescence with a TH costain was used to confirm expression of ArchT colocalized to VTA dopamine cell bodies. Floating coronal sections were washed 3 times in 1x PBS for 30 min and then blocked for 2 hr at room temperature in a solution of 3% normal donkey serum and 0.2% Triton X-100 dissolved in PBS. Sections were then washed 3 times in PBS for 15 min and incubated in blocking solution containing rabbit anti-TH antibody (1:1000; EMD Millipore, Burlington, MA) with gentle agitation at 4°C for 44-48 hr. Sections were next rinsed 3 times in PBS for 30 min and incubated with goat anti-rabbit IgG, Alexa Fluor 488 conjugate (1:500; Thermofisher Scientific, Waltham, MA) in blocking solution at room temperature for 2 hr. Sections were washed a final 2 times in PBS for 10 min. Immunofluorescence was also used to confirm expression of ArchT in axons and terminal in the BLA. Floating coronal sections were washed 2 times in 1x PBS for 10 min and then blocked for 2 hr at room temperature in a solution of 10% normal goat serum and 0.5% Triton X-100 dissolved in PBS. Sections were then washed 3 times in PBS for 15 min and incubated in blocking solution containing rabbit anti DsRed polyclonal antibody (1:1000; EMD Millipore, Burlington, MA) with gentle agitation at 4°C for 18-22 hr. Sections were next rinsed 3 times in blocking solution for 30 min and incubated with goat anti-rabbit IgG, Alexa Fluor 594 conjugate (1:500; Thermofisher Scientific) in blocking solution at room temperature for 2 hr. Sections were washed a final 2 times in PBS for 10 min.

Experiment 4: Outcome-specific Pavlovian blocking and Pavlovian-to-instrumental transfer

Subjects.

Thirty-two Male (*N* = 22) and Female (*N* = 10) Long Evans rats (Charles River) aged approximately 8 weeks at the start of the experiment were used in this study. Prior to the start of behavioral training, subjects were randomly assigned to Pavlovian blocking (Male: *N* = 11; Female: *N* = 5) or no-blocking control (Male: *N* = 11; Female: *N* = 5) groups.

Behavioral Procedures.

Magazine training and instrumental conditioning. Procedures were exactly as described in the previous experiments, with the exception that the house light was kept off. Lever-outcome pairings were counterbalanced within the groups.

Pavlovian conditioning. Rats received 12 sessions of Pavlovian conditioning (1 session/day on consecutive days) in a dark operant chamber to learn to associate each of two visual CSs (30 sec duration), house light or flashing stimulus lights (2hz) with a specific food reward, sucrose (20%, 0.1 ml/delivery) or grain pellets (45 mg; Bio-Serv). CS-reward pairings were counterbalanced within groups and with respect to instrumental lever-outcome pairings. For half the subjects in the Pavlovian blocking group, the house light terminated in the delivery of sucrose and flashing lights in the delivery of pellets, with the other half receiving the opposite arrangement. Each session consisted of 16 house light and 16 flashing light presentations. CSs were delivered pseudo-randomly with a variable 1.5-3 min ITI (mean = 2.5 min). Subjects in the control group learned to associate a distinct, third visual stimulus with both food rewards. The presentation of two alternating stimulus lights mounted to the outer walls of the operant chamber (0.25 hz alternating outside lights; 30 sec duration) terminated in the delivery of sucrose (20%, 0.1 ml/delivery) in half of the trials and in grain pellets (45 mg; Bio-Serv) in the other half. For subjects in this group,

each session consisted of 32 presentations of alternating outside lights with a variable 1.5-3min ITI (mean = 2.5 min).

Instrumental retraining and extinction. Instrumental retraining and extinction sessions were exactly as described in Experiment 3.

Preexposure. After instrumental extinction, rats received one day of preexposure to click and noise auditory stimuli. Click and noise were presented pseudo-randomly for 30 second durations, 8 times each with a variable 1.5m-3min ITI (mean = 2.5 min).

Compound conditioning. Subjects included in Pavlovian blocking experiments next received 4 days of compound conditioning where the previously learnt visual CSs were each presented in compound with distinct auditory stimuli, a click or noise. Visual CS-auditory CS pairings were counterbalanced within groups and with respect to Pavlovian and instrumental groupings. For all subjects, one compound stimulus (30 sec duration) consisted of the house light presented with click and the second compound stimulus (30 sec duration), flashing lights with noise. The other half of subjects received the opposite arrangement. Each compound conditioning session consisted of 8 presentations of each compound stimulus, terminating in the delivery of one of the food rewards. For subjects in the blocking group, each compound stimulus terminated in the outcome paired with the visual stimulus in initial Pavlovian conditioning. Compound stimulus-outcome pairings were counterbalanced across subjects in the control group. Compound stimuli were delivered pseudo-randomly with a variable 1.5-3 min ITI (mean = 2.5 min).

Outcome-specific Pavlovian-to-instrumental transfer tests. Procedures were exactly as described in Experiment 3, where both levers were available and the auditory CSs, conditioned here during compound training, were presented alone 4 times each.

Data collection. Lever presses and/or discrete entries into the food-delivery port were recorded continuously for each session.

Behavioral analysis.

Press rates and/or food-port entries during instrumental conditioning, Pavlovian conditioning and PIT were analyzed in the same way as Experiment 3. During compound conditioning sessions, entry rates during the 30 sec compound stimulus were compared to the preceding 30 sec preCS baseline window. Data were averaged across trials for each compound stimulus and then averaged across the two compound stimuli.

Experiment 5: VTA_{DA}→BLA stimulation during outcome-specific Pavlovian blocking

Subjects.

Twenty-four experimentally naïve Male (*N* = 11) and Female (*N* = 13) transgenic TH-cre+ (hemizygous) Long Evans rats between 9-12 weeks at the time of surgery were used in this study. Subjects with misplaced optical fibers (*N* = 2) or lacking viral expression (*N* = 2) were excluded prior to analysis.

Surgery.

Prior to the onset of behavioral training, Th-cre+ rats were randomly assigned to a viral group and were infused bilaterally with a cre-dependent AAV encoding either the excitatory opsin channelrhodopsin (ChR2; Females: *N* = 6; Males: *N* = 5; AAV5-EF1a-DIO-hChR2(H134R)-eYFP, University of North Carolina Vector Core) or an enhanced yellow fluorescent protein control (eYFP; Females: *N* = 7; Males: *N* = 6; pAAV5-Ef1a-DIO-eYFP, Addgene). Virus (0.2 µl) was infused bilaterally at a rate of 0.1 µl/min into the VTA (AP: -5.3; ML: ±0.7; DV: -8.3 mm from bregma) using a 28-gauge injector. Injectors were left in place for an additional 10 minutes following viral infusions. Optical fibers (200 µm core, 0.39 NA, Thorlabs, Newton, NJ) held in

ceramic ferrules (Kientec Systems, Stuart, FL) were implanted bilaterally in the BLA [AP: -2.7; ML: ±5.0; DV: -8.2] to allow subsequent light delivery to ChR2- or eYFP-expressing axon terminals in the BLA. Experiments commenced ~2 weeks after surgery to allow sufficient expression in VTA→BLA axon terminals at the time of optical manipulation (7-8 weeks after surgery).

Behavioral Procedures.

Behavioral procedures through PIT were identical to Experiment 4 with the following exceptions. Pavlovian conditioning and compound conditioning procedures were the same as those described for the blocking group, where visual CSs consisted of a house light and flashing stimulus lights. A separate control group receiving conditioning with outside lights was not included. A single PIT test initiating in a 5 min lever pressing extinction period was used for analysis. Counterbalancing across conditioning sessions and PIT was as described, but within viral groups.

Intracranial Self-Stimulation. Rats received two days of intracranial self-stimulation (ICSS) following PIT. Each day consisted of one 1 hr session where animals were free to nose poke in two ports positioned on the left and right side of the operant chamber wall opposite of the food-delivery port. For half of the subjects within each group, a nose poke in the left port would result in blue light delivery to either ChR2- or eYFP-expressing dopaminergic terminals in the BLA (active nose poke; stimulation parameters described below) whereas a nose poke into the right port would not result in light delivery (inactive nose poke). For the other half of subjects, active nose pokes were in the right port and inactive nose pokes in the left. To distinguish the context from prior conditioning and test sessions, opaque plexiglass cutouts covered the grid floor, and "No Parking" signs were used to occlude the magazine and levers of the operant chambers.

Data collection. Lever presses and/or discrete entries into the food-delivery port were recorded continuously for each session. Nose pokes were recorded continuously for ICSS session.

Behavioral analysis.

Behavioral analysis of training and PIT performance was identical to Experiment 4. To determine the effect of optically stimulating VTA_{DA}→BLA projections on reward collection during Pavlovian conditioning, entry rates during the 30 sec period following reward delivery were compared to the 30 sec preCS baseline window. For ICSS sessions, the total number of nose pokes into the active port were compared to the total number of nose pokes in the inactive port.

Optogenetic stimulation of VTA_{DA}→BLA terminals.

Optogenetic excitation was used to stimulate the activity of ChR2-expressing VTA_{DA}→BLA terminals at the time of each compound stimulus-outcome pairing during each compound conditioning session. Animals were habituated to the optical tether (200 μm, 0.22 NA, Doric) for at least the last two days of instrumental conditioning and the last two days of Pavlovian conditioning, but no light was delivered. During each compound conditioning session, blue light (473nm; 10 mW) was delivered to the BLA via a laser (Dragon Lasers, ChangChun) for 3 sec at a rate of 20Hz concurrent with each reward delivery. If the reward was retrieved (first food-port entry after reward delivery) while the light was still being delivered (i.e., within 3 sec of reward delivery), the light delivery was not extended. If the reward was retrieved after the laser had gone off, then the retrieval entry triggered an additional 3 sec of 20Hz illumination. Following Pavlovian conditioning, rats proceeded to the PIT tests as described above, during which they were tethered to the optical patch cords, but no light was delivered. For ICSS sessions, nose pokes into the active port triggered 1 sec of blue light (473nm; 10 mW) delivery to the BLA at a rate of 20Hz. Subsequent nose pokes during the 1 sec period of light delivery were recorded but did not extend light delivery.

Immunohistochemistry.

eYFP fluorescence was used to confirm expression of ChR2. A TH costain was used to confirm colocalization to VTA dopamine cell bodies. Staining procedures were as described in Experient 3 using a secondary goat anti-rabbit Alexa 594 antibody (Thermofisher Scientific). Immunofluorescence following procedures described for GFP amplification in Experiment 2 was also used to confirm expression of ChR2 in axons and terminals in the BLA.

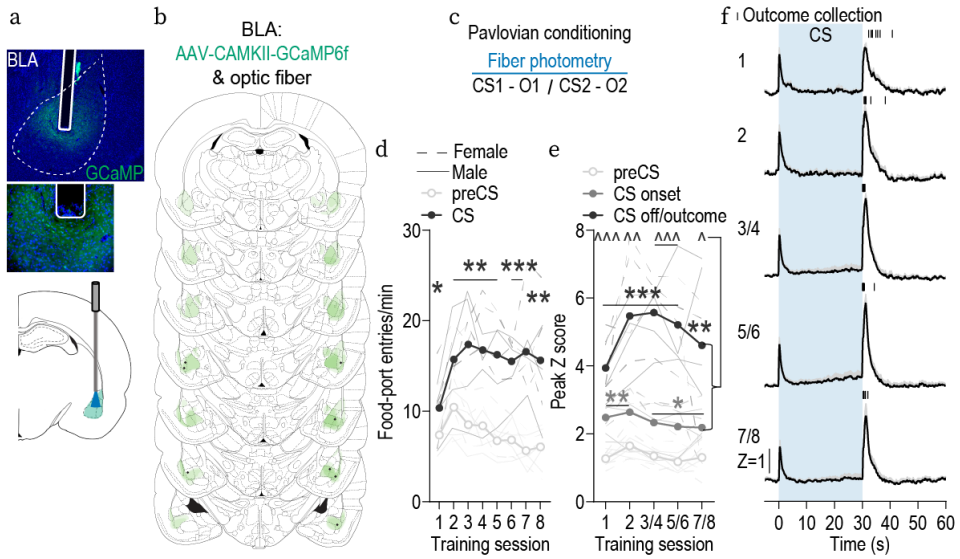

Figure 3-1: BLA neurons are activated during stimulus-outcome learning.

(a) Top: Representative fluorescent image of GCaMP6f expression and fiber placement in the BLA. Bottom: Schematic of fiber photometry approach for imaging bulk calcium activity in BLA neurons. **(b)** Schematic representation of GCaMP6f expression and placement of optical fiber tips in BLA for all subjects. Brain slides from Paxinos and Watson, 1998. **(c)** Procedure schematic. CS, conditional stimulus (white noise or click); O, outcome (sucrose solution or food pellet). **(d)** Food-port entry rates (entries/min) during the CS relative to the preCS period, averaged across trials and across the 2 CSs for each day of Pavlovian conditioning. Thin light lines represent individual subjects. $^{*}P < 0.05$, $^{**}P < 0.01$, $^{***}P < 0.001$ relative to preCS, Bonferroni correction. **(e)** Trial-averaged quantification of maximal (peak) GCaMP Z-scored ΔF/F during the 5 s period following CS onset or reward delivery compared to the equivalent baseline period immediately prior to CS onset. Thin light lines represent individual subjects. $^{*}P < 0.05$, $^{**}P < 0.01$, $^{***}P < 0.001$ relative to pre-event baseline. $^{\wedge}P < 0.05$, $^{\wedge\wedge}P < 0.01$, $^{\wedge\wedge\wedge}P < 0.001$ relative to CS onset, Bonferroni correction. **(f)** Trial-averaged GCaMP6f fluorescence changes (Z-scored ΔF/F) in response to CS presentation (blue box) or reward delivery across days of training. Shading reflects between-subjects s.e.m. Data from the last six sessions were averaged across two-session bins (3/4, 5/6, and 7/8). $N = 8$ (Male $N = 4$; Female $N = 4$).

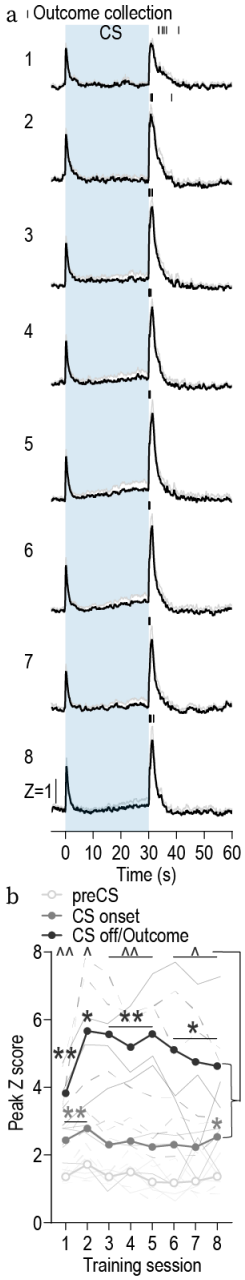

Figure 3-2: BLA neurons are activated during stimulus-outcome learning across each of the eight Pavlovian conditioning sessions.

(a) Trial-averaged GCaMP6f fluorescence changes (Z-scored ΔF/F) in response to CS presentation (blue box) or reward delivery from each of the 8 Pavlovian conditioning sessions. Shading reflects between-subjects s.e.m. **(b)** Trial-averaged quantification of maximal (peak) and GCaMP Z-scored ΔF/F during the 5 sec following CS onset or reward retrieval compared to the equivalent baseline period immediately prior CS onset. Thin light lines represent individual subjects. Both CS and reward delivery resulted in an elevated peak calcium response, which varied across training sessions (Training: $F_{(2.41, 12.06)} = 2.35$, $P = 0.13$; Event (preCS/CS onset/outcome delivery): $F_{(1.18, 5.92)} = 33.57$, $P = 0.001$; Training x Event: $F_{(3.08, 15.40)} = 3.85$, $P = 0.03$). Thin light lines represent individual subjects. *$P < 0.05$, **$P < 0.01$ relative to preCS baseline. ^$P < 0.05$, ^^$P < 0.01$ relative to CS onset, Bonferroni correction.

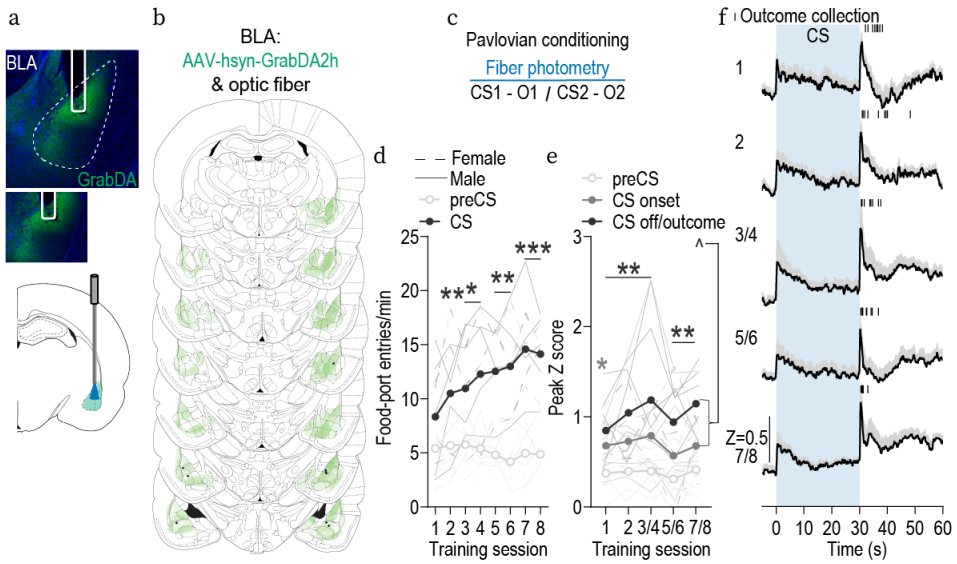

Figure 3-3: Dopamine is released in the BLA during stimulus-outcome learning.

(a) Top: Representative fluorescent image of GrabDA expression and fiber placement in the BLA. Bottom: Schematic of fiber photometry approach for imaging bulk calcium activity in BLA neurons. **(b)** Schematic representation of GrabDA expression and placement of optical fiber tips in BLA for all subjects. **(c)** Procedure schematic. CS, conditional stimulus (white noise or click); O, outcome (sucrose solution or food pellet). **(d)** Food-port entry rates (entries/min) during the CS relative to the preCS period, averaged across trials and across the 2 CSs for each day of Pavlovian conditioning. Thin light lines represent individual subjects. $^{*}P < 0.05$, $^{**}P < 0.01$, $^{***}P < 0.001$ relative to preCS, Bonferroni correction. **(e)** Trial-averaged quantification of maximal (peak) GCaMP Z-scored during the 5 s period following CS onset or reward delivery compared to the equivalent baseline period immediately prior to CS onset. Thin light lines represent individual subjects. $^{*}P < 0.05$, $^{**}P < 0.01$, relative to preCS baseline. $^{\wedge}P < 0.05$ relative to CS onset, Bonferroni correction. **(f)** Trial-averaged GrabDA fluorescence changes (Z-scored GrabDA) in response to CS presentation (blue box) or reward delivery across days of training. Shading reflects between-subjects s.e.m. Data from the last six sessions were averaged across two-session bins (3/4, 5/6, and 7/8). $N = 9$ (Male $N = 5$; Female $N = 4$).

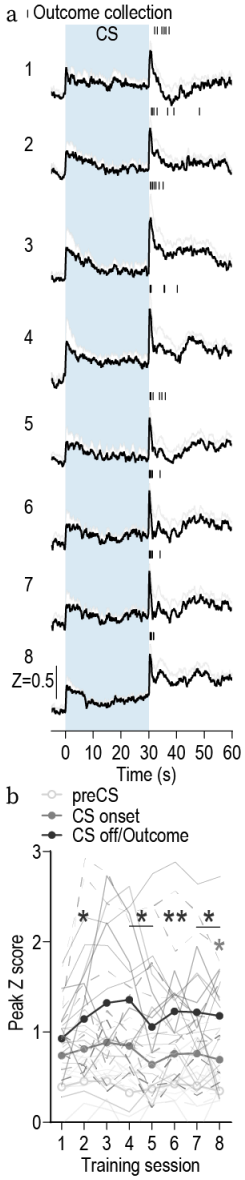

Figure 3-4: Dopamine is released in the BLA during stimulus-outcome learning across each of the eight Pavlovian conditioning sessions.

(a) Trial-averaged GrabDA fluorescence changes (Z-scored) in response to CS presentation (blue box) or reward delivery from $N = 7$ subjects with usable data from each of the 8 Pavlovian conditioning sessions. Shading reflects between-subjects s.e.m. **(b)** Trial-averaged quantification of maximal (peak) Z-scored GrabDA during the 5 sec following CS onset or reward retrieval compared to the equivalent baseline period immediately prior CS onset. Thin light lines represent individual subjects. Both CS and reward delivery resulted in an elevated peak calcium response (Training: $F_{(2.91,\ 17.46)} = 0.47$, $P = 0.70$; Event (preCS/CS onset/outcome delivery): $F_{(1.94,\ 11.65)} = 14.86$, $P = 0.0007$; Training x Event: $F_{(3.43,\ 20.60)} = 0.71$, $P = 0.57$). Thin light lines represent individual subjects. $^{*}P < 0.05$, $^{**}P < 0.01$ relative to preCS baseline, Bonferroni correction.

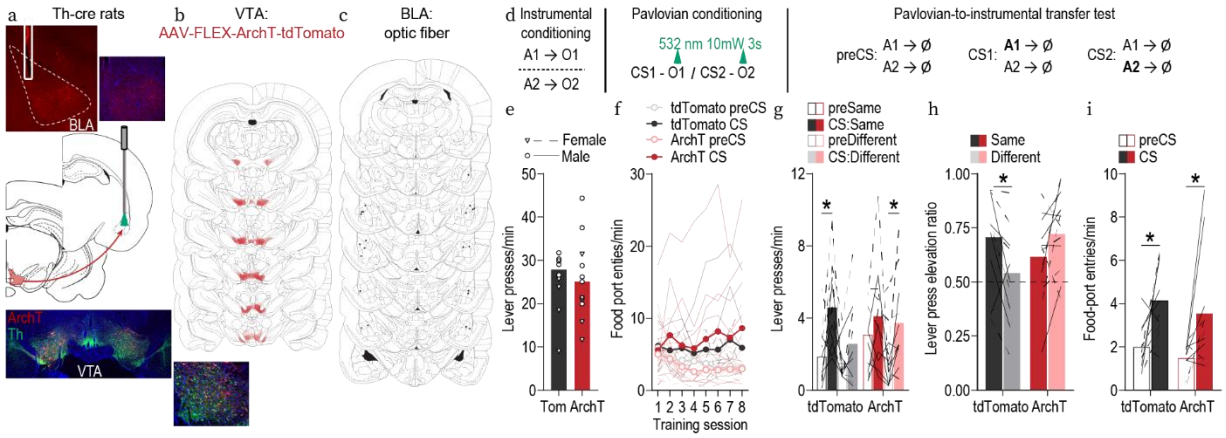

Figure 3-5: Optical inhibition of VTA_{DA} terminals in the BLA during stimulus-outcome pairing attenuates the encoding of stimulus-outcome memories.

(**a**) Top: Representative image of fiber placement in the vicinity of immunofluorescent ArchT-tdTomato-expressing VTA_{DA} axons and terminals in the BLA. Middle: Schematic of optogenetic strategy for bilateral inhibition of VTA_{DA} axons and terminals in the BLA. Bottom: Representative fluorescent image of ArchT-tdTomato expression in VTA cell bodies and coexpression of TH. (**b**) Schematic representation of ArchT-tdTomato expression in VTA and **(c)** placement of optical fiber tips in BLA for all subjects. **(d)** Procedure schematic. A, action (left or right lever press); O, outcome (sucrose solution or food pellet); CS, conditional stimulus (white noise or click). **(e)** Lever press rate (presses/min) averaged across levers and across the final 2 days of instrumental conditioning. (**f**) Food-port entry rates (entries/min) during the CS relative to the preCS period, averaged across trials and across the 2 CSs for each day of Pavlovian conditioning. Thin light lines represent individual subjects. **(g)** Trial-averaged lever press rates (presses/min) during preCS baseline periods compared with press rates during the CS periods separated for presses on the lever that, in training, delivered the same outcome as predicted by the CS (CS: Same) and pressing on the other available lever (CS: Different). *$P < 0.05$, planned comparisons pre: Same vs CS: Same and pre: Different vs CS: Different, uncorrected. (**h**) Elevation in lever presses on the lever that earned the same outcome as the presented CS (Same; [(presses on Same lever during CS)/(presses on Same lever during CS + Same presses during preCS)], averaged across trials and across CSs), relative to the elevation in responding on the alternate lever (Different; [(presses on Different lever during CS)/(presses on Different lever during CS + Different presses during preCS)], averaged across trials and across CSs) during the PIT test. Lines represent individual subjects. *$P < 0.05$, Bonferroni correction. **(i)** Food-port entry rates (entries/min) during the CS relative to the preCS period, averaged across trials and across the 2 CSs during the PIT test. Lines represent individual subjects. *$P < 0.05$, Bonferroni correction. ArchT, $N = 11$ (Males: $N = 6$, Females: $N = 5$); tdTomato, $N = 10$ (Males: $N = 5$, Females: $N = 5$).

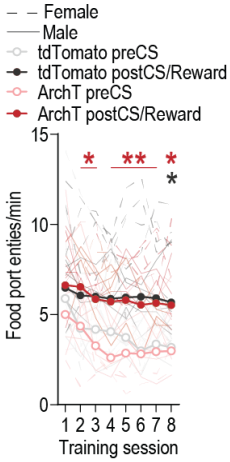

Figure 3-6: Optical inhibition of VTA_{DA}→BLA projections upon reward delivery does not affect reward collection

Food-port entry rates (entries/min) following reward delivery relative to the preCS period, averaged across trials and across the 2 CSs for each day of Pavlovian conditioning. Thin light lines represent individual subjects. Optical inhibition of VTA_{DA}→BLA terminals did not disrupt reward collection (Training: $F_{(3.13, 59.48)} = 8.51$; $P < 0.0001$; Virus: $F_{(1, 19)} = 0.47$. $P = 0.50$; CS period: $F_{(1, 19)} = 72.60$, $P < 0.0001$; Training x Virus: $F_{(7, 133)} = 0.65$, $P = 0.71$; Training x CS period: $F_{(4.94, 93.85)} = 3.00$, $P = 0.02$; Virus x CS period: $F_{(1, 19)} = 0.87$, $P = 0.36$; Training x Virus x CS period: $F_{(7, 133)} = 0.71$, $P = 0.66$).*$P < 0.05$, **$P < 0.01$, Bonferroni correction.

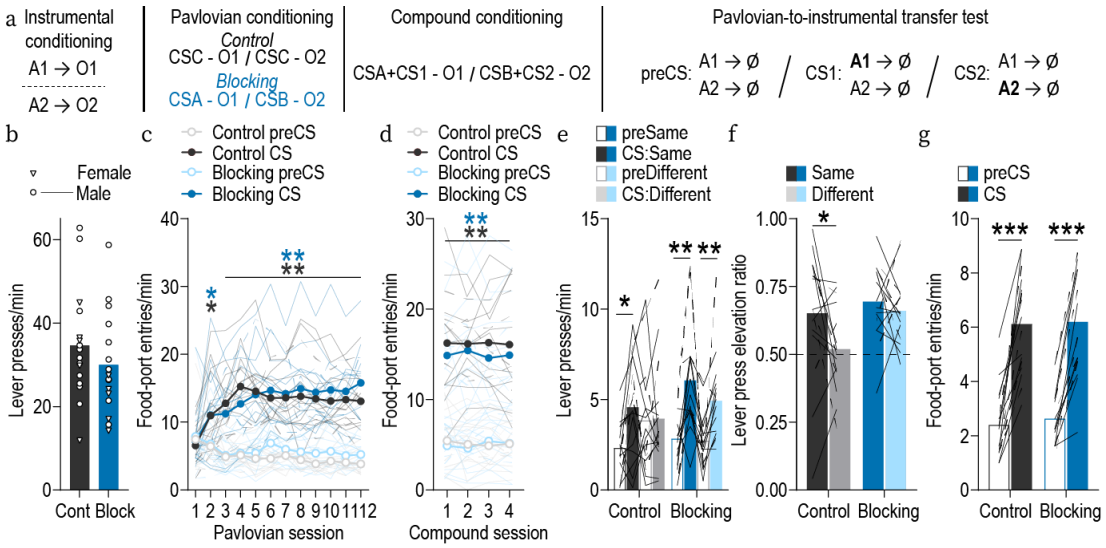

Figure 3-7: Pavlovian blocking suppresses encoding sensory-specific stimulus-outcome memories

(a) Procedure schematic. A, action (left or right lever press); O, outcome (sucrose solution or food pellet); CS, conditional stimulus (CSA/B: house light or flashing lights; CSC: outside lights; CS1/CS2: white noise or click). **(b)** Lever press rate (presses/min) averaged across levers and across the final 2 days of instrumental conditioning. (**c**) Food-port entry rates (entries/min) during the visual CS relative to the preCS period, averaged across trials and across the visual CSs for each day of Pavlovian conditioning. Thin light lines represent individual subjects. **P* < 0.05, ***P* < 0.01, Bonferroni correction. **(d)** Food-port entry rates (entries/min) during the compound stimulus relative to the preCS period, averaged across trials and across the 2 compound stimuli for each day of compound conditioning. Thin light lines represent individual subjects. ***P* < 0.01, Bonferroni correction **(e)** Trial-averaged lever press rates (presses/min) during preCS baseline periods compared with press rates during the auditory CS periods separated for presses on the lever that, in training, delivered the same outcome as predicted by the auditory CS (CS: Same) and pressing on the other available lever (CS: Different). **P* < 0.05, ***P* < 0.01, planned comparisons pre: Same vs CS: Same and pre: Different vs CS: Different, uncorrected. (**f**) Elevation in lever presses on the lever that earned the same outcome as the presented CS (Same; [(presses on Same lever during CS)/(presses on Same lever during CS + Same presses during preCS)], averaged across trials and across CSs), relative to the elevation in responding on the alternate lever (Different; [(presses on Different lever during CS)/(presses on Different lever during CS + Different presses during preCS)], averaged across trials and across CSs) during the PIT test. Lines represent individual subjects. **P* < 0.05, Bonferroni correction. **(g)** Food-port entry rates (entries/min) during the CS relative to the preCS period, averaged across trials and across the 2 CSs during the PIT test. Lines represent individual subjects. ****P* < 0.001, Bonferroni correction. Blocking, *N* = 16 (Males: *N* = 11, Females: *N* = 5); Control, *N* = 16 (Males: *N* = 11, Females: *N* = 5).

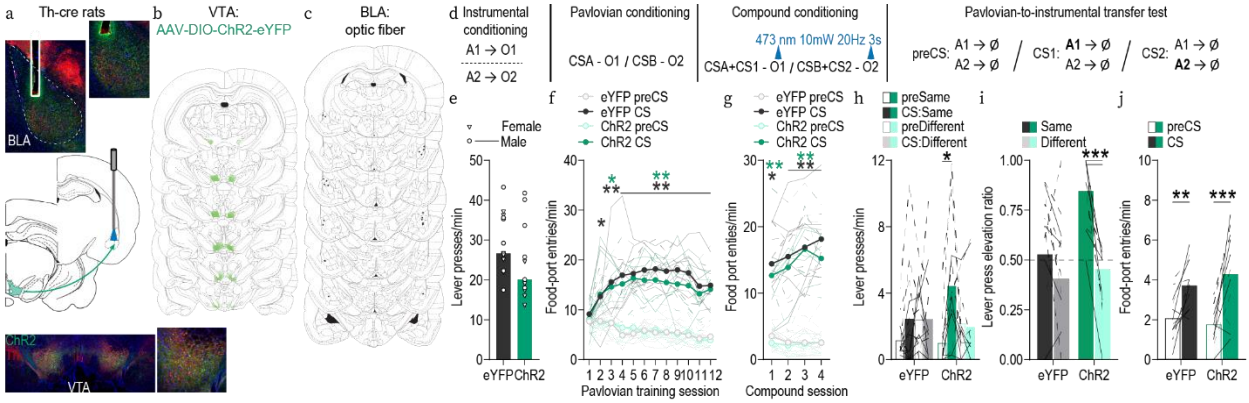

Figure 3-8: Optical stimulation of VTA_{DA} terminals in the BLA during stimulus-outcome pairing unblocks sensory-specific stimulus-outcome memories

(**a**) Top: Representative image of fiber placement in the vicinity of immunofluorescent ChR2-eYFP-expressing VTA_{DA} axons and terminals in the BLA. Middle: Schematic of optogenetic strategy for bilateral stimulation of VTA_{DA} axons and terminals in the BLA. Bottom: Representative fluorescent image of ChR2-eYFP expression in VTA cell bodies and co-expression of TH. (**b**) Schematic representation of ChR2-eYFP expression in VTA and **(c)** placement of optical fiber tips in BLA for all subjects. **(d)** Procedure schematic. A, action (left or right lever press); O, outcome (sucrose solution or food pellet); CS, conditional stimulus (CSA/B: house light or flashing lights; CS1/CS2: white noise or click). **(e)** Lever press rate (presses/min) averaged across levers and across the final 2 days of instrumental conditioning. (**f**) Food-port entry rates (entries/min) during the visual CS relative to the preCS period, averaged across trials and across the 2 visual CSs for each day of Pavlovian conditioning. Thin light lines represent individual subjects. *$P < 0.05$, **$P < 0.01$, Bonferroni correction. **(g)** Food-port entry rates (entries/min) during the compound stimulus relative to the preCS period, averaged across trials and across the 2 compound stimuli for each day of compound conditioning. Thin light lines represent individual subjects. *$P < 0.05$, **$P < 0.01$, Bonferroni correction **(h)** Trial-averaged lever press rates (presses/min) during preCS baseline periods compared with press rates during the auditory CS periods separated for presses on the lever that, in training, delivered the same outcome as predicted by the auditory CS (CS: Same) and pressing on the other available lever (CS: Different). *$P < 0.05$, planned comparisons pre: Same vs CS: Same and pre: Different vs CS: Different, uncorrected. (**i**) Elevation in lever presses on the lever that earned the same outcome as the presented CS (Same; [(presses on Same lever during CS)/(presses on Same lever during CS + Same presses during preCS)], averaged across trials and across CSs), relative to the elevation in responding on the alternate lever (Different; [(presses on Different lever during CS)/(presses on Different lever during CS + Different presses during preCS)], averaged across trials and across CSs) during the PIT test. Lines represent individual subjects. ***$P < 0.001$, Bonferroni correction. **(j)** Food-port entry rates (entries/min) during the CS relative to the preCS period, averaged across trials and across the 2 CSs during the PIT test. Lines represent individual subjects. **$P < 0.01$, ***$P < 0.001$, Bonferroni correction. ChR2, $N = 11$ (Males: $N = 5$, Females: $N = 6$); eYFP, $N = 13$ (Males: $N = 6$, Females: $N = 7$).

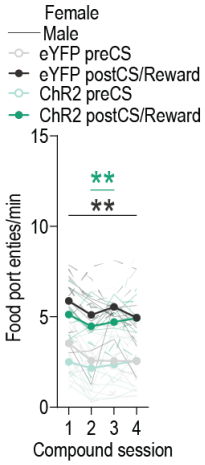

Figure 3-9: Optical stimulation of VTA_{DA}→BLA projections upon reward delivery does not affect reward collection

Food-port entry rates (entries/min) following reward delivery relative to the preCS period, averaged across trials and across the 2 CSs for each day of Pavlovian conditioning. Thin light lines represent individual subjects. Optical stimulation of VTA_{DA}→BLA terminals did not disrupt reward collection (Training: $F_{(1.50, 32.90)} = 3.70$, $P = 0.047$; Virus: $F_{(1, 22)} = 1.89$, $P = 0.18$; CS period: $F_{(1, 22)} = 46.80$, $P < 0.0001$; Training x Virus: $F_{(3, 66)} = 1.48$, $P = 0.23$; Training x CS period: $F_{(2.55, 56.04)} = 0.22$, $P = 0.85$; Virus x CS period: $F_{(1, 22)} = 0.04$, $P = 0.84$; Training x Virus x CS period: $F_{(3, 66)} = 0.51$, $P = 0.68$). $^{**}P < 0.01$, Bonferroni correction.

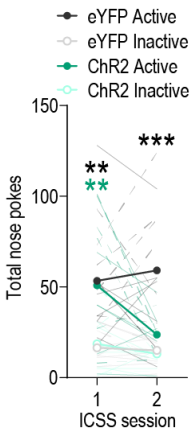

Figure 3-10: Stimulation of VTA_{DA} terminals in the BLA does not reinforce ICSS behavior

Total active nose pokes for VTA_{DA}→BLA terminal stimulation compared to inactive nose pokes across 2, 1-hr ICSS sessions. The number of active nose pokes attenuates in rats expressing ChR2 across sessions (Training: $F_{(1, 22)} = 3.05$, $P = 0.09$; Virus (ChR2 vs eYFP): $F_{(1, 22)} = 1.94$, $P = 0.18$; Nose poke (Active vs Inactive): $F_{(1, 22)} = 54.66$, $P < 0.0001$; Training x Virus: $F_{(1,22)} = 5.18$, $P = 0.03$; Training x Nose poke: $F_{(1, 22)} = 1.24$, $P = 0.28$; Virus x Nose poke: $F_{(1, 22)} = 5.18$, $P = 0.03$; Training x Virus x Nose poke: $F_{(1, 22)} = 5.00$, $P = 0.04$). $^{**}P < 0.01$, $^{***}P < 0.001$ relative to inactive nose pokes, Bonferroni correction.

Chapter 4: General Discussion

This work has investigated the neural circuitry mediating the encoding of sensory-specific stimulus-outcome memories and their subsequent use to guide adaptive decision making. In Chapter 2 I found that the BLA is an essential hub for sensory-specific appetitive associations. *In vivo* bulk calcium imaging revealed the BLA is robustly activated during stimulus-outcome learning. BLA activation at the time of reward delivery was essential for such encoding and optically inhibiting excitatory lOFC→BLA projections revealed that this was also dependent on lOFC inputs. Furthermore, I discovered that reciprocal lOFC→BLA→lOFC form a serial stimulus-outcome encoding and retrieval circuit. That is, lOFC→BLA activity enables the encoding of associative information that is later accessed through activation of BLA→lOFC outputs to promote selective cue-mediated instrumental choice.

VTA dopamine is a known contributor to model-based learning, but the projections through which it executes this role have largely been unidentified. Based on the above findings, I hypothesized that the BLA would be a likely target. *In vivo* fluorescent imaging of the dopamine sensor GrabDA revealed elevations in BLA dopamine during appetitive Pavlovian conditioning. Optically manipulating VTA_{DA}→BLA terminal activation during stimulus-outcome learning demonstrated these projections are necessary and sufficient for encoding model-based associative reward memories.

The BLA is active during sensory-specific stimulus-outcome learning

Monitoring BLA principal neuron population activity during outcome-specific Pavlovian conditioning revealed robust responses to reward delivery. But what information does this signal convey and how might it be contributing to learning? One possibility is that it represents an unsigned prediction error that facilitates learning through increasing CS associability, as suggested in attentional models of reinforcement learning (Pearce and Hall, 1980). Indeed, neural correlates of an associability signal have been found in the rodent BLA (Roesch et al., 2010; Esber et al., 2012) and human amygdala (Li et al., 2011b). Alternatively, this US-evoked activation could

encode a signed prediction error signal that alters the effectiveness of the US in modifying stimulus-outcome associations, as proposed by Rescorla-Wagner and temporal difference models (Rescorla and Wagner, 1972; Sutton, 1988). It is difficult to say which is the case with our data because in our Pavlovian conditioning tasks both USs are appetitive and would be expected to generate a positive prediction error early in learning. One way to determine if the increase at the time of reward delivery acts as an attentional "surprise" signal versus an RPE is with blocking (Holland, 1984). Although both models predict that an upshift in reward would unblock learning about a CS, they make opposite predictions about would happen in the event of a downshift (Holland and Schiffino, 2016). If BLA activation at the time of reward delivery in our task reflects an RPE signal, a downshift in the expected reward during blocking would result in a negative prediction error resulting in inhibitory effects on learning. If, however, the BLA signals an unsigned prediction error that guides attention, BLA activity would increase during this downshift leading to enhanced CS associability and unblocking. Some support for the latter has been found from studies lesioning the BLA (Chang et al., 2012; Esber and Holland, 2014). If the BLA facilitates sensory-specific associative learning through increasing CS associability, additional experiments would be useful in determining whether this attention signal enables learning stimulus-outcome contingencies more broadly, with further processing of outcome-specific content elsewhere, or whether the enhanced CS associability is itself outcome-specific.

Curiously, we did not detect an attenuation in activation upon reward delivery across training days. This seemingly contradicts an RPE interpretation, which predicts an attenuation in response to reward as it comes to be expected by the presence of an antecedent cue. Such findings have been reported in studies where single cue-reward contingencies are learnt (Lutas et al., 2019; Crouse et al., 2020). Our findings are also at odds with reports that unsigned prediction errors in the BLA, proposed to mediate stimulus processing, decline with contingency acquisition (Roesch et al., 2010; Esber et al., 2012). While it is possible that the reward responses we observed at the

end of training may have resulted from the subjects' not having yet acquired the stimulus-outcome associations, this seems unlikely given that these effects were replicated across two experiments. We also showed that this same conditioning protocol engendered stimulus-outcome encoding in separate groups of animals as evidenced by expression of the outcome-specific PIT effect. These discrepancies may arise from the nature of our task, which requires the subject to learn multiple stimulus-outcome associations in parallel. Further investigation is needed to determine how signed or unsigned prediction errors may evolve in this scenario. An additional caveat to consider is in one of our experiments, cues terminated in the delivery of reward. In this case, it is possible that BLA activation during this window could reflect the offset of the CS, independent of experiencing the reward. However, we also observed maintained responses to outcome collection in a task that disambiguates delivery from cue transitions, suggesting that it least in some circumstances, the BLA is persistently activated to rewards during detailed stimulus-outcome learning.

The BLA was additionally activated by the onset of the CS and this was consistent across training days. To further investigate the cue response present early in training, I recorded BLA responses to stimulus presentations in the absence of food rewards. BLA responses to unpaired cues habituated across days, consistent with previous reports (Bordi et al., 1993; Cromwell et al., 2005). It is therefore likely that these early responses are due to stimulus novelty or salience. Evidence for salience encoding in the BLA has been reported and reflects stimulus intensity (Shabel and Janak, 2009; Janak and Tye, 2015; Sengupta et al., 2018). In contrast to these early signals, activity elicited from cues in later sessions was restricted to those predicting reward and is consistent with associative encoding of reward predictive cues observed previously in BLA neurons (Schoenbaum et al., 1999; Tye and Janak, 2007; Tye et al., 2008). *In vivo* single unit recordings have revealed that during learning BLA neurons develop cue selectivity that reflects the associated outcome (Schoenbaum et al., 1999; Saddoris et al., 2005) and also encode inferred

outcome expectancies (Lucantonio et al., 2015). Blocking would again be a useful tool in determining whether acquired BLA responses to cues in our Pavlovian conditioning task encode the expectation of their specific associated reward. If this were the case, one might expect that inhibiting the BLA at the onset of the learnt cue (X) during compound training would diminish outcome expectancy. As a result, the delivery of the associated outcome (Z) would produce a prediction error capable of driving learning about the otherwise blocked cue (Y). Whether this is sufficient to promote the associative link between cue (Y) and the sensory-specific properties of outcome (Z) could be subsequently assessed by presentation of Y during outcome-specific PIT.

lOFC→BLA→lOFC projections form a serial encoding and retrieval circuit

That BLA principal neurons were activated during stimulus-outcome learning suggested that this activity might also be necessary for encoding outcome-specific associative reward memories. To test this, BLA principal neurons were optically inhibited during Pavlovian conditioning at the time of reward delivery, a window in which associative memories can be formed. While inactivation had no impact on the acquisition or expression of a Pavlovian conditional response, encoding the sensory specific details of the cue-reward relationships was impaired. These data reveal a specific *encoding* function for the BLA that links stimuli in the environment with the unique outcomes that they predict. Expanding upon this, we found that excitatory projections from the lOFC support the BLA in encoding detailed stimulus-outcome information and that this is later accessed through activation of reciprocal BLA→lOFC projections to guide adaptive decision making. That is, reciprocal lOFC→BLA→lOFC projections form a serial cue-reward encoding and retrieval circuit. These data clearly expand upon our prior knowledge of BLA and lOFC function in model-based decision making, revealing bidirectional involvement of these connections in specific phases of memory.

Previous work has demonstrated the lOFC is required to use reward predictive cues to bias instrumental choice and that this depends on inputs from the BLA (Ostlund and Balleine, 2007b;

Lichtenberg et al., 2017). These findings fit well within current frameworks of OFC function suggesting that this region integrates memories of stimuli, choices and rewards to represent the current task state, or situation (Wilson et al., 2014b; Wikenheiser and Schoenbaum, 2016; Sharpe et al., 2019; Gardner and Schoenbaum, 2021). From this perspective the OFC enables use of this state information, especially in perceptually ambiguous circumstances, to anticipate future rewards and deduce which actions will likely lead to those outcomes. Here we expand upon this, demonstrating that the lOFC not only makes use of reward memories, but also contributes to their formation through projections to the BLA. But how might encoding of these distinct stimulus-outcome memories be achieved?

Bradfield et al recently proposed that in navigating a cognitive map of action-outcome associations, the lOFC's primary function is to represent the *initial*, rather than the terminal task state (Bradfield and Hart, 2020). That is, the lOFC represents which actions are available, but not the consequences of those actions *per se*. In a similar fashion, it could be that during Pavlovian conditioning the lOFC may encode configurations of task elements that enables it to act as a general "state detector". Upon transitioning into a new state, the lOFC may direct the BLA to learn the associative structure of that state's defining features. Consistent with this idea, neurons in the BLA acquire responses to predictive cues with learning which reflects the valence of the outcomes they predict (Schoenbaum et al., 1999; Paton et al., 2006; Belova et al., 2007; Janak and Tye, 2015; Namburi et al., 2015). Critically, this rapid development of cue-selectivity in BLA neurons depends on lOFC input (Saddoris et al., 2005). The identity of appetitive food outcomes is also encoded in distinct neuronal ensembles, which could support the generation of sensory-specific reward memories (Liu et al., 2018; Courtin et al., 2022). Thus, BLA neurons are well positioned to facilitate the encoding of state-specific stimulus-outcome information. That this information is later accessed via reciprocal projections from the BLA back to the lOFC also raises the possibility that these memories are directly stored in the BLA, perhaps in distinct neuronal ensembles or engrams (Tonegawa et al., 2015; Ryan et al., 2021). It may be that upon cue presentation during

outcome-specific PIT, a specific stimulus-outcome memory is activated in the BLA and conveyed back to the lOFC for use in guiding action selection.

An alternative, though similar speculation, is that the role of the lOFC is not only to detect new states, but also to encode specific features of the elements in each state, including present stimuli and available outcomes. This is consistent with findings that the OFC encodes multiple elements of a task (Schoenbaum and Eichenbaum, 1995; Hirokawa et al., 2019), including reward identity (Howard and Kahnt, 2021). It is also known that the lOFC is needed to update outcome expectancies in the BLA (Lucantonio et al., 2015). Thus, during learning it might be the case that the lOFC signals to the BLA which particular outcome is available in the current state, driving the BLA to learn the relationship between that outcome and the antecedent cue. As described above, associative encoding in the BLA has been reported and BLA neurons also encode the contingency between cues and rewards (Bermudez and Schultz, 2010). BLA projections back to the lOFC could then update the contingency between task elements in separate states, which may be encoded in distinct neuronal ensembles in the lOFC (Schoenbaum et al., 1999; Schoenbaum et al., 2003). That is not to say that the BLA also doesn't maintain some aspect of the stimulus-outcome association since BLA→lOFC projections are clearly needed to enable cue-mediated selective choice during PIT. Activation of BLA→lOFC projections, upon cue presentation, may act to engage the appropriate task state representation in the lOFC during the novel test scenario.

Either of these speculations would account for deficits in encoding outcome-specific reward memories resulting from lOFC→BLA terminal inactivation. A role for lOFC→BLA projections in linking states to specific reward features also aligns with recent findings that these projections are required for encoding need state dependent incentive value (Malvaez et al., 2019). Future work is needed to clarify the precise information content conveyed from the lOFC to the BLA during reward learning.

The contribution of VTA→BLA projections to model-based appetitive learning

More than two decades ago it was discovered that dopamine neurons encode a prediction error – a robust phasic response to an unexpected reward that back propagates to an antecedent predictive cue (Ljungberg et al., 1992; Schultz et al., 1993). This gave rise to the popular theory that these signals serve as the teaching term in temporal difference algorithms which drives learning through endowing cues with cached value of future rewards (Schultz et al., 1997). However, this canonical model-free framework does not fully encapsulate dopamine's involvement in associative learning. Several studies have uncovered VTA dopamine broadcasts sensory prediction errors to support model-based associations that enable inferential decision making (Sadacca et al., 2016; Schultz, 2016; Sharpe et al., 2017; Takahashi et al., 2017; Langdon et al., 2018; Keiflin et al., 2019; Sharpe et al., 2020). I have added to our understanding of how dopamine contributes to such learning by uncovering an essential role for VTA_{DA}→BLA projections in encoding the link between predictive cues and the sensory features of rewards they predict.

I first uncovered evidence of robust dopamine release in the BLA in response to the delivery of distinct food outcomes throughout Pavlovian learning. Such responses early on in training have been consistently reported in VTA dopamine neurons (Schultz, 2016) and their downstream targets (Day et al., 2007), including the BLA (Lutas et al., 2019). It is likely that these responses reflect a prediction error that signals an unexpected significant event, though it is unlikely that it encodes the identity of the outcome itself (Takahashi et al., 2017). There is some debate on whether prediction errors in the amygdala drive associative learning directly or indirectly through modulating attention. As discussed above, there are reports of BLA "surprise" signals that are consistent with what is expected for signed prediction errors in attentional models of reinforcement learning (Roesch et al., 2010). The development of these attentional PEs is dependent on VTA inputs (Esber et al., 2012). This raises the possibility that signed dopamine prediction errors are locally translated in the BLA into signals that facilitate detailed learning through modulating attentional allocation to the relevant CS. Hybrid models incorporating

prediction errors and attention also suggest that these early dopamine prediction errors may drive stimulus-outcome learning directly, while attention signals modulate the rate of learning (Roesch et al., 2012). Although the Pavlovian task used in the research presented here is not designed to distinguish between these cognitive mechanisms of learning, I have demonstrated that neuronal and dopaminergic responses to reward in the BLA is necessary for encoding outcome-specific Pavlovian associations.

Like what was observed for BLA principal neuron activity, dopamine remained elevated upon reward delivery in the late stages of training. Although dopaminergic responses to rewards typically attenuate with the acquisition of appetitive associations (Schultz, 2016), this is often observed in tasks using single reinforcers and shorter cue durations than what was used here (Schultz et al., 1993; Day et al., 2007; Eshel et al., 2016; Sadacca et al., 2016; Lutas et al., 2019). Experiments varying the delay between CS onset and US delivery have revealed neuronal encoding of rewards in the VTA scales linearly with this duration and is present at longer (e. g., 16 second) CS-US intervals even after several days of conditioning (Fiorillo et al., 2008). Sustained dopamine release in the BLA upon reward delivery throughout training may therefore reflect some imprecision in the subjects' internal timing of outcome expectancy resulting from the longer 30 second cues used in our Pavlovian conditioning task. Alternatively, maintenance could result from increased task demands to learn multiple stimulus-outcomes contingencies or could reflect potential limitations of our conditioning paradigm. Regarding the later, it is important to consider that in our experiment BLA dopamine activity was monitored in the context of delayed Pavlovian conditioning, where cues terminated in food outcome delivery. It is therefore possible that these responses encode the offset of the cue, perhaps signaling a transition into a new state reflecting reward availability but is independent of experiencing the reward itself (Kalmbach et al., 2022). Future experiments would benefit from incorporation of a trace interval separating cue offset from outcome delivery to disambiguate responses to these events. Regardless of which of these specific task variables dopamine release corresponds to, restricting optical inactivation of

VTA_{DA}→BLA projections during cue offset/reward delivery to later phases of training would be useful in determining whether these late-stage responses are necessary for maintaining outcome-specific reward memories.

In addition to activation by reward delivery, phasic dopaminergic release was also present in early training sessions at the onset of the cues. Given that this occurs before the stimulus-outcome associations are learnt, this likely reflects a novelty response which has been reported in VTA dopamine neurons and habituates in the absence of motivationally significant outcomes (Schultz, 1998; Bunzeck and Düzel, 2006). But this does not imply that these signals are purely sensory and lack functional importance. As discussed previously, some models of reinforcement learning suggest stimulus novelty draws attention which strengthens its associability (Mackintosh, 1975; Pearce and Hall, 1980; Holland and Schiffino, 2016). In support of these theories, a recent study has found striatal dopamine modulates attentional allocation to a stimulus through encoding its perceived salience – a combination of its novelty and physical intensity (Kutlu et al., 2021). Dopaminergic novelty signals deterministically influence associative learning (Kutlu et al., 2022) and the associated development of conditional responses (Morrens et al., 2020). Whether dopaminergic novelty encoding in the BLA similarly influences detailed stimulus-outcome learning is an intriguing possibility.

Optically inhibiting VTA_{DA}→BLA projections during reward delivery in Pavlovian conditioning or stimulation of these projections upon outcome presentation in Pavlovian blocking revealed these inputs are necessary and sufficient for learning the association between distinct cues and the specific rewards they predict. Although the precise neural mechanisms underlying these effects were not tested, dopamine likely exerts its influence through modulating synaptic plasticity in the BLA during learning. Activation of D1 receptors enhances the excitability of BLA principal neurons and positively modulate LTP induction of cortical inputs onto BLA projection neurons through upregulation of cAMP (Li et al., 2011a; Li and Rainnie, 2014; Lutas et al., 2022). Synaptic plasticity in the BLA is also largely shaped by inhibitory interneurons (Ehrlich et al.,

2009; Perumal and Sah, 2021). Activation of presynaptic D2 receptors on inhibitory interneurons reduces GABAergic transmission (Bissière et al., 2003; Chu et al., 2012) and gates long term potentiation (LTP) of thalamic-BLA synapses through suppression of feedforward inhibition onto excitatory principal neurons (Bissière et al., 2003; Chang and Grace, 2015). Dopaminergic enhancement of feedforward inhibition onto inhibitory neurons is also D2 receptor mediated and similarly results in disinhibition of principal neurons (Bissière et al., 2003). Dopamine also attenuates prefrontal cortical suppression of sensory inputs to the BLA (Rosenkranz 2001), likely through D1 receptor mediated inactivation of GABAergic ITCs (Marowsky et al., 2005). Whether dopamine similarly disinhibits or directly facilitates potentiation of lOFC→BLA inputs is unknown but could be a potential mechanism underlying outcome-specific associative learning. In contrast to D1 mediated hyperpolarization of ITCs, activation of these receptors increases local inhibitory interneuron excitability (Bissière et al., 2003; Lorétan et al., 2004; Kröner et al., 2005). Resulting increases in spontaneous IPSC frequency in principal neurons may be important for counteracting responses to weaker inputs during learning. This would be akin to findings of dopaminergic enhancement of signal to noise in the prefrontal cortex, which facilitates aversive conditioning (Vander Weele et al., 2018; Ott and Nieder, 2019; Stalter et al., 2020).

Dopaminergic tuning of signal to noise in BLA principal neurons through potentiation of strong phasic inputs (i.e., gain modulation) and reduced spontaneous activity (i.e., noise reduction) would also have important implications for appetitive learning. Indeed, this has been substantiated at the behavioral level with one study reporting elevated dopamine in the BLA simultaneously enhanced cue-reward learning with a single reinforcer and suppressed responding to task irrelevant information (Tye et al., 2010). Within the context of outcome-specific associative learning, dopamine release in the BLA may be facilitating potentiation of lOFC inputs conveying state-relevant information (e.g., a specific outcome expectation during a given cue) while also suppressing BLA responses to weaker inputs conveying state irrelevant information (e.g., currently unavailable outcomes). This would mechanistically support my findings that both

lOFC→BLA and VTA_{DA}→BLA terminal inhibition impairs detailed stimulus-outcome learning to the extent that these associations cannot be used to adaptively bias choice selection during PIT. Interestingly, enhanced cue-induced pressing was biased for the action associated with the outcome that was different than what was predicted by the CS following VTA_{DA}→BLA inactivation during Pavlovian conditioning. These results might be expected if dopamine played a role in potentiating task relevant inputs and/or suppressing those that are irrelevant. Enhanced gain modulation could also explain why VTA_{DA}→BLA stimulation was sufficient to unblock stimulus-outcome encoding. During Pavlovian blocking, the acquisition of stimulus-outcome associations is prevented if the outcome is already predicted by another cue present in the environment. Dopamine neurons only weakly respond to the expected outcome in this scenario (Waelti et al., 2001). Under normal circumstances, dopamine release in the BLA may therefore be insufficient to potentiate synapses receiving information about the blocked cue. Alternatively, it is possible this small phasic increase in dopamine may even counteract BLA responses to the added stimulus through recruitment of inhibitory interneurons. Stimulating VTA_{DA}→BLA neurons might overcome this by sufficiently augmenting dopamine to tip the scale in favor of driving synaptic plasticity of the weaker inputs conveying information about the redundant cue. These mechanisms are of course speculative but present intriguing hypotheses that could be tested in future research.

Conclusions and Future Directions

Collectively, these data demonstrate the BLA is a central hub for outcome-specific reward memory, receiving excitatory inputs from the lOFC and modulation from VTA dopamine neurons to enable encoding of sensory-specific Pavlovian associations and their subsequent use through projections back to the lOFC. In multiplexing pathway-specific manipulations with complex behavioral paradigms, this work has uncovered neural substrates that enable model-based decision making and opens many exciting avenues for investigation. An obvious path forward is determining the precise information content that is being encoded by reciprocal BLA-OFC

projections and BLA dopamine release. This could be accomplished by combining calcium imaging techniques, such as fiber photometry or miniaturized microscopes (Siciliano and Tye, 2019), with behavioral tasks designed to test precise predictions posed by reinforcement learning theories. Whether unique stimulus-outcome associations are encoded by distinct neuronal ensembles in the BLA, lOFC or both could also be ascertained through recording neuronal populations with single cell resolution during Pavlovian conditioning. Pharmacological manipulation of dopamine receptors combined with *in vitro* slice physiology will be important for assessing how VTA dopamine might be shaping plasticity of lOFC→BLA synapses during learning. Finally, outcome expectancy in the OFC is updated by VTA inputs (Takahashi et al., 2009; Howard and Kahnt, 2018) and may therefore be an additional element of the circuitry needed to facilitate detailed stimulus-outcome encoding mediated by network communication with the BLA. But this remains to be tested.

Stepping through our cognitive map of the environment allows us to envision which specific rewards are available and the actions needed to obtain them. With this information we can make complex decisions based on our current needs and goals. Investigation into the neural mechanisms mediating associative learning advances our understanding of how these adaptive choices are made, but also provides insight into how decision making goes awry in mental illness. Model-based learning is disrupted in several psychiatric disorders (Hogarth et al., 2013; Chen et al., 2015; Culbreth et al., 2016; Bishop and Gagne, 2018; Radulescu and Niv, 2019) and abnormal amygdala, OFC or dopamine activity is a characteristic feature in many of these cases (Everitt and Robbins, 2005; Dayan, 2009; Schoenbaum et al., 2016; Sharp, 2017). In providing evidence that suggests a causal link between these cognitive and neural deficits, this research highlights potential targets for clinical interventions aimed to improve behavioral and circuit function in human patient populations.

References

Adams CD, Dickinson A (1981) Instrumental responding following reinforcer devaluation. The Quarterly Journal of Experimental Psychology 33:109-121.

Aggarwal M, Akamine Y, Liu AW, Wickens JR (2020) The nucleus accumbens and inhibition in the ventral tegmental area play a causal role in the Kamin blocking effect. Eur J Neurosci 52:3087-3109.

Aggleton JP, Burton MJ, Passingham RE (1980) Cortical and subcortical afferents to the amygdala of the rhesus monkey (Macaca mulatta). Brain Res 190:347-368.

Akam T, Walton ME (2021) What is dopamine doing in model-based reinforcement learning? Current Opinion in Behavioral Sciences 38:74-82.

Arguello AA, Richardson BD, Hall JL, Wang R, Hodges MA, Mitchell MP, Stuber GD, Rossi DJ, Fuchs RA (2017) Role of a Lateral Orbital Frontal Cortex-Basolateral Amygdala Circuit in Cue-Induced Cocaine-Seeking Behavior. Neuropsychopharmacology 42:727-735.

Balleine BW, Dickinson A (1998a) The role of incentive learning in instrumental outcome revaluation by sensory-specific satiety. Animal Learning & Behavior 26:46-59.

Balleine BW, Dickinson A (1998b) Goal-directed instrumental action: contingency and incentive learning and their cortical substrates. Neuropharmacology 37:407-419.

Balleine BW, O'Doherty JP (2009) Human and Rodent Homologies in Action Control: Corticostriatal Determinants of Goal-Directed and Habitual Action. Neuropsychopharmacology 35:48-69.

Balleine BW, Killcross AS, Dickinson A (2003) The Effect of Lesions of the Basolateral Amygdala on Instrumental Conditioning.

Balleine BW, Daw ND, O'Doherty JP (2009) Chapter 24 - Multiple Forms of Value Learning and the Function of Dopamine. In: Neuroeconomics (Glimcher PW, Camerer CF, Fehr E, Poldrack RA, eds), pp 367-387. London: Academic Press.

Baltz ET, Yalcinbas EA, Renteria R, Gremel CM (2018) Orbital frontal cortex updates state-induced value change for decision-making. Elife 7.

Barreiros IV, Panayi MC, Walton ME (2021) Organization of Afferents along the Anterior-posterior and Medial-lateral Axes of the Rat Orbitofrontal Cortex. Neuroscience 460:53-68.

Baxter DJ, Zamble E (1982) Reinforcer and response specificity in appetitive transfer of control. In: Animal Learning & Behavior, pp 201-210.

Baxter MG, Murray EA (2002) The amygdala and reward. Nat Rev Neurosci 3:563-573.

Baxter MG, Parker A, Lindner CC, Izquierdo AD, Murray EA (2000) Control of response selection by reinforcer value requires interaction of amygdala and orbital prefrontal cortex. J Neurosci 20:4311-4319.

Bayer HM, Glimcher PW (2005) Midbrain dopamine neurons encode a quantitative reward prediction error signal. Neuron 47:129-141.

Belova MA, Paton JJ, Salzman CD (2008) Moment-to-moment tracking of state value in the amygdala. J Neurosci 28:10023-10030.

Belova MA, Paton JJ, Morrison SE, Salzman CD (2007) Expectation modulates neural responses to pleasant and aversive stimuli in primate amygdala. Neuron 55:970-984.

Bermudez MA, Schultz W (2010) Responses of amygdala neurons to positive reward-predicting stimuli depend on background reward (contingency) rather than stimulus-reward pairing (contiguity). J Neurophysiol 103:1158-1170.

Berns GS, McClure SM, Pagnoni G, Montague PR (2001) Predictability modulates human brain response to reward. J Neurosci 21:2793-2798.

Beyeler A, Chang CJ, Silvestre M, Lévêque C, Namburi P, Wildes CP, Tye KM (2018) Organization of Valence-Encoding and Projection-Defined Neurons in the Basolateral Amygdala. Cell Rep 22:905-918.

Beyeler A, Namburi P, Glober GF, Simonnet C, Calhoon GG, Conyers GF, Luck R, Wildes CP, Tye KM (2016) Divergent Routing of Positive and Negative Information from the Amygdala during Memory Retrieval. Neuron 90:348-361.

Bindra D (1968) Neuropsychological interpretation of the effects of drive and incentive-motivation on general activity and instrumental behavior. Psychological Review 75:1-1.

Bindra D (1974) A motivational view of learning, performance, and behavior modification. Psychological Review 81:199-199.

Bishop SJ, Gagne C (2018) Anxiety, Depression, and Decision Making: A Computational Perspective. Annu Rev Neurosci 41:371-388.

Bissière S, Humeau Y, Lüthi A (2003) Dopamine gates LTP induction in lateral amygdala by suppressing feedforward inhibition. Nat Neurosci 6:587-592.

Blundell P, Hall G, Killcross S (2001) Lesions of the basolateral amygdala disrupt selective aspects of reinforcer representation in rats. J Neurosci 21:9018-9026.

Bolles RC (1972) Reinforcement, expectancy, and learning. Psychological Review 79:394-394.

Bolles RC, Holtz R, Dunn T, Hill W (1980) Comparisons of stimulus learning and response learning in a punishment situation. Learning and Motivation 11:78-96.

Bordi F, LeDoux J (1992) Sensory tuning beyond the sensory system: an initial analysis of auditory response properties of neurons in the lateral amygdaloid nucleus and overlying areas of the striatum. J Neurosci 12:2493-2503.

Bordi F, LeDoux J, Clugnet MC, Pavlides C (1993) Single-unit activity in the lateral nucleus of the amygdala and overlying areas of the striatum in freely behaving rats: rates, discharge patterns, and responses to acoustic stimuli. Behav Neurosci 107:757-769.

Bradfield LA, Hart G (2020) Rodent medial and lateral orbitofrontal cortices represent unique components of cognitive maps of task space. Neurosci Biobehav Rev 108:287-294.

Breton JM, Charbit AR, Snyder BJ, Fong PTK, Dias EV, Himmels P, Lock H, Margolis EB (2019) Relative contributions and mapping of ventral tegmental area dopamine and GABA neurons by projection target in the rat. J Comp Neurol 527:916-941.

Brinley-Reed M, McDonald AJ (1999) Evidence that dopaminergic axons provide a dense innervation of specific neuronal subpopulations in the rat basolateral amygdala. Brain Res 850:127-135.

Brogden WJ (1939) Sensory pre-conditioning. Journal of experimental psychology 25:323.

Bromberg-Martin ES, Matsumoto M, Hong S, Hikosaka O (2010) A pallidus-habenula-dopamine pathway signals inferred stimulus values. J Neurophysiol 104:1068-1076.

Bunzeck N, Düzel E (2006) Absolute coding of stimulus novelty in the human substantia nigra/VTA. Neuron 51:369-379.

Butler RK, Sharko AC, Oliver EM, Brito-Vargas P, Kaigler KF, Fadel JR, Wilson MA (2011) Activation of phenotypically-distinct neuronal subpopulations of the rat amygdala following exposure to predator odor. Neuroscience 175:133-144.

Carmichael ST, Price JL (1995) Limbic connections of the orbital and medial prefrontal cortex in macaque monkeys. J Comp Neurol 363:615-641.

Chang CH, Grace AA (2015) Dopaminergic Modulation of Lateral Amygdala Neuronal Activity: Differential D1 and D2 Receptor Effects on Thalamic and Cortical Afferent Inputs. Int J Neuropsychopharmacol 18.

Chang CY, Gardner M, Di Tillio MG, Schoenbaum G (2017) Optogenetic Blockade of Dopamine Transients Prevents Learning Induced by Changes in Reward Features. Curr Biol 27:3480-3486.e3483.

Chang CY, Esber GR, Marrero-Garcia Y, Yau HJ, Bonci A, Schoenbaum G (2016) Brief optogenetic inhibition of dopamine neurons mimics endogenous negative reward prediction errors. Nat Neurosci 19:111-116.

Chang SE, McDannald MA, Wheeler DS, Holland PC (2012) The effects of basolateral amygdala lesions on unblocking. Behav Neurosci 126:279-289.

Chen C, Takahashi T, Nakagawa S, Inoue T, Kusumi I (2015) Reinforcement learning in depression: A review of computational research. Neurosci Biobehav Rev 55:247-267.

Chen TW, Wardill TJ, Sun Y, Pulver SR, Renninger SL, Baohan A, Schreiter ER, Kerr RA, Orger MB, Jayaraman V, Looger LL, Svoboda K, Kim DS (2013) Ultrasensitive fluorescent proteins for imaging neuronal activity. Nature 499:295-300.

Chu H-Y, Ito W, Li J, Morozov A (2012) Target-Specific Suppression of GABA Release from Parvalbumin Interneurons in the Basolateral Amygdala by Dopamine.

Collins AL, Saunders BT (2020) Heterogeneity in striatal dopamine circuits: Form and function in dynamic reward seeking. J Neurosci Res 98:1046-1069.

Collins AL, Aitken TJ, Huang IW, Shieh C, Greenfield VY, Monbouquette HG, Ostlund SB, Wassum KM (2019) Nucleus Accumbens Cholinergic Interneurons Oppose Cue-Motivated Behavior. Biol Psychiatry.

Colwill RM, Rescorla RA (1985) Postconditioning Devaluation of a Reinforcer Affects Instrumental Responding. Journal of Experimental Psychology: Animal Behavior Processes 11:120-132.

Colwill RM, Rescorla RA (1986) Associative Structures In Instrumental Learning. Psychology of Learning and Motivation - Advances in Research and Theory 20:55-104.

Colwill RM, Motzkin DK (1994) Encoding of the unconditioned stimulus in Pavlovian conditioning. *Animal Learning & Behavior* 22:384-394.

Cone JJ, Fortin SM, McHenry JA, Stuber GD, McCutcheon JE, Roitman MF (2016) Physiological state gates acquisition and expression of mesolimbic reward prediction signals. Proc Natl Acad Sci U S A 113:1943-1948.

Constantinople CM, Piet AT, Bibawi P, Akrami A, Kopec C, Brody CD (2019) Lateral orbitofrontal cortex promotes trial-by-trial learning of risky, but not spatial, biases. Elife 8.

Corbit LH, Balleine BW (2005) Double dissociation of basolateral and central amygdala lesions on the general and outcome-specific forms of pavlovian-instrumental transfer. J Neurosci 25:962-970.

Corbit LH, Balleine BW (2016) Learning and Motivational Processes Contributing to Pavlovian-Instrumental Transfer and Their Neural Bases: Dopamine and Beyond. Curr Top Behav Neurosci.

Corbit LH, Leung BK, Balleine BW (2013) The role of the amygdala-striatal pathway in the acquisition and performance of goal-directed instrumental actions. J Neurosci 33:17682-17690.

Costa KM, Scholz R, Lloyd K, Moreno-Castilla P, Gardner MPH, Dayan P, Schoenbaum G (2022) The role of the orbitofrontal cortex in creating cognitive maps. bioRxiv:2022.2001.2025.477716.

Costa VD, Mitz AR, Averbeck BB (2019) Subcortical Substrates of Explore-Exploit Decisions in Primates. Neuron 103:533-545.e535.

Costa VD, Dal Monte O, Lucas DR, Murray EA, Averbeck BB (2016) Amygdala and Ventral Striatum Make Distinct Contributions to Reinforcement Learning. Neuron 92:505-517.

Courtin J, Bitterman Y, Müller S, Hinz J, Hagihara KM, Müller C, Lüthi A (2022) A neuronal mechanism for motivational control of behavior. Science 375:eabg7277.

Cromwell HC, Anstrom K, Azarov A, Woodward DJ (2005) Auditory inhibitory gating in the amygdala: single-unit analysis in the behaving rat. Brain Res 1043:12-23.

Crouse RB, Kim K, Batchelor HM, Girardi EM, Kamaletdinova R, Chan J, Rajebhosale P, Pittenger ST, Role LW, Talmage DA, Jing M, Li Y, Gao XB, Mineur YS, Picciotto MR (2020) Acetylcholine is released in the basolateral amygdala in response to predictors of reward and enhances the learning of cue-reward contingency. Elife 9.

Crow TJ (1972) Catecholamine-containing neurones and electrical self-stimulation. 1. A review of some data. Psychol Med 2:414-421.

Culbreth AJ, Westbrook A, Daw ND, Botvinick M, Barch DM (2016) Reduced model-based decision-making in schizophrenia. J Abnorm Psychol 125:777-787.

D'Ardenne K, McClure SM, Nystrom LE, Cohen JD (2008) BOLD Responses Reflecting Dopaminergic Signals in the Human Ventral Tegmental Area.

Davis M (1992) The role of the amygdala in fear and anxiety. Annu Rev Neurosci 15:353-375.

Daw ND, Niv Y, Dayan P (2005) Uncertainty-based competition between prefrontal and dorsolateral striatal systems for behavioral control. Nature Neuroscience 8:1704-1711.

Day JJ, Roitman MF, Wightman RM, Carelli RM (2007) Associative learning mediates dynamic shifts in dopamine signaling in the nucleus accumbens. Nat Neurosci 10:1020-1028.

Dayan P (2009) Dopamine, reinforcement learning, and addiction. Pharmacopsychiatry 42 Suppl 1:S56-65.

Dayan P, Berridge KC (2014) Model-based and model-free Pavlovian reward learning: revaluation, revision, and revelation. Cognitive, affective & behavioral neuroscience 14:473-492.

de Oliveira AR, Reimer AE, de Macedo CE, de Carvalho MC, Silva MA, Brandão ML (2011) Conditioned fear is modulated by D2 receptor pathway connecting the ventral tegmental area and basolateral amygdala. Neurobiol Learn Mem 95:37-45.

de Souza Caetano KA, de Oliveira AR, Brandão ML (2013) Dopamine D2 receptors modulate the expression of contextual conditioned fear: role of the ventral tegmental area and the basolateral amygdala. Behav Pharmacol 24:264-274.

Delamater AR (1995) Outcome-selective effects of intertrial reinforcement in a Pavlovian appetitive conditioning paradigm with rats. Animal Learning & Behavior 23:31-39.

Delamater AR (2007) The role of the orbitofrontal cortex in sensory-specific encoding of associations in pavlovian and instrumental conditioning. Ann N Y Acad Sci 1121:152-173.

Delamater AR (2012) On the nature of CS and US representations in Pavlovian learning. Learn Behav 40:1-23.

Delamater AR, Oakeshott S (2007) Learning about multiple attributes of reward in Pavlovian conditioning. Ann N Y Acad Sci 1104:1-20.

Derman RC, Bass CE, Ferrario CR (2020) Effects of hM4Di activation in CamKII basolateral amygdala neurons and CNO treatment on sensory-specific vs. general PIT: refining PIT circuits and considerations for using CNO. Psychopharmacology (Berl) 237:1249-1266.

Di Ciano P, Cardinal RN, Cowell RA, Little SJ, Everitt BJ (2001) Differential involvement of NMDA, AMPA/kainate, and dopamine receptors in the nucleus accumbens core in the acquisition and performance of pavlovian approach behavior. J Neurosci 21:9471-9477.

Dickinson A (1985) Actions and habits: the development of behavioural autonomy. Philosophical Transactions of the Royal Society of London B, Biological Sciences 308:67-78.

Dickinson A, Mulatero CW (1989) Reinforcer specificity of the suppression of instrumental performance on a non-contingent schedule. Behavioural Processes 19:167-180.

Dickinson A, Balleine B (1994) Motivational control of goal-directed action. Animal Learning & Behavior 22:1-18.

Dickinson A, Campos J, Varga ZI, Balleine B (1996) Bidirectional instrumental conditioning. Q J Exp Psychol B 49:289-306.

Dolan RJ, Dayan P (2013) Goals and habits in the brain. Neuron 80:312-325.

Drummond N, Niv Y (2020) Model-based decision making and model-free learning. Curr Biol 30:R860-R865.

Duvarci S, Pare D (2014) Amygdala microcircuits controlling learned fear. In: Neuron, pp 966-980: Cell Press.

Ehrlich I, Humeau Y, Grenier F, Ciocchi S, Herry C, Lüthi A (2009) Amygdala inhibitory circuits and the control of fear memory. Neuron 62:757-771.

Engelhard B, Finkelstein J, Cox J, Fleming W, Jang HJ, Ornelas S, Koay SA, Thiberge SY, Daw ND, Tank DW, Witten IB (2019) Specialized coding of sensory, motor and cognitive variables in VTA dopamine neurons. Nature 570:509-513.

Esber GR, Holland PC (2014) The basolateral amygdala is necessary for negative prediction errors to enhance cue salience, but not to produce conditioned inhibition. Eur J Neurosci 40:3328-3337.

Esber GR, Roesch MR, Bali S, Trageser J, Bissonette GB, Puche AC, Holland PC, Schoenbaum G (2012) Attention-related Pearce-Kaye-Hall signals in basolateral amygdala require the midbrain dopaminergic system. Biol Psychiatry 72:1012-1019.

Eshel N, Tian J, Bukwich M, Uchida N (2016) Dopamine neurons share common response function for reward prediction error. Nat Neurosci 19:479-486.

Estes WK (1948) Discriminative conditioning; effects of a Pavlovian conditioned stimulus upon a subsequently established operant response. J Exp Psychol 38:173-177.

Everitt BJ, Robbins TW (2005) Neural systems of reinforcement for drug addiction: from actions to habits to compulsion. Nat Neurosci 8:1481-1489.

Everitt BJ, Robbins TW (2016) Drug Addiction: Updating Actions to Habits to Compulsions Ten Years On. Annual Review of Psychology 67:23-50.

Everitt BJ, Cardinal RN, Hall J, Parkinson JA, Robbins TW (2000) Differential involvement of amygdala subsystems in appetitive conditioning and drug addiction. In: *The amygdala: A functional analysi*, pp 353-390.

Fallon J, Ciofi P (1992) Distribution of monoamines within the amygdala. In: The Amygdala, pp 97-114. New York: Academic Press.

Fanselow MS, LeDoux JE (1999) Why we think plasticity underlying Pavlovian fear conditioning occurs in the basolateral amygdala. Neuron 23:229-232.

Fanselow MS, Wassum KM (2015) The Origins and Organization of Vertebrate Pavlovian Conditioning. Cold Spring Harb Perspect Biol.

Feierstein CE, Quirk MC, Uchida N, Sosulski DL, Mainen ZF (2006) Representation of spatial goals in rat orbitofrontal cortex. Neuron 51:495-507.

Felsenberg J, Jacob PF, Walker T, Barnstedt O, Edmondson-Stait AJ, Pleijzier MW, Otto N, Schlegel P, Sharifi N, Perisse E, Smith CS, Lauritzen JS, Costa M, Jefferis GSXE, Bock DD, Waddell S (2018) Integration of Parallel Opposing Memories Underlies Memory Extinction. Cell 175:709-722.e715.

Fiorillo CD, Newsome WT, Schultz W (2008) The temporal precision of reward prediction in dopamine neurons. Nat Neurosci 11:966-973.

Fisher SD, Ferguson LA, Bertran-Gonzalez J, Balleine BW (2020) Amygdala-Cortical Control of Striatal Plasticity Drives the Acquisition of Goal-Directed Action. Curr Biol.

Fiuzat EC, Rhodes SE, Murray EA (2017) The role of orbitofrontal-amygdala interactions in updating action-outcome valuations in macaques. J Neurosci.

Fontanini A, Grossman SE, Figueroa JA, Katz DB (2009) Distinct subtypes of basolateral amygdala taste neurons reflect palatability and reward. J Neurosci 29:2486-2495.

Gallagher M, McMahan RW, Schoenbaum G (1999) Orbitofrontal cortex and representation of incentive value in associative learning. The Journal of neuroscience : the official journal of the Society for Neuroscience 19:6610-6614.

Gardner MPH, Schoenbaum G (2021) The orbitofrontal cartographer. Behav Neurosci 135:267-276.

Gilroy KE, Everett EM, Delamater AR (2014) Response-Outcome versus Outcome-Response Associations in Pavlovian-to-Instrumental Transfer: Effects of Instrumental Training Context. Int J Comp Psychol 27:585-597.

Glimcher PW (2011) Understanding dopamine and reinforcement learning: The dopamine reward prediction error hypothesis. Proceedings of the National Academy of Sciences of the United States of America 108:15647-15654.

Gläscher J, Daw N, Dayan P, O'Doherty JP (2010) States versus rewards: dissociable neural prediction error signals underlying model-based and model-free reinforcement learning. Neuron 66:585-595.

Goldstein RZ, Volkow ND (2011) Dysfunction of the prefrontal cortex in addiction: neuroimaging findings and clinical implications. Nat Rev Neurosci 12:652-669.

Grace AA, Rosenkranz JA (2002) Regulation of conditioned responses of basolateral amygdala neurons. Physiology & behavior 77.

Greba Q, Kokkinidis L (2000) Peripheral and intraamygdalar administration of the dopamine D1 receptor antagonist SCH 23390 blocks fear-potentiated startle but not shock reactivity or the shock sensitization of acoustic startle. Behav Neurosci 114:262-272.

Greba Q, Gifkins A, Kokkinidis L (2001) Inhibition of amygdaloid dopamine D2 receptors impairs emotional learning measured with fear-potentiated startle. Brain Res 899:218-226.

Grillon C (2002) Associative learning deficits increase symptoms of anxiety in humans. Biol Psychiatry 51:851-858.

Groman SM, Keistler C, Keip AJ, Hammarlund E, DiLeone RJ, Pittenger C, Lee D, Taylor JR (2019) Orbitofrontal Circuits Control Multiple Reinforcement-Learning Processes. Neuron.

Guarraci FA, Frohardt RJ, Kapp BS (1999a) Amygdaloid D1 dopamine receptor involvement in Pavlovian fear conditioning. Brain Res 827:28-40.

Guarraci FA, Frohardt RJ, Young SL, Kapp BS (1999b) A functional role for dopamine transmission in the amygdala during conditioned fear. Ann N Y Acad Sci 877:732-736.

Hall J, Parkinson JA, Connor TM, Dickinson A, Everitt BJ (2001) Involvement of the central nucleus of the amygdala and nucleus accumbens core in mediating Pavlovian influences on instrumental behaviour. Eur J Neurosci 13:1984-1992.

Hammond LJ (1980) The effect of contingency upon the appetitive conditioning of free-operant behavior. Journal of the Experimental Analysis of Behavior 34:297-304.

Harmer CJ, Phillips GD (1999) Enhanced dopamine efflux in the amygdala by a predictive, but not a non-predictive, stimulus: facilitation by prior repeated D-amphetamine. Neuroscience 90:119-130.

Hart AS, Rutledge RB, Glimcher PW, Phillips PE (2014) Phasic dopamine release in the rat nucleus accumbens symmetrically encodes a reward prediction error term. J Neurosci 34:698-704.

Hart EE, Sharpe MJ, Gardner MP, Schoenbaum G (2020) Responding to preconditioned cues is devaluation sensitive and requires orbitofrontal cortex during cue-cue learning. Elife 9.

Hatfield T, Han JS, Conley M, Gallagher M, Holland P (1996) Neurotoxic lesions of basolateral, but not central, amygdala interfere with Pavlovian second-order conditioning and reinforcer devaluation effects. J Neurosci 16:5256-5265.

Heath FC, Jurkus R, Bast T, Pezze MA, Lee JL, Voigt JP, Stevenson CW (2015) Dopamine D1-like receptor signalling in the hippocampus and amygdala modulates the acquisition of contextual fear conditioning. Psychopharmacology (Berl) 232:2619-2629.

Heilbronner SR, Rodriguez-Romaguera J, Quirk GJ, Groenewegen HJ, Haber SN (2016) Circuit-Based Corticostriatal Homologies Between Rat and Primate. Biol Psychiatry 80:509-521.

Hersman S, Allen D, Hashimoto M, Brito SI, Anthony TE (2020) Stimulus salience determines defensive behaviors elicited by aversively conditioned serial compound auditory stimuli. Elife 9.

Hikind N, Maroun M (2008) Microinfusion of the D1 receptor antagonist, SCH23390 into the IL but not the BLA impairs consolidation of extinction of auditory fear conditioning. Neurobiol Learn Mem 90:217-222.

Hirokawa J, Vaughan A, Masset P, Ott T, Kepecs A (2019) Frontal cortex neuron types categorically encode single decision variables. Nature 576:446-451.

Hogarth L, Balleine BW, Corbit LH, Killcross S (2013) Associative learning mechanisms underpinning the transition from recreational drug use to addiction. Ann N Y Acad Sci 1282:12-24.

Holland PC (1981) The effects of satiation after first- and second-order appetitive conditioning in rats. The Pavlovian journal of biological science 16:18-24.

Holland PC (1984) Unblocking in Pavlovian appetitive conditioning. J Exp Psychol Anim Behav Process 10:476-497.

Holland PC, Rescorla RA (1976) The effect of two ways of devaluing the unconditioned stimulus after first- and second-order appetitive conditioning. Journal of Experimental Psychology: Animal Behavior Processes 1:355-355.

Holland PC, Straub JJ (1980) Differential effects of two ways of devaluing the unconditioned stimulus after Pavlovian appetitive conditioning. Journal of Experimental Psychology: Animal Behavior Processes 5:65-65.

Holland PC, Schiffino FL (2016) Mini-review: Prediction errors, attention and associative learning. Neurobiol Learn Mem 131:207-215.

Howard JD, Kahnt T (2017) Identity-specific reward representations in orbitofrontal cortex are modulated by selective devaluation. Journal of Neuroscience 37:2627-2638.

Howard JD, Kahnt T (2018) Identity prediction errors in the human midbrain update reward-identity expectations in the orbitofrontal cortex. Nat Commun 9:1611.

Howard JD, Kahnt T (2021) To be specific: The role of orbitofrontal cortex in signaling reward identity. Behav Neurosci 135:210-217.

Howard JD, Gottfried JA, Tobler PN, Kahnt T (2015) Identity-specific coding of future rewards in the human orbitofrontal cortex. Proc Natl Acad Sci U S A 112:5195-5200.

Hull CL (1943) Principles of behavior: an introduction to behavior theory. New York: Appleton-Century.

Iglesias S, Mathys C, Brodersen KH, Kasper L, Piccirelli M, den Ouden HE, Stephan KE (2013) Hierarchical prediction errors in midbrain and basal forebrain during sensory learning. Neuron 80:519-530.

Izquierdo A, Suda RK, Murray EA (2004) Bilateral orbital prefrontal cortex lesions in rhesus monkeys disrupt choices guided by both reward value and reward contingency. J Neurosci 24:7540-7548.

Izquierdo A, Darling C, Manos N, Pozos H, Kim C, Ostrander S, Cazares V, Stepp H, Rudebeck PH (2013) Basolateral amygdala lesions facilitate reward choices after negative feedback in rats. J Neurosci 33:4105-4109.

Janak PH, Tye KM (2015) From circuits to behaviour in the amygdala. Nature 517:284-292.

Johansen JP, Tarpley JW, LeDoux JE, Blair HT (2010) Neural substrates for expectation-modulated fear learning in the amygdala and periaqueductal gray. Nat Neurosci 13:979-986.

Johnson AW, Gallagher M, Holland PC (2009) The basolateral amygdala is critical to the expression of pavlovian and instrumental outcome-specific reinforcer devaluation effects. J Neurosci 29:696-704.

Jones JL, Esber GR, McDannald MA, Gruber AJ, Hernandez A, Mirenzi A, Schoenbaum G (2012) Orbitofrontal cortex supports behavior and learning using inferred but not cached values. Science 338:953-956.

Kalmbach A, Winiger V, Jeong N, Asok A, Gallistel CR, Balsam PD, Simpson EH (2022) Dopamine encodes real-time reward availability and transitions between reward availability states on different timescales. Nat Commun 13:3805.

Kamin LJ (1968) "Attention-like" processes in classical conditioning. In: Miami symposium on the prediction of behavior: aversive stimulation, M. Jones Edition, pp 9-31. Miami: University of Miami Press.

Keiflin R, Reese RM, Woods CA, Janak PH (2013) The orbitofrontal cortex as part of a hierarchical neural system mediating choice between two good options. J Neurosci 33:15989-15998.

Keiflin R, Pribut HJ, Shah NB, Janak PH (2019) Ventral Tegmental Dopamine Neurons Participate in Reward Identity Predictions. Curr Biol 29:93-103.e103.

Keramati M, Dezfouli A, Piray P (2011) Speed/accuracy trade-off between the habitual and the goal-directed processes. PLoS Comput Biol 7:e1002055.

Killcross S, Robbins TW, Everitt BJ (1997) Different types of fear-conditioned behaviour mediated by separate nuclei within amygdala. Nature 388:377-380.

Kim H, Shimojo S, O'Doherty JP (2006) Is avoiding an aversive outcome rewarding? Neural substrates of avoidance learning in the human brain. PLoS Biol 4:e233.

Klein-Flügge MC, Barron HC, Brodersen KH, Dolan RJ, Behrens TE (2013) Segregated encoding of reward-identity and stimulus-reward associations in human orbitofrontal cortex. J Neurosci 33:3202-3211.

Kochli DE, Keefer SE, Gyawali U, Calu DJ (2020) Basolateral Amygdala to Nucleus Accumbens Communication Differentially Mediates Devaluation Sensitivity of Sign- and Goal-Tracking Rats. Front Behav Neurosci 14:593645.

Konorski J (1967) Integrative activity of the brain: An interdisciplinary approach. Chicago: University of Chicago Press.

Kruse JM, Overmier JB, Konz WA, Rokke E (1983) Pavlovian conditioned stimulus effects upon instrumental choice behavior are reinforcer specific. Learning and Motivation 14:165-181.

Kröner S, Rosenkranz JA, Grace AA, Barrionuevo G (2005) Dopamine modulates excitability of basolateral amygdala neurons in vitro. J Neurophysiol 93:1598-1610.

Kutlu MG, Zachry JE, Melugin PR, Cajigas SA, Chevee MF, Kelly SJ, Kutlu B, Tian L, Siciliano CA, Calipari ES (2021) Dopamine release in the nucleus accumbens core signals perceived saliency. Curr Biol 31:4748-4761.e4748.

Kutlu MG, Zachry JE, Melugin PR, Tat J, Cajigas S, Isiktas AU, Patel DD, Siciliano CA, Schoenbaum G, Sharpe MJ, Calipari ES (2022) Dopamine signaling in the nucleus accumbens core mediates latent inhibition. Nat Neurosci 25:1071-1081.

Lamont EW, Kokkinidis L (1998) Infusion of the dopamine D1 receptor antagonist SCH 23390 into the amygdala blocks fear expression in a potentiated startle paradigm. Brain Res 795:128-136.

Langdon AJ, Sharpe MJ, Schoenbaum G, Niv Y (2018) Model-based predictions for dopamine. Curr Opin Neurobiol 49:1-7.

Larkin JD, Jenni NL, Floresco SB (2016) Modulation of risk/reward decision making by dopaminergic transmission within the basolateral amygdala. Psychopharmacology (Berl) 233:121-136.

Lasseter HC, Wells AM, Xie X, Fuchs RA (2011) Interaction of the basolateral amygdala and orbitofrontal cortex is critical for drug context-induced reinstatement of cocaine-seeking behavior in rats. Neuropsychopharmacology 36:711-720.

Lee JH, Lee S, Kim JH (2017) Amygdala Circuits for Fear Memory: A Key Role for Dopamine Regulation. Neuroscientist 23:542-553.

Levin JR, Serlin, R.C., Seaman, M.A. (1994) A controlled powerful multiple-comparison strategy for several situations . Psychological Bulletin 115:153-159.

Lex A, Hauber W (2008) Dopamine D1 and D2 receptors in the nucleus accumbens core and shell mediate Pavlovian-instrumental transfer. Learn Mem 15:483-491.

Li C, Rainnie DG (2014) Bidirectional regulation of synaptic plasticity in the basolateral amygdala induced by the D1-like family of dopamine receptors and group II metabotropic glutamate receptors. The Journal of physiology 592.

Li C, Dabrowska J, Hazra R, Rainnie DG (2011a) Synergistic activation of dopamine D1 and TrkB receptors mediate gain control of synaptic plasticity in the basolateral amygdala. PLoS One 6:e26065.

Li J, Schiller D, Schoenbaum G, Phelps EA, Daw ND (2011b) Differential roles of human striatum and amygdala in associative learning. Nat Neurosci 14:1250-1252.

Lichtenberg NT, Wassum KM (2016) Amygdala mu-opioid receptors mediate the motivating influence of cue-triggered reward expectations. Eur J Neurosci.

Lichtenberg NT, Sepe-Forrest L, Pennington ZT, Lamparelli AC, Greenfield VY, Wassum KM (2021) The Medial Orbitofrontal Cortex-Basolateral Amygdala Circuit Regulates the Influence of Reward Cues on Adaptive Behavior and Choice. J Neurosci 41:7267-7277.

Lichtenberg NT, Pennington ZT, Holley SM, Greenfield VY, Cepeda C, Levine MS, Wassum KM (2017) Basolateral amygdala to orbitofrontal cortex projections enable cue-triggered reward expectations. J Neurosci.

Liu H, Tang Y, Womer F, Fan G, Lu T, Driesen N, Ren L, Wang Y, He Y, Blumberg HP, Xu K, Wang F (2014) Differentiating patterns of amygdala-frontal functional connectivity in schizophrenia and bipolar disorder. Schizophr Bull 40:469-477.

Liu J, Lyu C, Li M, Liu T, Song S, Tsien JZ (2018) Neural Coding of Appetitive Food Experiences in the Amygdala. Neurobiol Learn Mem 155:261-275.

Ljungberg T, Apicella P, Schultz W (1992) Responses of monkey dopamine neurons during learning of behavioral reactions. J Neurophysiol 67:145-163.

Lopatina N, McDannald MA, Styer CV, Sadacca BF, Cheer JF, Schoenbaum G (2015) Lateral orbitofrontal neurons acquire responses to upshifted, downshifted, or blocked cues during unblocking. Elife 4:e11299.

Lopes G, Bonacchi N, Frazão J, Neto JP, Atallah BV, Soares S, Moreira L, Matias S, Itskov PM, Correia PA, Medina RE, Calcaterra L, Dreosti E, Paton JJ, Kampff AR (2015) Bonsai: an event-based framework for processing and controlling data streams. Front Neuroinform 9:7.

Lorétan K, Bissière S, Lüthi A (2004) Dopaminergic modulation of spontaneous inhibitory network activity in the lateral amygdala. Neuropharmacology 47:631-639.

Lucantonio F, Caprioli D, Schoenbaum G (2014) Transition from 'model-based' to 'model-free' behavioral control in addiction: Involvement of the orbitofrontal cortex and dorsolateral striatum. Neuropharmacology 76 Pt B:407-415.

Lucantonio F, Gardner MP, Mirenzi A, Newman LE, Takahashi YK, Schoenbaum G (2015) Neural Estimates of Imagined Outcomes in Basolateral Amygdala Depend on Orbitofrontal Cortex. J Neurosci 35:16521-16530.

Ludvig EA, Sutton RS, Kehoe EJ (2012) Evaluating the TD model of classical conditioning. Learning and Behavior 40:305-319.

Lutas A, Fernando K, Zhang SX, Sambangi A, Andermann ML (2022) History-dependent dopamine release increases cAMP levels in most basal amygdala glutamatergic neurons to control learning. Cell Rep 38:110297.

Lutas A, Kucukdereli H, Alturkistani O, Carty C, Sugden AU, Fernando K, Diaz V, Flores-Maldonado V, Andermann ML (2019) State-specific gating of salient cues by midbrain dopaminergic input to basal amygdala. Nat Neurosci 22:1820-1833.

Lázaro-Muñoz G, LeDoux JE, Cain CK (2010) Sidman instrumental avoidance initially depends on lateral and basal amygdala and is constrained by central amygdala-mediated Pavlovian processes. Biol Psychiatry 67:1120-1127.

Machado CJ, Bachevalier J (2007) The effects of selective amygdala, orbital frontal cortex or hippocampal formation lesions on reward assessment in nonhuman primates. Eur J Neurosci 25:2885-2904.

Mackintosh NJ (1975) A theory of attention: Variations in the associability of stimuli with reinforcement. Psychological review 82:276.

Maes EJP, Sharpe MJ, Usypchuk AA, Lozzi M, Chang CY, Gardner MPH, Schoenbaum G, Iordanova MD (2020) Causal evidence supporting the proposal that dopamine transients function as temporal difference prediction errors. Nature Neuroscience 23:176-178.

Maltais S, C té S, Drolet G, Falardeau P (2000) Cellular colocalization of dopamine D1 mRNA and D2 receptor in rat brain using a D2 dopamine receptor specific polyclonal antibody. Prog Neuropsychopharmacol Biol Psychiatry 24:1127-1149.

Malvaez M, Shieh C, Murphy MD, Greenfield VY, Wassum KM (2019) Distinct cortical-amygdala projections drive reward value encoding and retrieval. Nat Neurosci 22:762-769.

Malvaez M, Greenfield VY, Wang AS, Yorita AM, Feng L, Linker KE, Monbouquette HG, Wassum KM (2015) Basolateral amygdala rapid glutamate release encodes an outcome-specific representation vital for reward-predictive cues to selectively invigorate reward-seeking actions. Sci Rep 5:12511.

Marowsky A, Yanagawa Y, Obata K, Vogt K (2005) A specialized subclass of interneurons mediates dopaminergic facilitation of amygdala function. Neuron 48.

McDannald MA, Esber GR, Wegener MA, Wied HM, Liu TL, Stalnaker TA, Jones JL, Trageser J, Schoenbaum G (2014) Orbitofrontal neurons acquire responses to 'valueless' Pavlovian cues during unblocking. Elife 3:e02653.

McDonald A (1992) Cell types and intrinsic connections of the amygdala. The amygdala: neurobiological aspects of emotion, memory, and mental dysfunction (Aggleton JP, ed):67-96.

McDonald AJ (1998) Cortical pathways to the mammalian amygdala. Prog Neurobiol 55:257-332.

McDonald AJ, Augustine JR (1993) Localization of GABA-like immunoreactivity in the monkey amygdala. Neuroscience 52:281-294.

Menegas W, Babayan BM, Uchida N, Watabe-Uchida M (2017) Opposite initialization to novel cues in dopamine signaling in ventral and posterior striatum in mice. Elife 6.

Miller KJ, Botvinick MM, Brody CD (2018) Value Representations in Orbitofrontal Cortex Drive Learning, not Choice. bioRxiv:245720.

Millhouse OE, DeOlmos J (1983) Neuronal configurations in lateral and basolateral amygdala. Neuroscience 10:1269-1300.

Morecraft RJ, Geula C, Mesulam MM (1992) Cytoarchitecture and neural afferents of orbitofrontal cortex in the brain of the monkey. J Comp Neurol 323:341-358.

Morrens J, Aydin Ç, Janse van Rensburg A, Esquivelzeta Rabell J, Haesler S (2020) Cue-Evoked Dopamine Promotes Conditioned Responding during Learning. Neuron 106:142-153.e147.

Morse AK, Leung BK, Heath E, Bertran-Gonzalez J, Pepin E, Chieng BC, Balleine BW, Laurent V (2020) Basolateral Amygdala Drives a GPCR-Mediated Striatal Memory Necessary for Predictive Learning to Influence Choice. Neuron 106:855-869.e858.

Muller J, Corodimas KP, Fridel Z, LeDoux JE (1997) Functional inactivation of the lateral and basal nuclei of the amygdala by muscimol infusion prevents fear conditioning to an explicit conditioned stimulus and to contextual stimuli. Behav Neurosci 111:683-691.

Muramoto K, Ono T, Nishijo H, Fukuda M (1993) Rat amygdaloid neuron responses during auditory discrimination. Neuroscience 52:621-636.

Murray EA, Izquierdo A (2007) Orbitofrontal cortex and amygdala contributions to affect and action in primates. Ann N Y Acad Sci 1121:273-296.

Málková L, Gaffan D, Murray EA (1997) Excitotoxic lesions of the amygdala fail to produce impairment in visual learning for auditory secondary reinforcement but interfere with reinforcer devaluation effects in rhesus monkeys. J Neurosci 17:6011-6020.

Nader K, LeDoux JE (1999) Inhibition of the mesoamygdala dopaminergic pathway impairs the retrieval of conditioned fear associations. Behav Neurosci 113:891-901.

Namburi P, Beyeler A, Yorozu S, Calhoon GG, Halbert SA, Wichmann R, Holden SS, Mertens KL, Anahtar M, Felix-Ortiz AC, Wickersham IR, Gray JM, Tye KM (2015) A circuit mechanism for differentiating positive and negative associations. Nature 520:675-678.

Nasser HM, Calu DJ, Schoenbaum G, Sharpe MJ (2017) The Dopamine Prediction Error: Contributions to Associative Models of Reward Learning. Front Psychol 8:244.

Niv Y (2019) Learning task-state representations. Nat Neurosci 22:1544-1553.

O'Doherty JP, Dayan P, Friston K, Critchley H, Dolan RJ (2003) Temporal difference models and reward-related learning in the human brain. Neuron 38:329-337.

Orsini CA, Hernandez CM, Singhal S, Kelly KB, Frazier CJ, Bizon JL, Setlow B (2017) Optogenetic Inhibition Reveals Distinct Roles for Basolateral Amygdala Activity at Discrete Time Points during Risky Decision Making. J Neurosci 37:11537-11548.

Ostlund SB, Balleine BW (2007a) The contribution of orbitofrontal cortex to action selection. Ann N Y Acad Sci 1121:174-192.

Ostlund SB, Balleine BW (2007b) Orbitofrontal cortex mediates outcome encoding in Pavlovian but not instrumental conditioning. J Neurosci 27:4819-4825.

Ostlund SB, Balleine BW (2008) Differential involvement of the basolateral amygdala and mediodorsal thalamus in instrumental action selection. J Neurosci 28:4398-4405.

Ott T, Nieder A (2019) Dopamine and Cognitive Control in Prefrontal Cortex. Trends Cogn Sci 23:213-234.

Overmier JB, Bull JA, Trapold MA (1972) Discriminative cue properties of different fears and their role in response selection in dogs. Journal of Comparative and Physiological Psychology 76:478-478.

Pan WX, Schmidt R, Wickens JR, Hyland BI (2005) Dopamine cells respond to predicted events during classical conditioning: evidence for eligibility traces in the reward-learning network. J Neurosci 25:6235-6242.

Parkes SL, Balleine BW (2013) Incentive memory: evidence the basolateral amygdala encodes and the insular cortex retrieves outcome values to guide choice between goal-directed actions. J Neurosci 33:8753-8763.

Parkinson JA, Robbins TW, Everitt BJ (2000) Dissociable roles of the central and basolateral amygdala in appetitive emotional learning. Eur J Neurosci 12:405-413.

Passamonti L, Fairchild G, Fornito A, Goodyer IM, Nimmo-Smith I, Hagan CC, Calder AJ (2012) Abnormal anatomical connectivity between the amygdala and orbitofrontal cortex in conduct disorder. PLoS One 7:e48789.

Paton JJ, Belova MA, Morrison SE, Salzman CD (2006) The primate amygdala represents the positive and negative value of visual stimuli during learning. Nature 439:865-870.

Pavlov IP (1927) Conditioned reflexes: an investigation of the physiological activity of the cerebral cortex: Oxford University Press.

Paxinos G, Watson C (1998) The rat brain in stereotaxic coordinates, 4th Edition: Academic Press.

Pearce JM, Hall G (1980) A model for Pavlovian learning: variations in the effectiveness of conditioned but not of unconditioned stimuli. Psychol Rev 87:532-552.

Perumal MB, Sah P (2021) Inhibitory Circuits in the Basolateral Amygdala in Aversive Learning and Memory. Front Neural Circuits 15:633235.

Pezze MA, Feldon J (2004) Mesolimbic dopaminergic pathways in fear conditioning. Prog Neurobiol 74:301-320.

Pickens CL, Saddoris MP, Gallagher M, Holland PC (2005) Orbitofrontal lesions impair use of cue-outcome associations in a devaluation task. Behav Neurosci 119:317-322.

Pickens CL, Saddoris MP, Setlow B, Gallagher M, Holland PC, Schoenbaum G (2003) Different roles for orbitofrontal cortex and basolateral amygdala in a reinforcer devaluation task. J Neurosci 23:11078-11084.

Pignatelli M, Beyeler A (2019) Valence coding in amygdala circuits. Curr Opin Behav Sci 26:97-106.

Price JL (2007) Definition of the orbital cortex in relation to specific connections with limbic and visceral structures and other cortical regions. Ann N Y Acad Sci 1121:54-71.

Pritchard TC, Edwards EM, Smith CA, Hilgert KG, Gavlick AM, Maryniak TD, Schwartz GJ, Scott TR (2005) Gustatory neural responses in the medial orbitofrontal cortex of the old world monkey. J Neurosci 25:6047-6056.

Radulescu A, Niv Y (2019) State representation in mental illness. Curr Opin Neurobiol 55:160-166.

Rescorla R (1999) Learning about qualitatively different outcomes during a blocking procedure. Animal Learning & Behavior 27:140-151.

Rescorla RA (1973) Effects of US habituation following conditioning. Journal of Comparative and Physiological Psychology 82:137-137.

Rescorla RA (1974) Effect of inflation of the unconditioned stimulus value following conditioning. Journal of Comparative and Physiological Psychology 86:101-101.

Rescorla RA, Solomon RL (1967) Two-process learning theory: Relationships between Pavlovian conditioning and instrumental learning. Psychological Review 74:151-151.

Rescorla RA, Wagner AR (1972) A theory of Pavlovian conditioning: Variations in the effectiveness of reinforcement and nonreinforcement. In: Classical Conditioning II: Current Research and Theory (Black AH, Prokasy WF, eds), pp 64-69. New York: Appleton-Century-Crofts.

Ressler KJ, Mayberg HS (2007) Targeting abnormal neural circuits in mood and anxiety disorders: from the laboratory to the clinic. Nat Neurosci 10:1116-1124.

Reynolds JNJ, Hyland BI, Wickens JR (2001) A cellular mechanism of reward-related learning. Nature 413:67-70.

Rhodes SE, Murray EA (2013) Differential effects of amygdala, orbital prefrontal cortex, and prelimbic cortex lesions on goal-directed behavior in rhesus macaques. J Neurosci 33:3380-3389.

Riceberg JS, Shapiro ML (2017) Orbitofrontal Cortex Signals Expected Outcomes with Predictive Codes When Stable Contingencies Promote the Integration of Reward History. J Neurosci 37:2010-2021.

Rich EL, Wallis JD (2016) Decoding subjective decisions from orbitofrontal cortex. Nat Neurosci 19:973-980.

Robbins TW, Costa RM (2017) Habits. Current Biology 27:R1200-R1206.

Roesch MR, Calu DJ, Esber GR, Schoenbaum G (2010) Neural correlates of variations in event processing during learning in basolateral amygdala. J Neurosci 30:2464-2471.

Roesch MR, Esber GR, Li J, Daw ND, Schoenbaum G (2012) Surprise! Neural correlates of Pearce-Hall and Rescorla-Wagner coexist within the brain. European Journal of Neuroscience 35:1190-1200.

Romanski LM, Clugnet MC, Bordi F, LeDoux JE (1993) Somatosensory and auditory convergence in the lateral nucleus of the amygdala. Behav Neurosci 107:444-450.

Rudebeck P, Rich E (2018) Orbitofrontal cortex. Current Biology 28:R1083-R1088.

Rudebeck PH, Murray EA (2014) The orbitofrontal oracle: cortical mechanisms for the prediction and evaluation of specific behavioral outcomes. Neuron 84:1143-1156.

Rudebeck PH, Mitz AR, Chacko RV, Murray EA (2013) Effects of amygdala lesions on reward-value coding in orbital and medial prefrontal cortex. Neuron 80:1519-1531.

Rudebeck PH, Ripple JA, Mitz AR, Averbeck BB, Murray EA (2017) Amygdala contributions to stimulus-reward encoding in the macaque medial and orbital frontal cortex during learning. J Neurosci.

Ryan TJ, Ortega-de San Luis C, Pezzoli M, Sen S (2021) Engram cell connectivity: an evolving substrate for information storage. Curr Opin Neurobiol 67:215-225.

Sadacca BF, Jones JL, Schoenbaum G (2016) Midbrain dopamine neurons compute inferred and cached value prediction errors in a common framework. Elife 5.

Sadacca BF, Wied HM, Lopatina N, Saini GK, Nemirovsky D, Schoenbaum G (2018) Orbitofrontal neurons signal sensory associations underlying model-based inference in a sensory preconditioning task. Elife 7.

Saddoris MP, Gallagher M, Schoenbaum G (2005) Rapid associative encoding in basolateral amygdala depends on connections with orbitofrontal cortex. Neuron 46:321-331.

Salinas-Hernández XI, Duvarci S (2021) Dopamine in Fear Extinction. Front Synaptic Neurosci 13:635879.

Saunders BT, Richard JM, Margolis EB, Janak PH (2018) Dopamine neurons create Pavlovian conditioned stimuli with circuit-defined motivational properties. Nat Neurosci 21:1072-1083.

Scarlet J, Delamater AR, Campese V, Fein M, Wheeler DS (2012) Differential involvement of the basolateral amygdala and orbitofrontal cortex in the formation of sensory-specific associations in conditioned flavor preference and magazine approach paradigms. Eur J Neurosci 35:1799-1809.

Schoenbaum G, Eichenbaum H (1995) Information coding in the rodent prefrontal cortex. I. Single-neuron activity in orbitofrontal cortex compared with that in pyriform cortex. J Neurophysiol 74:733-750.

Schoenbaum G, Roesch M (2005) Orbitofrontal cortex, associative learning, and expectancies. Neuron 47:633-636.

Schoenbaum G, Chiba AA, Gallagher M (1998) Orbitofrontal cortex and basolateral amygdala encode expected outcomes during learning. Nat Neurosci 1:155-159.

Schoenbaum G, Chiba AA, Gallagher M (1999) Neural encoding in orbitofrontal cortex and basolateral amygdala during olfactory discrimination learning. J Neurosci 19:1876-1884.

Schoenbaum G, Chiba AA, Gallagher M (2000) Changes in functional connectivity in orbitofrontal cortex and basolateral amygdala during learning and reversal training. J Neurosci 20:5179-5189.

Schoenbaum G, Setlow B, Saddoris MP, Gallagher M (2003) Encoding predicted outcome and acquired value in orbitofrontal cortex during cue sampling depends upon input from basolateral amygdala. Neuron 39:855-867.

Schoenbaum G, Chang CY, Lucantonio F, Takahashi YK (2016) Thinking Outside the Box: Orbitofrontal Cortex, Imagination, and How We Can Treat Addiction. Neuropsychopharmacology 41:2966-2976.

Schuck NW, Cai MB, Wilson RC, Niv Y (2016) Human Orbitofrontal Cortex Represents a Cognitive Map of State Space. Neuron 91:1402-1412.

Schultz W (1998) Predictive reward signal of dopamine neurons. J Neurophysiol 80:1-27.

Schultz W (2016) Dopamine reward prediction error coding. Dialogues in Clinical Neuroscience 18:23-32.

Schultz W, Apicella P, Ljungberg T (1993) Responses of monkey dopamine neurons to reward and conditioned stimuli during successive steps of learning a delayed response task. J Neurosci 13:900-913.

Schultz W, Dayan P, Montague PR (1997) A neural substrate of prediction and reward. Science 275:1593-1599.

See RE, Kruzich PJ, Grimm JW (2001) Dopamine, but not glutamate, receptor blockade in the basolateral amygdala attenuates conditioned reward in a rat model of relapse to cocaine-seeking behavior. Psychopharmacology (Berl) 154:301-310.

Seitz BM, Blaisdell AP, Sharpe MJ (2021) Higher-Order Conditioning and Dopamine: Charting a Path Forward. Front Behav Neurosci 15:745388.

Sengupta A, Yau JOY, Jean-Richard-Dit-Bressel P, Liu Y, Millan EZ, Power JM, McNally GP (2018) Basolateral Amygdala Neurons Maintain Aversive Emotional Salience. J Neurosci 38:3001-3012.

Servonnet A, Hernandez G, El Hage C, Rompré PP, Samaha AN (2020) Optogenetic Activation of the Basolateral Amygdala Promotes Both Appetitive Conditioning and the Instrumental Pursuit of Reward Cues. J Neurosci 40:1732-1743.

Shabel SJ, Janak PH (2009) Substantial similarity in amygdala neuronal activity during conditioned appetitive and aversive emotional arousal. Proc Natl Acad Sci U S A 106:15031-15036.

Sharp BM (2017) Basolateral amygdala and stress-induced hyperexcitability affect motivated behaviors and addiction. Transl Psychiatry 7:e1194.

Sharpe MJ, Schoenbaum G (2016) Back to basics: Making predictions in the orbitofrontal-amygdala circuit. Neurobiol Learn Mem 131:201-206.

Sharpe MJ, Stalnaker T, Schuck NW, Killcross S, Schoenbaum G, Niv Y (2019) An Integrated Model of Action Selection: Distinct Modes of Cortical Control of Striatal Decision Making. Annu Rev Psychol 70:53-76.

Sharpe MJ, Batchelor HM, Mueller LE, Yun Chang C, Maes EJP, Niv Y, Schoenbaum G (2020) Dopamine transients do not act as model-free prediction errors during associative learning. Nat Commun 11:106.

Sharpe MJ, Chang CY, Liu MA, Batchelor HM, Mueller LE, Jones JL, Niv Y, Schoenbaum G (2017) Dopamine transients are sufficient and necessary for acquisition of model-based associations. Nat Neurosci 20:735-742.

Shi YW, Fan BF, Xue L, Wen JL, Zhao H (2017) Regulation of Fear Extinction in the Basolateral Amygdala by Dopamine D2 Receptors Accompanied by Altered GluR1, GluR1-Ser845 and NR2B Levels. Front Behav Neurosci 11:116.

Sias A, Morse A, Wang S, Greenfield V, Goodpaster C, Wrenn T, Wikenheiser A, Holley S, Cepeda C, Levine M, Wassum K (2021) A bidirectional corticoamygdala circuit for the encoding and retrieval of detailed reward memories. eLife 10.

Siciliano CA, Tye KM (2019) Leveraging calcium imaging to illuminate circuit dysfunction in addiction. Alcohol 74:47-63.

Sladky R, Höflich A, Küblböck M, Kraus C, Baldinger P, Moser E, Lanzenberger R, Windischberger C (2015) Disrupted effective connectivity between the amygdala and orbitofrontal cortex in social anxiety disorder during emotion discrimination revealed by dynamic causal modeling for FMRI. Cereb Cortex 25:895-903.

Solomon RL, Corbit JD (1974) An opponent-process theory of motivation. I. Temporal dynamics of affect. Psychol Rev 81:119-145.

Spence KW (1956) Behavior theory and conditioning. New Haven: Yale University Press.

Stalnaker TA, Franz TM, Singh T, Schoenbaum G (2007) Basolateral amygdala lesions abolish orbitofrontal-dependent reversal impairments. Neuron 54:51-58.

Stalnaker TA, Liu TL, Takahashi YK, Schoenbaum G (2018) Orbitofrontal neurons signal reward predictions, not reward prediction errors. Neurobiol Learn Mem 153:137-143.

Stalnaker TA, Roesch MR, Franz TM, Burke KA, Schoenbaum G (2006) Abnormal associative encoding in orbitofrontal neurons in cocaine-experienced rats during decision-making. Eur J Neurosci 24:2643-2653.

Stalnaker TA, Cooch NK, McDannald MA, Liu TL, Wied H, Schoenbaum G (2014) Orbitofrontal neurons infer the value and identity of predicted outcomes. Nature Communications 5:1-13.

Stalnaker TA, Howard JD, Takahashi YK, Gershman SJ, Kahnt T, Schoenbaum G (2019) Dopamine neuron ensembles signal the content of sensory prediction errors. Elife 8.

Stalter M, Westendorff S, Nieder A (2020) Dopamine Gates Visual Signals in Monkey Prefrontal Cortex Neurons. Cell Rep 30:164-172.e164.

Steinberg EE, Keiflin R, Boivin JR, Witten IB, Deisseroth K, Janak PH (2013) A causal link between prediction errors, dopamine neurons and learning. Nature Neuroscience 16:966-973.

Stolyarova A, Rakhshan M, Hart EE, O'Dell TJ, Peters MAK, Lau H, Soltani A, Izquierdo A (2019) Contributions of anterior cingulate cortex and basolateral amygdala to decision confidence and learning under uncertainty. Nat Commun 10:4704.

Suarez JA, Howard JD, Schoenbaum G, Kahnt T (2019) Sensory prediction errors in the human midbrain signal identity violations independent of perceptual distance.

Sugase-Miyamoto Y, Richmond BJ (2005) Neuronal signals in the monkey basolateral amygdala during reward schedules. J Neurosci 25:11071-11083.

Sun F, Zhou J, Dai B, Qian T, Zeng J, Li X, Zhuo Y, Zhang Y, Wang Y, Qian C, Tan K, Feng J, Dong H, Lin D, Cui G, Li Y (2020) Next-generation GRAB sensors for monitoring dopaminergic activity in vivo. Nat Methods 17:1156-1166.

Sutton RS (1988) Learning to Predict by the Methods of Temporal Differences. Machine Learning 3:9-44.

Suzuki S, Cross L, O'Doherty JP (2017) Elucidating the underlying components of food valuation in the human orbitofrontal cortex. Nat Neurosci 20:1780-1786.

Suzuki T, Ishigooka J, Watanabe S, Miyaoka H (2002) Enhancement of delayed release of dopamine in the amygdala induced by conditioned fear stress in methamphetamine-sensitized rats. Eur J Pharmacol 435:59-65.

Takahashi H, Takano H, Kodaka F, Arakawa R, Yamada M, Otsuka T, Hirano Y, Kikyo H, Okubo Y, Kato M, Obata T, Ito H, Suhara T (2010) Contribution of dopamine D1 and D2 receptors to amygdala activity in human. J Neurosci 30:3043-3047.

Takahashi YK, Batchelor HM, Liu B, Khanna A, Morales M, Schoenbaum G (2017) Dopamine Neurons Respond to Errors in the Prediction of Sensory Features of Expected Rewards. Neuron 95:1395-1405.e1393.

Takahashi YK, Roesch MR, Stalnaker TA, Haney RZ, Calu DJ, Taylor AR, Burke KA, Schoenbaum G (2009) The orbitofrontal cortex and ventral tegmental area are necessary for learning from unexpected outcomes. Neuron 62:269-280.

Takahashi YK, Chang CY, Lucantonio F, Haney RZ, Berg BA, Yau HJ, Bonci A, Schoenbaum G (2013) Neural estimates of imagined outcomes in the orbitofrontal cortex drive behavior and learning. Neuron 80:507-518.

Tang W, Kochubey O, Kintscher M, Schneggenburger R (2020) A VTA to Basal Amygdala Dopamine Projection Contributes to Signal Salient Somatosensory Events during Fear Learning. J Neurosci 40:3969-3980.

Tian J, Huang R, Cohen JY, Osakada F, Kobak D, Machens CK, Callaway EM, Uchida N, Watabe-Uchida M (2016) Distributed and Mixed Information in Monosynaptic Inputs to Dopamine Neurons. Neuron 91:1374-1389.

Tonegawa S, Pignatelli M, Roy DS, Ryan TJ (2015) Memory engram storage and retrieval. Curr Opin Neurobiol 35:101-109.

Touzani K, Bodnar RJ, Sclafani A (2013) Glucose-conditioned flavor preference learning requires co-activation of NMDA and dopamine D1-like receptors within the amygdala. Neurobiol Learn Mem 106:95-101.

Trapold MA (1970) Are expectancies based upon different positive reinforcing events discriminably different? Learning and Motivation 1:129-140.

Tremblay L, Schultz W (2000) Modifications of reward expectation-related neuronal activity during learning in primate orbitofrontal cortex. J Neurophysiol 83:1877-1885.

Tye KM (2018) Neural Circuit Motifs in Valence Processing. Neuron 100:436-452.

Tye KM, Janak PH (2007) Amygdala neurons differentially encode motivation and reinforcement. J Neurosci 27:3937-3945.

Tye KM, Stuber GD, de Ridder B, Bonci A, Janak PH (2008) Rapid strengthening of thalamo-amygdala synapses mediates cue-reward learning. Nature 453:1253-1257.

Tye KM, Tye LD, Cone JJ, Hekkelman EF, Janak PH, Bonci A (2010) Methylphenidate facilitates learning-induced amygdala plasticity. Nat Neurosci 13:475-481.

Tye KM, Prakash R, Kim SY, Fenno LE, Grosenick L, Zarabi H, Thompson KR, Gradinaru V, Ramakrishnan C, Deisseroth K (2011) Amygdala circuitry mediating reversible and bidirectional control of anxiety. Nature 471:358-362.

van Duuren E, Escámez FA, Joosten RN, Visser R, Mulder AB, Pennartz CM (2007) Neural coding of reward magnitude in the orbitofrontal cortex of the rat during a five-odor olfactory discrimination task. Learn Mem 14:446-456.

Vander Weele CM, Siciliano CA, Matthews GA, Namburi P, Izadmehr EM, Espinel IC, Nieh EH, Schut EHS, Padilla-Coreano N, Burgos-Robles A, Chang CJ, Kimchi EY, Beyeler A, Wichmann R, Wildes CP, Tye KM (2018) Dopamine enhances signal-to-noise ratio in cortical-brainstem encoding of aversive stimuli. Nature 563:397-401.

Waelti P, Dickinson A, Schultz W (2001) Dopamine responses comply with basic assumptions of formal learning theory. Nature 412:43-48.

Wallis JD, Miller EK (2003) Neuronal activity in primate dorsolateral and orbital prefrontal cortex during performance of a reward preference task. Eur J Neurosci 18:2069-2081.

Wang F, Howard JD, Voss JL, Schoenbaum G, Kahnt T (2020) Targeted Stimulation of an Orbitofrontal Network Disrupts Decisions Based on Inferred, Not Experienced Outcomes. J Neurosci 40:8726-8733.

Wassum KM, Izquierdo A (2015) The basolateral amygdala in reward learning and addiction. Neurosci Biobehav Rev 57:271-283.

Wellman LL, Gale K, Malkova L (2005) GABAA-mediated inhibition of basolateral amygdala blocks reward devaluation in macaques. J Neurosci 25:4577-4586.

West EA, Forcelli PA, Murnen AT, McCue DL, Gale K, Malkova L (2012) Transient inactivation of basolateral amygdala during selective satiation disrupts reinforcer devaluation in rats. Behav Neurosci 126:563-574.

Wikenheiser AM, Schoenbaum G (2016) Over the river, through the woods: cognitive maps in the hippocampus and orbitofrontal cortex. Nat Rev Neurosci 17:513-523.

Wilson RC, Takahashi YK, Schoenbaum G, Niv Y (2014a) Orbitofrontal cortex as a cognitive map of task space. Neuron 81:267-279.

Wilson RC, Takahashi YK, Schoenbaum G, Niv Y (2014b) Orbitofrontal cortex as a cognitive map of task space. Neuron 81:267-279.

Witten IB, Steinberg EE, Lee SY, Davidson TJ, Zalocusky KA, Brodsky M, Yizhar O, Cho SL, Gong S, Ramakrishnan C, Stuber GD, Tye KM, Janak PH, Deisseroth K (2011) Recombinase-driver rat lines: tools, techniques, and optogenetic application to dopamine-mediated reinforcement. Neuron 72:721-733.

Wunderlich K, Smittenaar P, Dolan RJ (2012) Dopamine enhances model-based over model-free choice behavior. Neuron 75:418-424.

Zeeb FD, Winstanley CA (2013) Functional disconnection of the orbitofrontal cortex and basolateral amygdala impairs acquisition of a rat gambling task and disrupts animals' ability to alter decision-making behavior after reinforcer devaluation. J Neurosci 33:6434-6443.

Zhang X, Kim J, Tonegawa S (2020) Amygdala Reward Neurons Form and Store Fear Extinction Memory. Neuron 105:1077-1093.e1077.

Zhou J, Montesinos-Cartagena M, Wikenheiser AM, Gardner MPH, Niv Y, Schoenbaum G (2019a) Complementary Task Structure Representations in Hippocampus and Orbitofrontal Cortex during an Odor Sequence Task. Curr Biol 29:3402-3409.e3403.

Zhou J, Gardner MPH, Stalnaker TA, Ramus SJ, Wikenheiser AM, Niv Y, Schoenbaum G (2019b) Rat Orbitofrontal Ensemble Activity Contains Multiplexed but Dissociable

Representations of Value and Task Structure in an Odor Sequence Task. Curr Biol 29:897-907.e893.